

**Synthetic and Structural Studies of Permethylscandocene and  
Permethyltantalocene Derivatives**

**Thesis by  
Martin A. St. Clair**

**In Partial Fulfillment of the Requirements  
for the Degree of  
Doctor of Philosophy**

**California Institute of Technology  
Pasadena, California**

**1989**

**(submitted February 22, 1989)**

## ACKNOWLEDGEMENTS

First and foremost, I would like to thank the members of the Bercaw group with whom I have worked over the past five years. In particular, Tippy (Mark Thompson) was both a good housemate and taught me most of what I know about Bercaw high-vacuum techniques, scandium chemistry, and cross-country skiing. Van (Allan van Asselt) was also a wonderful housemate and friend, who helped keep chemistry in proper perspective, and introduced me (with the help of Jeff (Leon) Gelles) to the wonders of bluegrass. And of course, I would especially like to thank John Bercaw for support and for showing me how to do careful, interesting, good science.

The assistance of Bernie Santarsiero and Bill Schaefer with solving the crystal structures in this thesis was greatly appreciated, as was the assistance of Doug Meinhart, Dave Wheeler, and Donnie Cotter in obtaining NMR spectra and Kathy Kanes in obtaining Raman spectra. The gift of  $(\text{C}_6\text{H}_{11})\text{C}\equiv\text{C}-\text{C}\equiv\text{C}(\text{C}_6\text{H}_{11})$  from Professor George Zweifel of UC Davis is gratefully acknowledged. Funding for this work was provided by the National Science Foundation, Department of Energy, and the Shell Companies Foundation.

I would also like to thank my parents, who have always allowed me the freedom to pursue my own interests, and yet, by example, have shown me what things are really worth pursuing. Fr. Michael Kennedy, the staff and guests of *Casa Rutilio Grande*, and my friends at All Saints have taught me more during my stay in Southern California than any Ph.D. program imaginable. Finally, and most importantly, I am grateful to Cindy for her constant support and love, for continuing to challenge me, and for helping me to grow.

## ABSTRACT

$\text{Cp}^*_2\text{Sc-H}$  reacts with  $\text{H}_2$  and  $\text{CO}$  at  $-78^\circ\text{C}$  to yield  $\text{Cp}^*_2\text{ScOCH}_3$ . A stepwise reduction of  $\text{CO}$  to an alkoxide is observed when  $\text{CO}$  reacts with  $\text{Cp}^*_2\text{ScC}_6\text{H}_4\text{CH}_3$ -*p* to give the  $\eta^2$ -acyl  $\text{Cp}^*_2\text{Sc}(\text{CO})\text{C}_6\text{H}_4\text{CH}_3$ -*p*, which then reacts with  $\text{H}_2$  to produce  $\text{Cp}^*_2\text{ScOCH}_2\text{C}_6\text{H}_4\text{CH}_3$ -*p*.  $\text{Cp}^*_2\text{ScCH}_3$  and  $\text{Cp}^*_2\text{ScH}(\text{THF})$  react with  $\text{CO}$  to give uncharacterizable products.  $\text{Cp}^*_2\text{ScH}$  and  $\text{Cp}^*_2\text{ScCH}_3$  react with  $\text{Cp}_2\text{MCO}$  ( $\text{M} = \text{Mo}, \text{W}$ ) to give scandoxycarbenes,  $\text{Cp}_2\text{M}=\text{C}(\text{CH}_3)\text{OScCp}^*_2$ , while a wide variety of  $\text{Cp}^*_2\text{ScX}$  ( $\text{X} = \text{H}, \text{CH}_3, \text{N}(\text{CH}_3)_2, \text{CH}_2\text{CH}_2\text{C}_6\text{H}_5$ ) reacts with  $\text{CpM}(\text{CO})_2$  ( $\text{M} = \text{Co}, \text{Rh}$ ) to yield similar carbene complexes. An x-ray crystal structure determination of  $\text{Cp}(\text{CO})\text{Co}=\text{C}(\text{CH}_3)\text{-OScCp}^*_2$  revealed a  $\mu^2: \eta^1, \eta^1$  carbonyl interaction between the  $\text{Co-CO}$  and  $\text{Sc}$ .

$\text{CO}_2$  inserts cleanly into  $\text{Sc-phenyl}$  bonds at  $-78^\circ\text{C}$  to produce a carboxylate complex,  $\text{Cp}^*_2\text{Sc}(\text{O}_2\text{C})\text{C}_6\text{H}_4\text{CH}_3$ -*p*. The structure of this compound was determined by x-ray crystallographic techniques.

Excess  $\text{C}_2\text{H}_2$  reacts with  $\text{Cp}^*_2\text{ScR}$  ( $\text{R} = \text{H}, \text{alkyl}, \text{aryl}, \text{alkenyl}, \text{alkynyl}, \text{amide}$ ) at temperatures below  $-78^\circ\text{C}$  to form the alkynyl species  $\text{Cp}^*_2\text{Sc-C}\equiv\text{C-H}$ , which then reacts with the remaining acetylene to form polyacetylene.  $\text{Cp}^*_2\text{Sc-C}\equiv\text{C-H}$  further reacts to yield  $\text{Cp}^*_2\text{Sc-C}\equiv\text{C-ScCp}^*_2$ . This unusual  $\text{C}_2$  bridged dimer was characterized by x-ray crystallography.

Attempts were made to model the C-N bond breaking step of hydrodenitrogenation by synthesizing  $\text{Cp}^*_2\text{TaH}(\eta^2\text{-H}_2\text{C}=\text{N}(\text{C}_6\text{H}_4\text{X}))$  and studying its rearrangement to  $\text{Cp}^*_2\text{Ta}(=\text{N}(\text{C}_6\text{H}_4\text{X}))(\text{CH}_3)$ . The 1,2 addition/elimination reactions of  $\text{Cp}^*_2\text{Ta}(\eta^2\text{-H}_2\text{C}=\text{N}(\text{CH}_3)\text{H})$  and  $\text{Cp}^*_2\text{Ta}(=\text{X})\text{H}$  ( $\text{X}=\text{O}, \text{S}, \text{NH}, \text{N}(\text{C}_6\text{H}_5)$ ) were investigated.  $\text{Cp}^*_2\text{Ta}(=\text{NH})\text{H}$  was found to react with  $\text{D}_2$  to give  $\text{Cp}^*_2\text{Ta}(=\text{ND})\text{H}$ , implying a non-symmetric amide-dihydride intermediate for the addition/elimination process.  $\text{Cp}^*_2\text{Ta}(=\text{S})\text{H}$  and  $\text{H}_2\text{O}$  equilibrate with  $\text{Cp}^*_2\text{Ta}(=\text{O})\text{H}$  and  $\text{H}_2\text{S}$ , which allowed determination of the difference in bond strengths for  $\text{Ta=O}$  and  $\text{Ta=S}$ .  $\text{Ta=O}$  was found to be approximately 41 kcal/mole stronger than  $\text{Ta=S}$ .

## TABLE OF CONTENTS

	<u>page</u>
Acknowledgements	ii
Abstract	iii
Introduction	1
Chapter 1	6
Insertion of CO, Organic Carbonyls, and Inorganic Carbonyls Into $\text{Cp}^*\text{Sc-R}$ Bonds	
References	42
Chapter 2	47
Insertion of $\text{CO}_2$ Into $\text{Cp}^*\text{Sc-R}$ Bonds	
References	63
Chapter 3	65
Reaction of Acetylenes With $\text{Cp}^*\text{ScR}$	
References	90
Chapter 4	94
Synthesis and Reactivity of $\text{Cp}^*\text{Ta}(\eta^2\text{-H}_2\text{C=NR})\text{H}$ and $\text{Cp}^*\text{Ta(=X)H}$	
References	111



## INTRODUCTION

The synthesis, characterization, and reactions of early transition metal complexes constitute a relatively recent development in the area of organometallic chemistry. Advances in air- and water-free techniques, when combined with synthetic strategies such as the use of sterically demanding ligands, have made the left side of the d-block elements an area of active research for many research groups. A few examples of reaction types involving these metals include the thermal activation of alkanes<sup>1</sup>, alkene and alkyne polymerization<sup>2</sup>, ring opening metathesis polymerization<sup>3</sup>, dinitrogen reduction<sup>4</sup>, and carbon monoxide activation<sup>5</sup>. Current interest has turned to oxidation and related processes, which involve metal-oxygen, -nitrogen, and -sulfur bonds.<sup>6</sup> The research described herein involves a number of these areas: activation of CO, CO<sub>2</sub>, and C<sub>2</sub>H<sub>2</sub> by the earliest of the transition metals, scandium, and the reactions of tantalum-oxygen, -nitrogen, and -sulfur bonds with simple substrates such as H<sub>2</sub>O, H<sub>2</sub>S, and NH<sub>3</sub>. With both scandium and tantalum, the research reported was made possible by synthetic pathways developed in these labs to the [Cp<sup>\*</sup><sub>2</sub>M] systems, where Cp<sup>\*</sup> = [η<sup>5</sup>-((CH<sub>3</sub>)<sub>5</sub>C<sub>5</sub>)].<sup>7</sup> The sterically demanding Cp<sup>\*</sup> ligands provide a monomeric, well-defined active site at the metal, thus making these systems attractive as models for mechanistically complicated catalytic systems.

Early transition metals exhibit a number of modes of reactivity toward CO. Perhaps the best known is insertion of CO into the metal carbon bond, with coordination of O to the metal center to give an η<sup>2</sup> acyl complex.<sup>8</sup> This coordination mode activates the CO toward further reaction, as evidenced by observed dimerization and tetramerization of η<sup>2</sup> acyl ligands to form complex enediolate complexes.<sup>6</sup> An alternative strategy to activate CO with early transition metals is to coordinate an oxophilic metal center to the oxygen of a metal carbonyl ligand. Coordination of the metal to the oxygen results in polarization of the CO and weakening of the CO bond, rendering it more susceptible to

nucleophilic attack. Both of these strategies are examined in Chapter 1, in which the reactions of  $[\text{Cp}^*_2\text{Sc}]$  compounds with CO and metal carbonyls are reported.

A related reaction involves the insertion of  $\text{CO}_2$  into metal-carbon bonds. While this reaction has not been studied as extensively as the insertion of CO, use of  $\text{CO}_2$  to synthesize more useful chemicals is attractive due to  $\text{CO}_2$ 's low cost and plentiful supply. As is the case with CO, unusual reactivity is observed with early transition metals, including reduction of  $\text{CO}_2$  to  $-\text{OCH}_3$ .<sup>9</sup> Thus, it was deemed to be of interest to study the reactions of  $[\text{Cp}^*_2\text{Sc}]$  compounds with  $\text{CO}_2$ . These results, along with an x-ray crystal structure of a scandium carboxylate, are found in Chapter 2.

These same  $[\text{Cp}^*_2\text{Sc}]$  compounds have been found to be active as ethylene polymerization catalysts.<sup>10</sup> However, only stoichiometric reaction via  $\sigma$ -bond metathesis is observed for propylene. Propyne reacts rapidly with  $\text{Cp}^*_2\text{Sc-R}$  to give RH and  $\text{Cp}^*_2\text{Sc-C}\equiv\text{C-CH}_3$  followed by insertion into the Sc-C bond to give the enyne product. Subsequent  $\sigma$ -bond metathesis yields the free enyne and  $\text{Cp}^*_2\text{Sc-C}\equiv\text{C-CH}_3$ , completing a catalytic cycle for the production of the enyne. However, reaction of the simplest alkyne,  $\text{C}_2\text{H}_2$ , with  $[\text{Cp}^*_2\text{Sc}]$  compounds had not been investigated. The results of these investigations, including the x-ray crystal structure determination of an unusual  $\text{Cp}^*_2\text{Sc-C}\equiv\text{C-ScCp}^*_2$  dimer, are given in Chapter 3.

A great deal of current work in organometallic chemistry focuses on attempting to elucidate the mechanisms of industrially important processes such as oxidation, hydrodenitrogenation, and hydrodesulfurization.<sup>7</sup> As is often the case, the heterogeneous processes in use are poorly understood mechanistically, making it advantageous to study simpler model systems. A system that has shown itself to be quite versatile in forming such model compounds is  $[\text{Cp}^*_2\text{Ta}]$ . A number of routes have been developed to synthesize  $[\text{Cp}^*_2\text{Ta}]$  compounds with single and double bonds to O, S, and N; some of the reactivity of these compounds has been previously reported.<sup>11</sup> In Chapter 4, the

reactivity of these complexes is further explored, and relative bond strengths of Ta=O, Ta=S, and Ta=NR are discussed.

## REFERENCES

1. a.) For examples, see: Thompson, M.E.; Baxter, S.M.; Bulls, A.R.; Burger, B.J.; Nolan, M.C.; Santarsiero, B.D.; Bercaw, J.E. *J. Am. Chem. Soc.* **1987**, *109*, 203-219.  
b.) Watson, P.L. *J. Am. Chem. Soc.* **1983**, *105*, 6491-6493.
2. For examples, see: a.) Eisch, J.J.; Piotrowski, A.M.; Brownstein, S.K.; Gabe, E.J.; Lee, F.L. *J. Am. Chem. Soc.* **1985**, *107*, 7219-7221. b.) Jordan, R.F.; Bajgur, C.S.; Willet, R.; Scott, B. *J. Am. Chem. Soc.* **1986**, *108*, 7410-7411. c.) Watson, P. *J. Am. Chem. Soc.* **1982**, *104*, 337-339. d.) see reference 3a.
3. For examples, see: a.) Wallace, K.C.; Liu, A.H.; Dewan, J.C.; Schrock, R.R. *J. Am. Chem. Soc.* **1988**, *110*, 4964-4977. b.) Swager, T.M.; Grubbs, R.H. *J. Am. Chem. Soc.* **1987**, *109*, 894-896.
4. For a recent review, see Dillworth, J.R.; Richards, R.L. In *Comprehensive Organometallic Chemistry*; Wilkinson, G.; Stone, F.G.A.; Abel, E.W., Eds.; Pergamon: New York, 1982; Volume 8, Chapter 20.
5. Examples include: a.) Fagan, P.J.; Manriquez, J.M.; Marks, T.J.; Day, V.W.; Vollmer, S.J.; Day, C.S. *J. Am. Chem. Soc.* **1980**, *102*, 7112-7114. b.) Butts, S.B.; Holt, E.M.; Strauss, S.H.; Alcock, N.W.; Stimson, R.E.; Shriver, D.F. *J. Am. Chem. Soc.* **1979**, *101*, 5864-5866. c.) Manriquez, J.M.; McAlister, D.R.; Sanner, R.D.; Bercaw, J.E. *J. Am. Chem. Soc.* **1978**, *100*, 2716-2724.
6. Mayer, J.M.; Nugent, W. "Metal-Ligand Multiple Bonds"; Wiley-Interscience: New York, 1988.
7. a.)  $[\text{Cp}^*_2\text{Sc}]$  - see reference 3a. b.) Gibson, V.C.; Bercaw, J.E.; Bruton, W.J.; Sanner, R.D. *Organometallics* **1986**, *5*, 976-979.

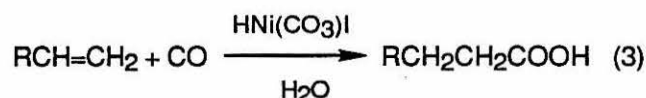
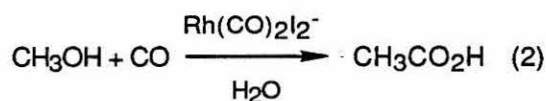
8. For a recent review, see Kuhlmann, E.J.; Alexander, J.J. *Coord. Chem. Rev.* **1980**, *33*, 195-225.
9. a.) Fachinetti, G.; Floriani, C.; Roselli, A.; Pucci, S. *J. Chem. Soc., Chem. Commun.* **1978**, 269-270. b.) Gambarotta, S.; Strologo, S.; Floriani, C.; Chiesi-Villa, A.; Guastini, C. *J. Am. Chem. Soc.* **1985**, *107*, 6278-6282.
10. See reference 6 and Burger, B.J., Ph.D dissertation, California Institute of Technology, Pasadena, California, 1987.
11. a.) van Asselt, A.; Burger, B.J.; Gibson, V.C.; Bercaw, J.E. *J. Am. Chem. Soc.* **1986**, *108*, 5347-5349. b.) Parkin, G.; Bunel, E.; Burger, B.J.; Trimmer, M.S.; van Asselt, A.; Bercaw, J.E. *J. Mol. Catal.* **1987**, *41*, 21-39. c.) Parkin, G.; Bercaw, J.E. *Polyhedron* **1988**, *7*, 2053-2082.

## **Chapter 1**

### **Insertion of CO, Organic Carbonyls, and Inorganic Carbonyls Into $\text{Cp}^*_2\text{Sc-R}$ Bonds\***

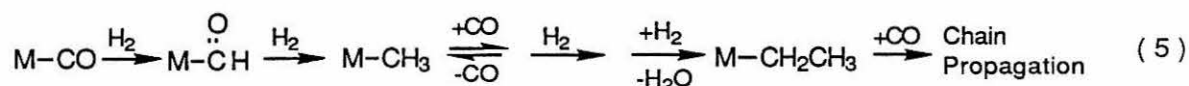
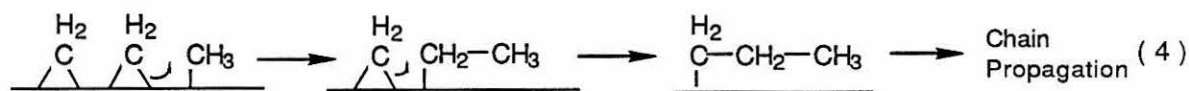
## INTRODUCTION

The insertion of carbon monoxide into metal carbon bonds is one of the most extensively studied processes in organometallic chemistry. As a C-C bond forming reaction, it represents a pathway to functionalize simpler hydrocarbons and convert them into more valuable organic chemicals. Industrially important examples include the hydroformylation, or "oxo", reaction (eq. 1), in which olefins are converted to aldehydes or alcohols; the Monsanto acetic acid synthesis (eq. 2), in which methanol



is converted into acetic acid; and the Reppe synthesis, which yields acids or esters from olefins.<sup>1</sup>

Of related interest is the Fischer-Tropsch process, by which  $\text{H}_2$  and  $\text{CO}$  are combined to yield a variety of hydrocarbons, olefins, alcohols, aldehydes, and ketones. Several mechanisms have been proposed to account for the observed product distribution and rates. Of these, two are currently favored. The carbide/methylene mechanism (4), originally proposed by Fischer and Tropsch, postulates the dissociative chemisorption of



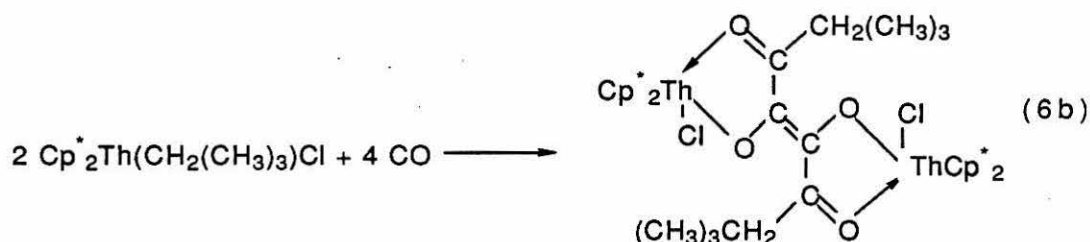
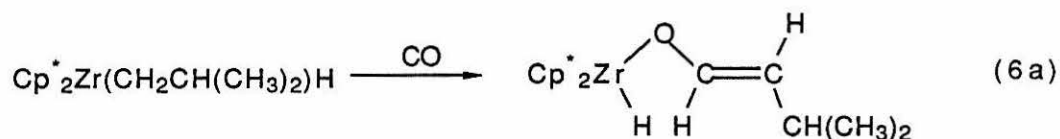
CO on the surface of the catalyst to generate carbides. These species can then react with hydrogen to form methylene units, which polymerize to form longer chain alkanes. Alternatively (5), initiation could occur via insertion of CO into a surface M-H to give a formyl. This species is then reduced to give a surface methyl, which would then insert CO, thus lengthening the chain. The actual mechanism is likely to combine several of these steps, or both mechanisms may be operating in parallel.<sup>2</sup>

A great deal of effort has gone into attempts to understand the mechanisms of these reactions. Under actual operating conditions, however, the systems are difficult to study. As a result, model systems of more easily investigated complexes involving every transition metal, as well as some  $d^0$  and  $d^{10}$  complexes, have been examined and observed to undergo CO insertion.<sup>3</sup> In most cases, the reaction proceeds via migration of the alkyl to the C of the CO ligand, rather than "insertion" of the CO into the M-C bond. In recent years, a great deal of attention has been focused on the reaction of CO with metal carbon bonds of early transition metals, lanthanides, and actinides. In these cases, the acyl ligand coordinates to the oxophilic metal center in an  $\eta^2$  fashion. This reaction has been studied in considerable detail, both experimentally and theoretically. In reactions with the well-studied bis-Cp "bent sandwich" compounds, CO is believed to attack laterally, bonding to the empty  $1a_1$  orbital of the metal center. Overlap between the alkyl  $\sigma$  donor orbital and the CO  $\pi^*$  orbital then facilitates migration of the alkyl to the carbonyl.<sup>4</sup> In  $Cp_2ML_2$  systems, extended Hückel calculations find an  $\eta^1$  acyl intermediate as the acyl ligand pivots from the initial  $\eta^2$  O-out isomer to the final  $\eta^2$  O-in isomer.<sup>5</sup> However, an *ab initio* GVB calculation on the insertion of CO into the Sc-H bond of  $Cl_2ScH$  found no stable  $\eta^1$  intermediate on the reaction coordinate.<sup>6</sup> The HOMO of the  $\eta^2$  acyl product appears to result from interaction of the acyl lone pair combination and empty  $d\sigma$  orbitals at the metal center, while the LUMO is an acyl C-O  $\pi^*$  orbital, which is primarily carbon p in character. Both calculations agree that the carbon atom



of the acyl ligand should be very electrophilic, which accounts for a great deal of the chemistry observed for this ligand experimentally.

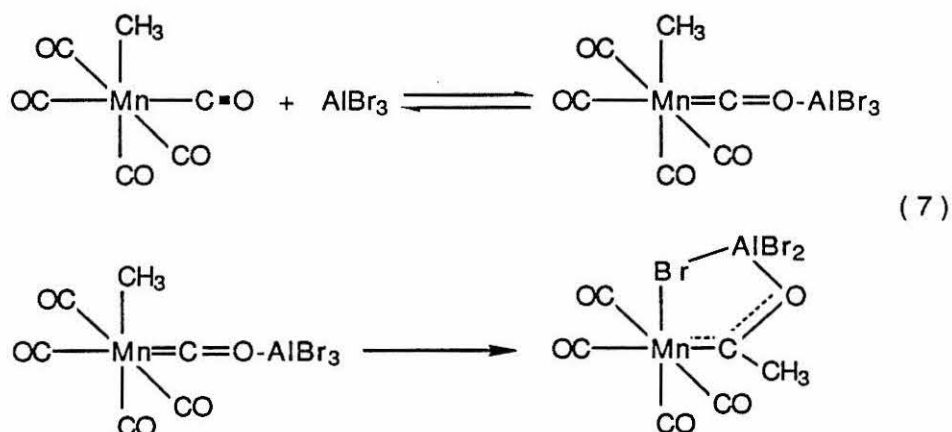
Examples of the reactive character of this acyl carbon include rearrangement of the insertion product of CO with  $\text{Cp}^*_2\text{Zr}(\text{CH}_2\text{CHMe}_2)\text{H}$  at low temperatures to give *trans*- $\text{Cp}^*_2\text{Zr}(\text{H})(\text{OCH}=\text{CHCHMe}_2)$  via insertion of the oxy-carbene fragment into the Zr-H bond and  $\beta$ -H elimination of the resulting isovaleraldehyde adduct (6a).<sup>7</sup> Another illustration is the tetramerization observed by Marks upon reacting  $\text{Cp}^*_2\text{Th}(\text{CH}_2(\text{CH}_3)_3)\text{Cl}$  with excess CO (6b).<sup>8</sup> These types of rearrangements



and couplings are unprecedented in middle and late transition metal acyls, indicating that the  $\eta^2$  acyl believed to be initially formed in each of these reactions may be the key to subsequent reactivity.

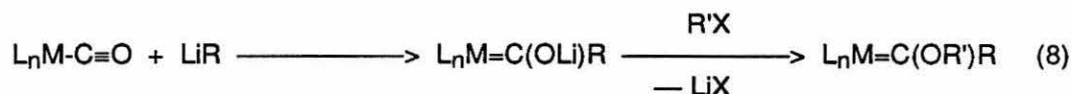
Given the variety of products observed for the reaction of CO with early transition metal and actinide organometallic compounds, it was of considerable interest to investigate the reactions of  $\text{Cp}^*_2\text{Sc-R}$  with CO. Sc(III)'s size and oxophilicity are intermediate between the transition metals and the f-block elements<sup>9</sup>, and, as a coordinatively unsaturated 14 electron complex,  $\text{Cp}^*_2\text{Sc-R}$  should be extremely reactive toward CO.

An alternative strategy for the activation of CO involves the use of two metals. This tactic has been explored in considerable detail by Shriver using  $\text{RMn}(\text{CO})_5$  and  $\text{AlR}'_3$ .<sup>10</sup> As shown below (7), O-coordination of Al to the Mn-CO accelerates the process of migration by the migrating group by a factor of at least  $10^3$ . Acceleration is also



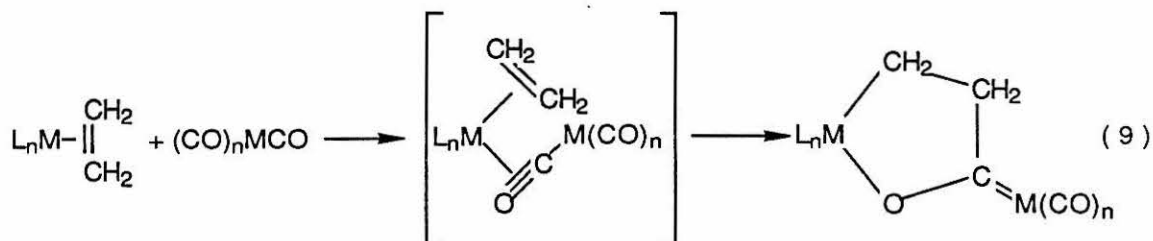
observed in systems where cations can ion-pair with the carbonyl oxygen.<sup>11</sup> This reactivity is explained by reduction of the bond order of the CO moiety, and by polarization of the CO, which makes the CO more susceptible to nucleophilic attack (in this case, migration of R). This mechanistic pathway is well known in organic chemistry, where addition of  $\text{M-X}$  ( $\text{X} = \text{H}, \text{R}; \text{M} = \text{B}, \text{Al}$ ) to  $\text{C}=\text{O}$  is a well developed synthetic tool.<sup>12</sup> However, similar reactivity is seldom seen for reactions of main group Lewis acids with metal carbonyls.<sup>13</sup> The presence of the metal center presumably makes the CO ligand more difficult to polarize by delocalizing its electron density out onto the carbonyl. Thus it takes a potent Lewis acid with highly nucleophilic substituents, or a more basic carbonyl group, to add  $\text{M-R}$  across the carbonyl bond of  $\text{M-CO}$ . The best known example is the reaction of  $\text{AlH}_3$  and  $\text{BH}_3$  with metal carbonyls to produce hydrocarbons; initial coordination of the metal center to the carbonyl O is followed by nucleophilic attack of the  $\text{H}^-$  on the CO carbon.<sup>14</sup>

As the Lewis structure shown for the Al adduct in Figure 7 suggests, these Lewis acid complexes of M-CO could be expected to have substantial metal carbon multiple bond character. This points to a possible application for this type of CO activation. Despite the extensive chemistry which has been developed for "Fischer carbene" complexes, the original synthesis, with slight variations, has remained the principal route into this important class of compounds (8).<sup>15</sup>



While this method has been used to prepare a wide range of derivatives, it does not appear to be general; for example, very few carbene complexes of cobalt have been synthesized by this route.<sup>14b</sup>

Several reports of novel routes into this class of compounds have recently appeared. Lappert and others have utilized electron-rich olefins to synthesize bis-amine substituted carbenes.<sup>16</sup> Erker<sup>17</sup> has utilized olefin complexes of the Group 4 transition metals to effect the synthesis of metallacyclic carbenes from metal carbonyls, including those of cobalt, likely via a concerted electrocyclic ring closure (9). Recently Mashima<sup>18</sup> has used this strategy to prepare exocyclic titanoxycarbenes of Cr, Mo, W and Re.



Some of the recently developed synthetic routes into carbenes take advantage of the above-noted metal-carbon multiple bond character induced by coordination of an

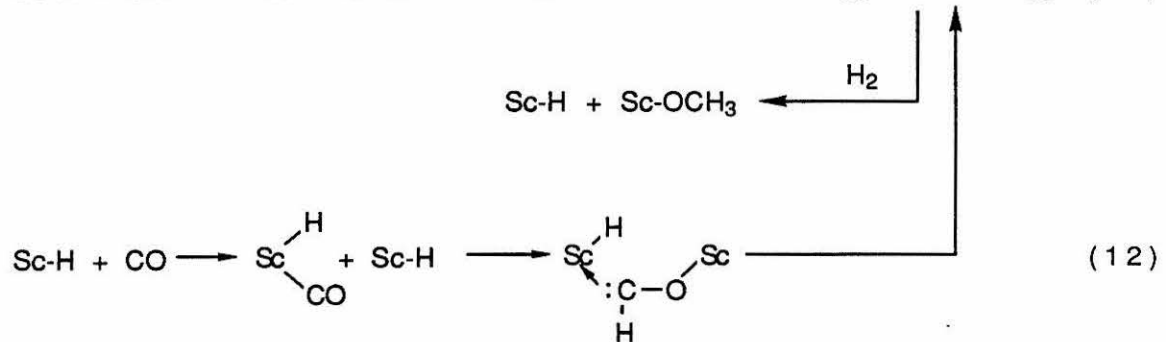
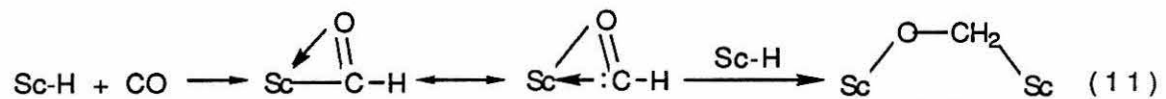
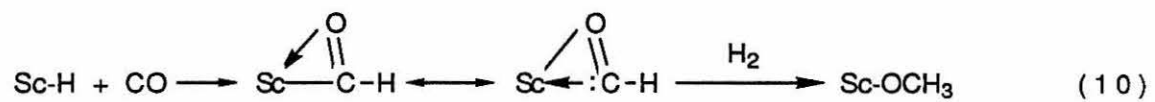
electrophilic center to the carbonyl oxygen. Reactions of metal carbonyls with titanium or aluminum amides to yield  $\text{NMe}_2$ -substituted "titanoxy" or "alumoxy" carbenes have been reported by Petz<sup>19</sup>. Earlier work from these laboratories demonstrated that  $\text{Cp}^*_2\text{ZrH}_2$  and  $\text{Cp}^*_2\text{ZrHX}$  are effective reagents for converting metal carbonyls to hydrogen-substituted "zirconoxycarbenes",  $\text{L}_n\text{M}=\text{C}(\text{H})\text{OZrXCp}^*_2$  ( $\text{X} = \text{H}$ , halide).<sup>20</sup>

All of these methods lack generality and are apparently specific in affording exocyclic,  $-\text{NR}_2$  or  $-\text{H}$  substituted carbenes. Thus it was of interest to study the reactions of these strongly Lewis acidic  $\text{Cp}^*_2\text{Sc-R}$  complexes with metal carbonyls in order to determine whether the enhanced Lewis acidity of these compounds might result in a more general entrance into oxycarbene compounds.

## RESULTS AND DISCUSSION

### CO Insertion

$\text{Cp}^*_2\text{Sc-H}$  (prepared in situ by the reaction of  $\text{Cp}^*_2\text{ScMe}$  with  $\text{H}_2$ ) reacts at  $-78^\circ\text{C}$  with one equivalent of CO and excess  $\text{H}_2$  to give  $\text{Cp}^*_2\text{ScOMe}$ . ( $\text{Cp}^*_2\text{ScOMe}$  can be independently synthesized by the reaction of  $\text{Cp}^*_2\text{ScMe}$  with  $\text{MeOH}$ .<sup>21</sup>) Several mechanistic pathways are conceivable for this reaction and are shown below: insertion of CO into the Sc-H bond to give a formyl, which then reacts with  $\text{H}_2$  to give the observed methoxy ligand (10); intermolecular attack by a ScH on the Sc-formyl to give a bridged species, which could then react with  $\text{H}_2$  to give the observed methoxide and Sc-H (11); or formation of a Sc-CO species, which could then be reduced intermolecularly by Sc-H (12). Each of these mechanisms has some type of precedent among CO insertions of the early transition metals and f-block elements. Insertion of CO into an M-H bond has been shown to occur in the  $\text{Cp}^*_2\text{Th}(\text{OR})\text{H}$  system to give the formyl. Marks also reports hydrogenation of the acyl to the alkoxide in the presence of a catalytic amount of  $(\text{Cp}^*_2\text{ThH}_2)_2$ .<sup>22</sup> The stoichiometric reduction of an acyl by a metal hydride has been reported by a number of workers.  $\text{Cp}_2\text{Zr}(\text{COCH}_3)\text{CH}_3$ , for example, reacts with  $\text{Cp}_2\text{ReH}$



**Scheme 1.** Possible mechanisms for the conversion of  $\text{Sc-H} + \text{CO} + \text{H}_2$  to  $\text{Sc-OCH}_3$ .

to give  $\text{CpRe}(\text{CHCH}_3)\text{OZr}(\text{CH}_3)\text{Cp}_2$ .<sup>23</sup> The reaction of  $\text{H}_2$  with Sc-C bonds, in the final step, is well established.<sup>24</sup> The reduction of metal carbonyls by metal hydrides, followed by migratory insertion of the oxycarbene into the metal-H bond has been suggested as a possible general mechanism for CO hydrogenation to oxygenates.<sup>25</sup> While no Sc-CO compound has been detected,  $d^0$  metal carbonyls have been characterized.<sup>26</sup> Further reduction to the alkoxide is in line with that observed in the reaction of  $\text{Cp}^*_2\text{ZrH}_2$  with  $\text{Cp}^*_2\text{Zr}(\text{CO})_2$ .<sup>27</sup>

Several lines of evidence point to (10) as a reasonable mechanism, though the others cannot be ruled out. Reaction of  $\text{Cp}^*_2\text{ScC}_6\text{H}_4\text{CH}_3\text{-}p$  with one equivalent of CO at  $-78^\circ\text{C}$  gives, in good yield, the  $\eta^2$  acyl  $\text{Cp}^*_2\text{Sc}(\text{CO})\text{C}_6\text{H}_4\text{CH}_3\text{-}p$ . Upon treatment with 4 atm of  $\text{H}_2$ , this compound is cleanly converted to  $\text{Cp}^*_2\text{ScOCH}_2\text{C}_6\text{H}_4\text{CH}_3\text{-}p$  (identified by  $^1\text{H}$  NMR by comparison to a sample of  $\text{Cp}^*_2\text{ScOCH}_2\text{C}_6\text{H}_5$  prepared by the reaction of benzyl alcohol with  $\text{Cp}^*_2\text{ScMe}$ ). No  $\text{Cp}^*_2\text{ScH}$  is observed in solution, indicating that, if present, its concentration is less than 5%. This does not mean that a small amount of  $\text{Cp}^*_2\text{ScH}$  is not catalyzing the reaction. However,  $\text{Cp}^*_2\text{Sc}(\text{CO})\text{C}_6\text{H}_4\text{CH}_3\text{-}p$  is unreactive with  $\text{Cp}^*_2\text{ScH}(\text{THF})$ ,  $\text{Cp}_2\text{WH}_2$ ,  $\text{LiAlH}_4$ , and  $\text{NaBH}_4$ .

Characterization of  $\text{Cp}^*_2\text{Sc}(\text{CO})\text{C}_6\text{H}_4\text{CH}_3\text{-}p$  indicates that it is structurally similar to other early transition metal and actinide acyls that have been isolated. Of particular importance are the  $\nu(\text{CO})$  of  $1450\text{ cm}^{-1}$  (which shifts to  $1418\text{ cm}^{-1}$  on labeling with  $^{13}\text{CO}$ ) and the  $^{13}\text{C}$  NMR resonance of  $324.7\text{ ppm}$ . These are comparable to other  $\eta^2$  acyls, as shown in Table 1.

Attempts to directly synthesize the formyl  $\text{Cp}^*_2\text{ScCHO}$  were unsuccessful. Reactions of CO with either  $\text{Cp}^*_2\text{ScH}$  or  $\text{Cp}^*_2\text{ScH}(\text{THF})$  yielded only decomposition products. Efforts to observe the methyl acyl were fruitless as well. Low temperature NMR studies were inconclusive, and attempts at synthesis yielded only decomposition products. Intriguingly, treatment of a THF solution of  $\text{Cp}^*_2\text{ScCH}_3$  with one equivalent of CO at  $-78^\circ\text{C}$  results in an intense dark blue color, which persists on warming to room

**Table 1.** Spectroscopic Data on  $\eta^2$  Acyl Compounds

<u>Compound</u>	<u><math>\nu(\text{CO})</math> (<math>\text{cm}^{-1}</math>)</u>	<u><math>\delta_{\text{acyl}}</math></u>	<u>Ref.</u>
$\text{Cp}^*_2\text{Sc}(\text{CO})\text{C}_6\text{H}_4\text{CH}_3\text{-}p$	1450	324.7	this work
$\text{Cp}^*_2\text{Th}(\text{Cl})\text{COCH}_2\text{CCH}_3$	1469	360.2	8
$\text{Cp}_2\text{LuCOC}(\text{CH}_3)_3$	1490	380.6	28
$\text{Cp}^*_2\text{Zr}(\text{CH}_3)\text{COCH}_3$	1537	-	29
$\text{Cp}^*_2\text{Ti}(\text{Cl})\text{COCH}_3$	1620	-	30
$\text{Cp}^*_2\text{TiCO}(\text{CH}_3)\text{C}=\text{CH}(\text{CH}_3)$	1482	-	31

temperature and removal of volatiles.  $^1\text{H}$  NMR, however, again shows a mixture of products. Signals indicative of olefinic Hs were observed irreproducibly, indicating the possibility of  $\text{Cp}^*_2\text{ScOCH}=\text{CH}_2$  as an intermediate which then decomposes to unknown products. Similar rearrangements have been reported in Zr and Th systems where the alkyl is larger, and is attributed to H migration to the "carbene-like" carbon of the  $\eta^2$  acyl. Attempts were made to capture this "carbene-like" reactivity intramolecularly by synthesizing  $\text{Cp}^*_2\text{ScCH}_2\text{Si}(\text{CH}_3)_3$  and reacting it with CO. In  $\text{Cp}^*_2\text{ThCl}(\text{CH}_2\text{Si}(\text{CH}_3)_3)$ , insertion of CO is followed by migration of the silyl group to the acyl carbon.<sup>32</sup> In this case,  $^1\text{H}$  NMR again showed only decomposition products. Thus, the only stable acyl product observed was from insertion into a Sc-phenyl bond, where (presumably) decomposition pathways are limited. Interestingly, this type of reactivity is quite similar to that observed by Teuben *et al.* for the  $\text{Cp}^*_2\text{TiR}$  system. Only the product of CO insertion into the Ti-alkenyl bond was isolated; other Rs, such as alkyl and aryl derivatives, proceeded "beyond the  $\eta^2$  stage, with formation of products difficult to identify."<sup>31</sup>

### Insertion of organic carbonyls into Sc-R bonds

$\text{Cp}^*_2\text{ScCH}_3$  reacts readily with organic carbonyls to form products analogous to those found in the reaction of alkyl aluminum reagents with carbonyls.<sup>12</sup> For example, the addition of formaldehyde to a solution of  $\text{Cp}^*_2\text{ScCH}_3$  gives  $\text{Cp}^*_2\text{ScOCH}_2\text{CH}_3$ , presumably via insertion of the  $\text{CH}_2\text{O}$  unit into the Sc-CH<sub>3</sub> bond. The reaction is apparently quite sensitive to impurities in the organic carbonyl, as decomposition is observed if reagents are not rigorously purified. Decomposition is also observed with most of the aldehydes tried (with the exception of benzaldehyde) and with acetone. As the reaction is not likely to be of significant synthetic usefulness, and appears to go via the same mechanism as  $\text{Al}(\text{CH}_3)_3$  addition, it was not pursued.

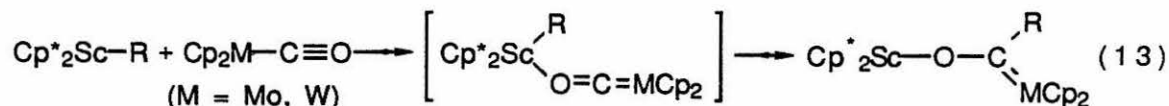
Insertion of a  $\overline{\text{CH}_2\text{CH}_2\text{O}}$  unit into an Sc-C bond is observed when ethylene oxide is reacted with  $\text{Cp}^*_2\text{ScCH}_3$ . Initial adduct formation to give  $\text{Cp}^*_2\text{ScCH}_3(\overline{\text{OCH}_2\text{CH}_2})$  is followed by formation of  $\text{Cp}^*_2\text{ScOCH}_2\text{CH}_2\text{CH}_3$  at room temperature over a period of 48 hours. Analogous chemistry has been observed for the  $\text{Cp}^*_2\text{ScH}(\text{THF})$  adduct.<sup>21</sup>

### Insertion of M-CO into Sc-R bonds

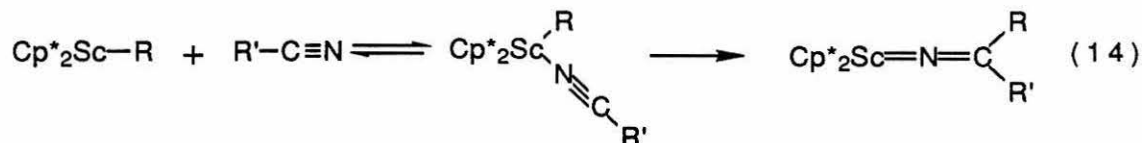
Reactivity of  $\text{Cp}^*_2\text{ScR}$  with  $\text{Cp}_2\text{MCO}$  (R = H, CH<sub>3</sub>, C<sub>6</sub>H<sub>5</sub>, CH<sub>2</sub>CH<sub>2</sub>C<sub>6</sub>H<sub>5</sub>, N(CH<sub>3</sub>)<sub>2</sub>; M = Mo, W).

Both  $\text{Cp}^*_2\text{ScH}(\text{THF})$  and  $\text{Cp}^*_2\text{ScCH}_3$  react with  $\text{Cp}_2\text{MCO}$  at 25°C to give  $\text{Cp}_2\text{M}=\text{C}(\text{R})\text{OScCp}^*_2$  in 50-60% yield. No intermediates are observed by NMR during the course of the reaction. On the other hand, when  $\text{Cp}_2\text{WCO}$  is treated with  $\text{Cp}^*_2\text{ScCl}$ , an adduct is formed with  $\nu(\text{CO}) = 1835 \text{ cm}^{-1}$ , 70  $\text{cm}^{-1}$  lower than  $\nu(\text{CO})$  of  $\text{Cp}_2\text{WCO}$ , indicative of a Lewis acid-base interaction between the highly electrophilic scandium center and the carbonyl oxygen, analogous to the interaction between  $\text{AlCl}_3$  and metal carbonyls.<sup>10</sup> Presumably, the reaction of the hydride and methyl compounds also proceed by initial adduct formation with polarization of the CO bond, followed by intramolecular nucleophilic attack by the scandium substituent (13).



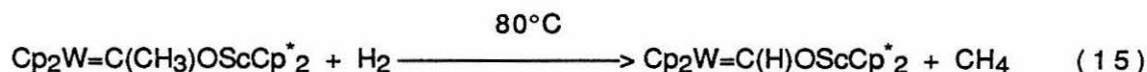


This sequence resembles the reaction of  $\text{Cp}^*_2\text{ScR}$  with cyanides, for which initial N-coordination of the nitrile is followed by a 1,3 alkyl shift to give azomethine complexes (14)<sup>33</sup>.

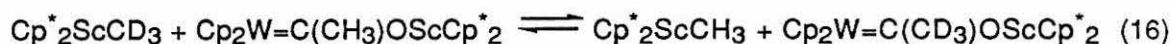


The  $^1\text{H}$  NMR spectra and color of these scandoxycarbenes  $\text{Cp}_2\text{M}=\text{C}(\text{CH}_3)\text{OScCp}^*_2$  (M = Mo, W) are very similar to those for the zirconoxycarbenes of molybdenocene and tungstenocene,  $\text{Cp}_2\text{M}=\text{C}(\text{H})\text{OZr}(\text{X})\text{Cp}^*_2$  (M = Mo, W), reported earlier.<sup>20</sup> Particularly characteristic is the inequivalence of the ( $\eta^5\text{-C}_5\text{H}_5$ ) ligands, indicating that the carbene substituents,  $[\text{OScCp}^*_2]$  and  $[\text{CH}_3]$  or  $[\text{H}]$ , point toward the cyclopentadienyl rings of the bent metallocene.  $\pi$ -bonding between the carbene carbon and the transition metal dictates this sterically least favorable orientation. Steric interactions with the cyclopentadienyl ligands apparently limit the size of groups that may be added to the  $\text{Cp}_2\text{MCO}$  system. Thus,  $\text{Cp}^*_2\text{ScCH}_2\text{CH}_2\text{C}_6\text{H}_5$ ,  $\text{Cp}^*_2\text{ScN}(\text{CH}_3)_2$ , and  $\text{Cp}^*_2\text{ScC}_6\text{H}_5$  show no reactivity toward  $\text{Cp}_2\text{MCO}$  (M = Mo, W) even at elevated temperatures. Both  $\text{Cp}^*_2\text{Zr}(\text{CH}_3)_2$  and  $\text{Cp}_2\text{Zr}(\text{CH}_3)_2$  fail to react with  $\text{Cp}_2\text{MCO}$  at  $80^\circ\text{C}$ . In the latter case it is not clear whether steric effects or the large Zr-CH<sub>3</sub> bond dissociation energy predominate.<sup>34</sup>

The scandoxycarbene complexes, when heated in benzene for days at  $80^\circ\text{C}$ , slowly decompose to unidentified products. However, when heated to  $80^\circ\text{C}$  under  $\text{H}_2$ ,  $\text{Cp}_2\text{W}=\text{C}(\text{CH}_3)\text{OScCp}^*_2$  is cleanly converted to  $\text{Cp}_2\text{W}=\text{C}(\text{H})\text{OScCp}^*_2$  and  $\text{CH}_4$  (15).



The possibility that reaction (15) is reversible was therefore addressed by examining the reactivity of  $\text{Cp}_2\text{W}=\text{C}(\text{CH}_3)\text{OScCp}^*_2$  with  $\text{Cp}^*_2\text{ScCD}_3$ . Only  $\text{Cp}^*_2\text{ScCD}_3$  is observed in the  $^2\text{H}$  NMR ( $\delta = 0.15$ ) spectrum of this mixture at room temperature; however, after several minutes at  $80^\circ\text{C}$  a peak at  $\delta = 2.08$  corresponding to  $\text{Cp}_2\text{W}=\text{C}(\text{CD}_3)\text{OScCp}^*_2$  appears, indicative of a dynamic equilibrium between  $\text{Cp}_2\text{WCO}$ ,  $\text{Cp}^*_2\text{ScCH}_3$  and  $\text{Cp}_2\text{W}=\text{C}(\text{CH}_3)\text{OScCp}^*_2$ .



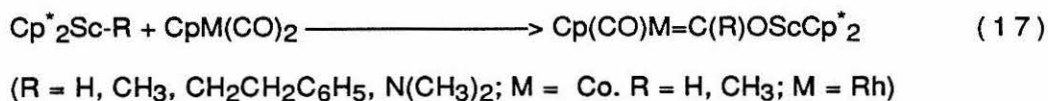
Considering equilibrium (16) and the very high reactivity of  $\text{Cp}^*_2\text{ScCH}_3$  with dihydrogen<sup>24</sup>, the mechanism of conversion of  $\text{Cp}_2\text{W}=\text{C}(\text{CH}_3)\text{OScCp}^*_2$  and dihydrogen to  $\text{Cp}_2\text{W}=\text{C}(\text{H})\text{OScCp}^*_2$  and methane is readily apparent: the  $\text{Cp}^*_2\text{ScCH}_3$  from equilibrium (16) is converted to  $\text{CH}_4$  and  $\text{Cp}^*_2\text{ScH}$ , which subsequently reacts rapidly with  $\text{Cp}_2\text{WCO}$  to form  $\text{Cp}_2\text{W}=\text{C}(\text{H})\text{OScCp}^*_2$ .

Attempts to replace the scandoxycarbene ligand with other functional groups were unsuccessful. No reaction is observed between  $\text{Cp}_2\text{M}=\text{C}(\text{R})\text{OScCp}^*_2$  and  $\text{HN}(\text{CH}_3)_2$ , despite the fact that this is a common route to convert Fischer-type carbenes to analogous substituted amine derivatives.<sup>35</sup> Treatment with methanol leads instead to cleavage of an  $\text{Sc}-(\eta^5\text{-C}_5\text{Me}_5)$  bond and subsequent decomposition. Efforts to make the reaction catalytic in Sc by exchanging the oxycarbene with a  $\text{CH}_3$  group on  $\text{Al}(\text{CH}_3)_3$  were also not productive.

Reactivity of  $\text{Cp}^*_2\text{ScR}$  ( $\text{R} = \text{H}, \text{CH}_3, \text{CH}_2\text{CH}_2\text{C}_6\text{H}_5, \text{CH}(\text{SiCH}_3)_2, \text{C}_6\text{H}_5, \text{C}\equiv\text{C}(\text{CH}_3), \text{N}(\text{CH}_3)_2$ ) with  $\text{CpM}(\text{CO})_2$  ( $\text{M} = \text{Co}, \text{Rh}$ ).

Earlier work by Barger<sup>36</sup> has shown that when  $\text{CpM}(\text{CO})_2$  ( $\text{M} = \text{Co}, \text{Rh}$ ) is treated with  $\text{Cp}^*_2\text{ZrHX}$  ( $\text{X} = \text{H}, \text{Cl}, \text{F}$ ), two possible pathways may be followed, depending upon the nature of X. When  $\text{X} = \text{H}$ , elimination of  $\text{H}_2$  occurs, and a metal-metal bonded species with a bridging and semi-bridging carbonyl is formed. A possible intermediate is observed in this reaction ( $\text{M} = \text{Rh}$ ), which is believed to be a zirconoxycarbene. When  $\text{X} = \text{Cl}$  or  $\text{F}$ , the products are the chloro- or fluoro-substituted zirconoxycarbenes.

Because reductive elimination of  $\text{RH}$  ( $\text{R} = \text{H}$ , alkyl, etc.) is unavailable in the  $\text{Cp}^*_2\text{ScR}$  system, the reactivity observed is similar to that seen for  $\text{Cp}^*_2\text{ZrHX}$  ( $\text{X} = \text{Cl}$  or  $\text{F}$ ). Moreover, several  $\text{Cp}^*_2\text{ScR}$  complexes ( $\text{R} = \text{H}, \text{CH}_3, \text{CH}_2\text{CH}_2\text{C}_6\text{H}_5, \text{N}(\text{CH}_3)_2$ ), react quickly and cleanly with  $\text{CpM}(\text{CO})_2$  to give the R-substituted scandoxycarbene products in good yield (50-70%).



These sterically much-less-encumbered monocyclopentadienyl systems do not constrain as severely the type of R group that may be added. Once again, however, neither  $\text{Cp}^*_2\text{Zr}(\text{CH}_3)_2$  nor  $\text{Cp}_2\text{Zr}(\text{CH}_3)_2$  react, suggesting that the higher Lewis acidity of the  $\text{Cp}^*_2\text{ScR}$  derivatives is the main factor responsible for the facility of the addition of Sc-C bonds to coordinated carbon monoxide.

Interestingly, even when  $\beta\text{-H}$  elimination is available, as in the phenethylscandium derivative, simple addition of the intact  $[\text{CH}_2\text{CH}_2\text{C}_6\text{H}_5]$  substituent to a carbonyl of  $\text{CpCo}(\text{CO})_2$  occurs. By contrast, addition of 2-butyne to a variety of alkyl complexes of the type  $\text{Cp}^*_2\text{ScCH}_2\text{CH}_2\text{R}$  (including  $\text{Cp}^*_2\text{ScCH}_2\text{CH}_2\text{C}_6\text{H}_5$ )

invariably results in  $\beta$ -H elimination of  $\text{CH}_2=\text{CHR}$  and subsequent formation of  $\text{Cp}^*_2\text{ScC}(\text{CH}_3)=\text{C}(\text{CH}_3)\text{H}$ .<sup>37</sup>

Two resonances are observed in the  $^1\text{H}$  and  $^{13}\text{C}$  NMR spectra of  $\text{Cp}^*_2\text{ScO}(\text{N}(\text{CH}_3)_2)\text{CCo}(\text{CO})\text{Cp}$  for the  $\text{N}(\text{CH}_3)_2$  group, indicating restricted rotation about the C-N bond. The inequivalence of the methyl groups at  $25^\circ\text{C}$  implies some double bond character, and has been observed for other amine substituted carbenes.<sup>38</sup>

With bulkier alkyl substituents such as  $\text{CH}[\text{Si}(\text{CH}_3)_3]_2$ , no reaction of  $\text{Cp}^*_2\text{ScR}$  with  $\text{CpM}(\text{CO})_2$  ( $\text{M} = \text{Co}, \text{Rh}$ ) occurs, even at  $80^\circ\text{C}$ . No reaction is observed with  $\text{Cp}^*_2\text{ScC}_6\text{H}_5$  or  $\text{Cp}^*_2\text{ScC}\equiv\text{CCH}_3$ ; however, in these cases, the strong Sc-C bonds are probably the cause of their lower reactivities.<sup>36</sup>

While the spectroscopic features of the scandoxycarbene ligands of cobalt and rhodium complexes are consistent with their formulation, a low frequency CO stretch at approximately  $1800\text{ cm}^{-1}$  is apparent in their infrared spectra, suggesting some type of interaction of the remaining carbonyl with the coordinatively unsaturated Sc center. Moreover,  $^{13}\text{C}$  NMR spectra for  $\text{Cp}(\text{CO})\text{Rh}=\text{C}(\text{CH}_3)\text{OScCp}^*_2$  exhibit two downfield resonances with rather different Rh- $^{13}\text{C}$  coupling constants ( $\delta = 206.7$ ,  $J_{\text{Rh-C}} = 114\text{ Hz}$  and  $\delta 279.1$ ,  $J_{\text{Rh-C}} = 56\text{ Hz}$ ; cf.  $\text{Cp}(\text{CO})\text{RhCN}(\text{CH}_3)\text{CH}_2\text{CH}_2\text{NCH}_3$ ,  $\delta 196.84$ ,  $J_{\text{Rh-C}} = 92.9\text{ Hz}$  and  $\delta = 207.72$ ,  $J_{\text{Rh-C}} = 62.9\text{ Hz}$ <sup>16</sup>).

In order to clarify the nature of this interaction, a single crystal x-ray diffraction study of  $\text{CpCo}(\mu^2-\eta^1, \eta^1-\text{CO})(=\text{C}(\text{CH}_3)\text{OScCp}^*_2)$  was carried out. The molecular structure is shown in Figure 1, and a skeletal view is shown in Figure 2. As is readily apparent, the low  $\nu(\text{CO})$  and the additional downfield  $^{13}\text{C}$  NMR shift are attributable to the  $\mu^2-\eta^1, \eta^1$  carbonyl. Whereas O2 is obviously bonded to the Sc ( $d(\text{Sc-O2}) = 2.331(2)\text{\AA}$ ), C2 is beyond a reasonable bonding distance ( $d(\text{Sc-C2}) = 2.979(4)\text{\AA}$ ). By contrast, the  $\mu^2-\eta^1, \eta^2$  carbonyl for  $(\eta^5-\text{C}_5\text{H}_5)\text{Co}(\mu-\text{CO})(\mu^2-\eta^1, \eta^2-\text{CO})\text{Zr}(\eta^5-\text{C}_5(\text{CH}_3)_5)_2$  shows a Zr-O distance of  $2.431(5)\text{\AA}$  and Zr-C of

**Figure 1.** An ORTEP drawing of  $\text{Cp}^*_2\text{ScOC}(\text{CH}_3)\text{Co}(\text{CO})\text{Cp}$ . Thermal ellipsoids are drawn at the 20% probability level.

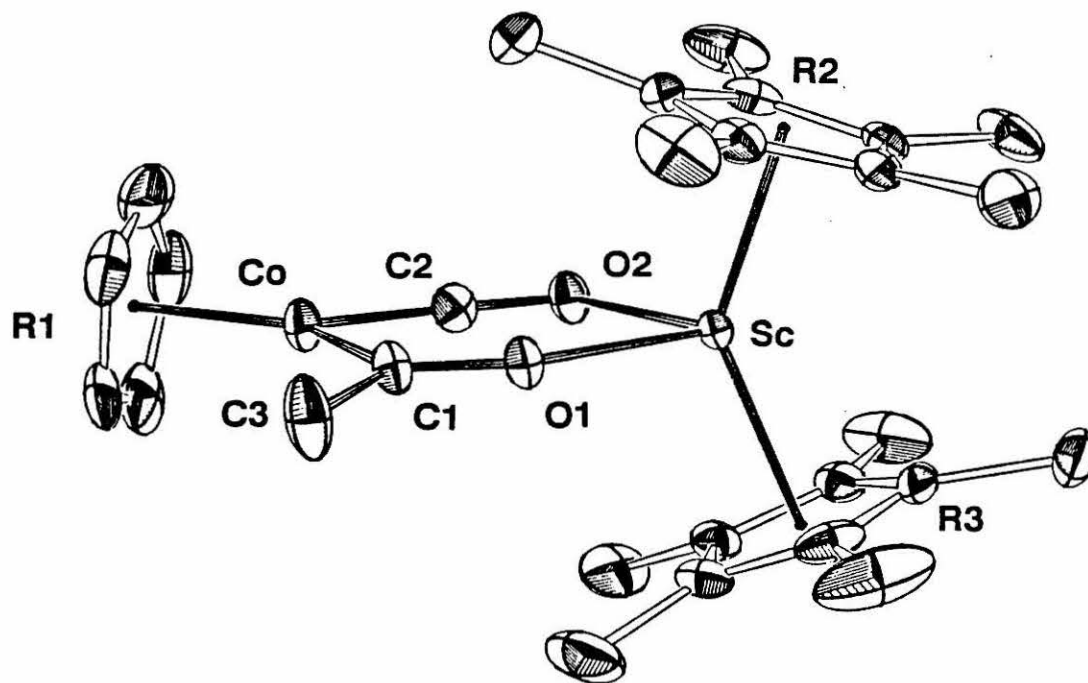
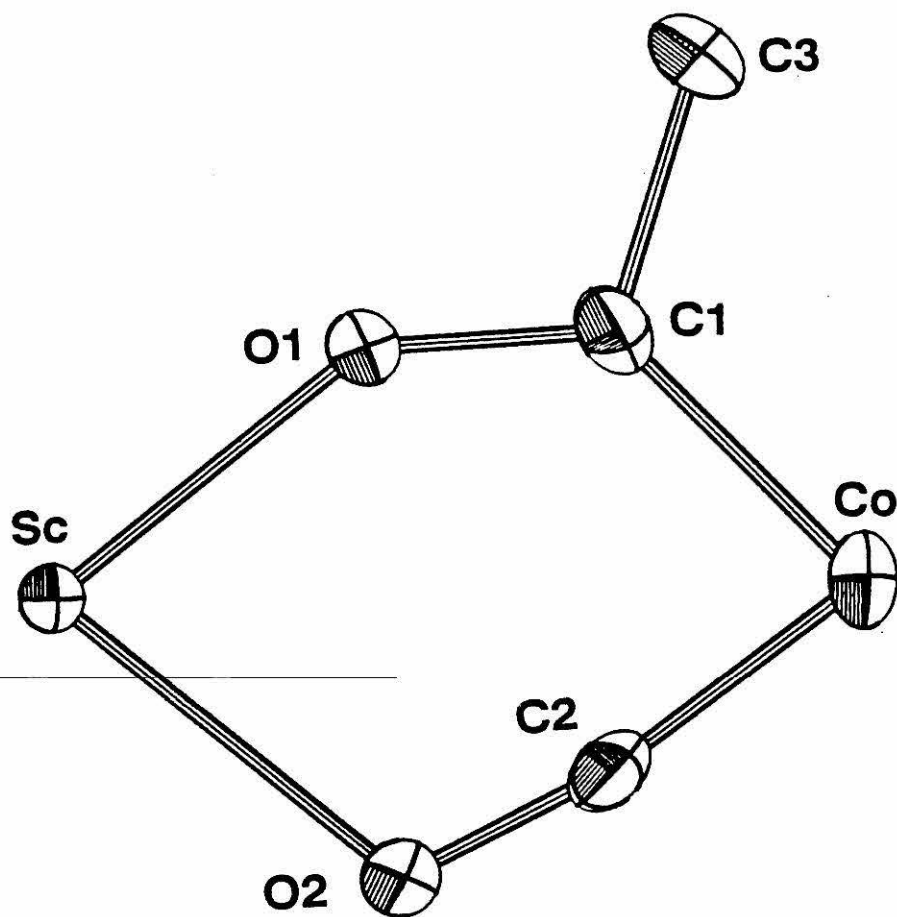
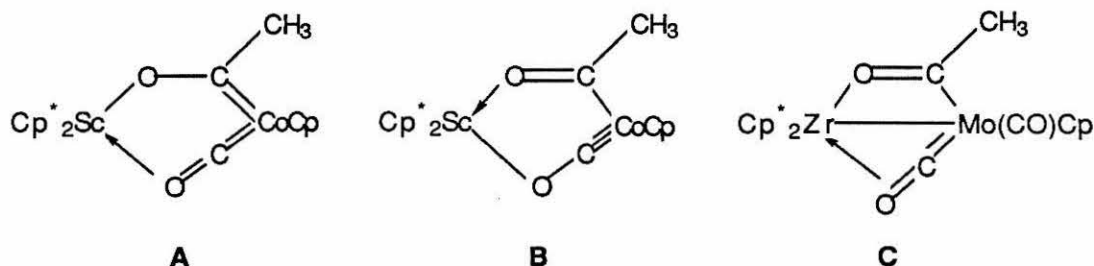


**Figure 2.** Skeletal view of  $\text{Cp}^*_2\text{ScOC}(\text{CH}_3)\text{Co}(\text{CO})\text{Cp}$  with Cps and  $\text{Cp}^*$ s omitted for clarity.



2.272(8)Å; hence the  $\mu^2\text{-}\eta^1, \eta^1$  designation for the bridging carbonyl of  $\text{Cp}(\text{CO})\text{Co}=\text{C}(\text{CH}_3)\text{OScCp}^*_2$ .

The compound most closely analogous to  $\text{CpCo}(\mu^2\text{-}\eta^1, \eta^1\text{-CO})(=\text{C}(\text{CH}_3)\text{OScCp}^*_2)$  (structures A and B) is  $\text{Cp}(\text{CO})\text{Mo}(\mu^2\text{-}\eta^1, \eta^2\text{-CO})(=\text{C}(\text{CH}_3)\text{OZrCp}^*_2)$  (structure C, below).<sup>39</sup> The bonding shown in C gives rise to 18-electron valence shells for both molybdenum and zirconium. Thus, there are two major differences between these two structures: (a) a metal-metal bond for C, as indicated by the relatively short Zr-Mo



bond distance (3.297(1)Å; cf. the 4.118(1)Å Sc-Co distance), and (b) the bridging carbonyl is of the  $\mu^2\text{-}\eta^1, \eta^2$ -type ( $\nu(\text{CO}) = 1536 \text{ cm}^{-1}$ ,  $d(\text{C-O}) = 1.241(4)\text{Å}$ ) for  $\text{Cp}(\text{CO})\text{Mo}(\mu^2\text{-}\eta^1, \eta^2 \text{ CO})(=\text{C}(\text{CH}_3)\text{OZrCp}^*_2)$ , compared with the  $\mu^2\text{-}\eta^1, \eta^1$ -carbonyl for  $\text{CpCo}(\mu^2\text{-}\eta^1, \eta^1 \text{ CO})(=\text{C}(\text{CH}_3)\text{OScCp}^*_2)$  ( $\nu(\text{CO}) = 1795 \text{ cm}^{-1}$ ,  $d(\text{C-O}) = 1.202(4)\text{Å}$ ). Caulton has earlier noted that the acetyl/oxycarbene ligand is quite flexible, spanning metal-metal distances from 2.57-3.52Å.<sup>39b</sup> The non-bonding Sc-Co distance of 4.118(1)Å indicates that even greater metal-metal distances may be accommodated. Other examples of complexes having a ( $\mu^2\text{-}\eta^1, \eta^1 \text{ CO}$ ) ligand are given in Table 2. Norton has noted that carbonyl stretching frequencies for  $\mu^2\text{-}\eta^1, \eta^1$  and  $\mu^2\text{-}\eta^1, \eta^2$  types are so similar that the position may not be used as diagnostic.<sup>39a</sup> Interestingly, the  $\nu(\text{CO})$  for the  $\mu^2\text{-}\eta^1, \eta^1 \text{ CO}$  of  $\text{CpCo}(\mu^2\text{-}\eta^1, \eta^1 \text{ CO})(=\text{C}(\text{CH}_3)\text{OScCp}^*_2)$  (1795  $\text{cm}^{-1}$ ) is substantially greater than the 1530 - 1630  $\text{cm}^{-1}$  region observed for other members of these two series. The modest distortion from a linear Co-C-O

**Table 2.** Structural Characteristics of Compounds Containing ( $\mu^2\text{:}\eta^1,\eta^1\text{-CO}$ ) Ligands

	$\angle\text{M-C-O}$	$\angle\text{M-O-C}$	$d(\text{C-O})$	$\nu(\text{CO})$	Ref.
$\text{Cp}(\text{CO})_2\text{MoCQTi}(\text{THF})\text{Cp}_2$	178.0°	135.4°	1.201	1650	40
$\text{Cp}(\text{CO})_2\text{MoCQTi}(\text{CH}_3)\text{Cp}_2$	178.8°	144.3°	1.212	1623	41
$\text{Cp}(\text{CO})_2\text{MoCQZr}(\text{CH}_3)\text{Cp}_2$	178.2°	145.5°	1.236	1545	42
$(\text{CO})_3\text{CoCQYb}(\text{THF})\text{Cp}^*_2$	177.8°	163.0°	1.188	1798, 1761	43
$(\text{Cp}(\text{CO})_2\text{MoCQ})_2\text{ZrCp}^*_2$	177.8°	170.7°	1.217	1578, 1533	44
$\text{Cp}(\text{CO})_2(\text{C}(\text{CH}_3)\text{O})\text{MoCQ-}$ $\text{Zr}(\text{CH}_3)\text{Cp}_2$	172.3°	77.6°	1.241	1600	39b
$\text{Cp}(\mu\text{-C}(\text{CH}_3)\text{O})\text{CoCQScCp}^*_2$	169.9°	110.9°	1.268	1795	this work

arrangement (169.9(3)°) in the six-membered ring likely reduces back bonding from the cobalt.

The structural features of the  $\text{Cp}^*_2\text{Sc}$  unit are unexceptional in comparison to other structurally characterized  $[\text{Cp}^*_2\text{Sc}]$  compounds.<sup>24,45</sup> The Sc-O distances compare with those for the carboxylate derivative  $\text{Cp}^*_2\text{ScO}_2\text{CC}_6\text{H}_4\text{CH}_3$  ( $d(\text{Sc-O}) = 2.167(3)$  and  $2.176(3)\text{\AA}$ ).<sup>45</sup>

The carbon-oxygen bond for the bridging methyl-scandoxycarbene ligand (1.268(4) $\text{\AA}$ ) is significantly longer than that for the  $\mu^2\text{-}\eta^1,\eta^1$  CO ligand, indicating a substantially lower C-O bond order. The cobalt-carbon bond length (1.654(3) $\text{\AA}$ ) for the  $\mu^2\text{-}\eta^1,\eta^1$  carbonyl is roughly the same as for  $\text{CpCo}(\text{CO})_2$  (1.679(4) $\text{\AA}$ )<sup>46</sup>, and the cobalt-carbene carbon distance is ca. 0.2 $\text{\AA}$  longer (1.850(4) $\text{\AA}$ ). This modest lengthening of the metal-carbon bond on conversion to an oxy-carbene is normal, although multiple metal-carbon bonding is maintained (cf. a typical Co-C single bond length  $\approx 2.0\text{\AA}$ <sup>47</sup>). Several other cobalt carbene compounds have been structurally characterized, and some structural parameters are summarized in Table 3. The bond



distances and angles are most indicative of resonance structure A, although the small difference in  $d(\text{C1-O1})$  and  $d(\text{C2-O2})$  could be taken as signifying some B character. The chelating oxygen ligation about the scandium center for  $\text{CpCo}(\mu^2\text{-}\eta^1, \eta^1 \text{CO})(=\text{C}(\text{CH}_3)\text{OScCp}^*_2)$  leads to a lower reactivity. For example, in contrast to  $\text{Cp}_2\text{W}=\text{C}(\text{CH}_3)\text{O-ScCp}^*_2$ ,  $\text{CpCo}(\mu^2\text{-}\eta^1, \eta^1 \text{CO})(=\text{C}(\text{CH}_3)\text{OScCp}^*_2)$  does not react with  $\text{H}_2$  after days at  $80^\circ\text{C}$ .

**Table 3.** Co=C and C-O Bond lengths for Carbene Complexes of Cobalt

	<u><math>d(\text{Co}=\text{C})</math> (Å)</u>	<u><math>d(\text{C-O})</math> (Å)</u>	<u>Ref.</u>
$(\text{Ge}(\text{C}_6\text{H}_5)_3)(\text{CO})_3\text{Co}=\text{C}(\text{OCH}_2\text{CH}_3)(\text{CH}_2\text{CH}_3)$	1.913(11)	1.289(10)	48
$\text{Cp}(\text{CO})\text{Co}=\text{CCH}_2(\eta^3\text{-CHCHCH}_2)\text{OZrCp}_2$	1.815(4)	1.287(4)	17b
$(\eta^5\text{-C}_5\text{H}_4\text{Cl})(\text{CO})\text{Co}=\text{CCH}_2(\eta^3\text{-CHCHCH}_2)\text{OZrCp}_2$	1.829(5)	1.286(6)	17c
$\text{Cp}(\text{C}_6\text{H}_5\text{S})\text{Co}=\text{CN}(\text{CH}_3)\text{CH}_2\text{CH}_2\text{N}(\text{CH}_3)$	1.902(3)	--	16a
$(\text{PPh}_3)(\text{CO})(\text{NO})\text{Co}=\text{CN}(\text{CH}_3)\text{CH}_2\text{CH}(\text{CH}_3)\text{N}(\text{CH}_3)$	1.974(15)	--	49
$\text{CpCo}(\mu^2\text{-}\eta^1, \eta^1\text{-CO})(=\text{C}(\text{CH}_3)\text{OScCp}^*_2)$	1.850(4)	1.268(4)	this work

## CONCLUSIONS

$\text{Cp}^*_2\text{Sc-H}$  reacts with CO and excess  $\text{H}_2$  at low temperatures to give  $\text{Cp}^*_2\text{Sc-OCH}_3$ .  $\text{Cp}^*_2\text{Sc-R}$  reacts rapidly with CO at low temperatures to form  $\eta^2$  acyl complexes; in the case of  $\text{R} = \text{p-tolyl}$ , the product can be isolated and characterized. However, when  $\text{R} = \text{H}$ , alkyl, the resulting product is apparently also quite reactive and decomposes.

The increased Lewis acidity of the 14 electron Sc center results in greater reactivity toward activation of metal carbonyls, relative to other early transition metal or aluminum compounds. The resulting polarization of the carbonyl C-O bond results in a greater susceptibility to nucleophilic attack (at carbon) by the migrating R group. When  $\text{L}_n\text{M-CO}$  is  $\text{Cp}_2\text{MCO}$  ( $\text{M} = \text{Mo}, \text{W}$ ), the type of R that may be added is limited by steric interactions with the Cp rings. When  $\text{L}_n\text{M-CO}$  is  $\text{CpM}(\text{CO})_2$  ( $\text{M} = \text{Co}, \text{Rh}$ ),

bulkier alkyls and amides may be added. The structure of  $\text{CpCo}(\mu^2\text{-}\eta^1, \eta^1\text{CO})(=\text{C}(\text{CH}_3)\text{OScCp}^*_2)$  illustrates, once again, the oxophilic nature of the Sc center as it coordinates both carbonyl oxygens.

## EXPERIMENTAL

### General Considerations

All manipulations of air- and/or water-sensitive materials were carried out using high vacuum techniques or in a dry box under an atmosphere of dinitrogen as described elsewhere.<sup>50</sup> Solvents were dried and purified by prolonged reflux over a suitable drying agent followed by distillation under an atmosphere of dinitrogen. Etheral solvents were stored over sodium benzophenone ketyl, and hydrocarbon solvents were stored over titanocene.<sup>51</sup> Ethylene oxide and CO (Matheson) were used as received.  $\text{Cp}^*_2\text{ScCH}_3$ <sup>24</sup>,  $\text{Cp}^*_2\text{ScCD}_3$ <sup>24</sup>,  $\text{Cp}^*_2\text{ScH(THF)}$ <sup>24</sup>,  $\text{Cp}^*_2\text{ScC}_6\text{H}_5$ <sup>24</sup>,  $\text{Cp}^*_2\text{ScC}\equiv\text{CCH}_3$ <sup>24</sup>,  $\text{Cp}^*_2\text{ScN(CH}_3)_2$ <sup>33</sup>,  $\text{Cp}^*_2\text{ScCH}_2\text{CH}_2\text{C}_6\text{H}_5$ <sup>37</sup>,  $\text{Cp}^*_2\text{ScCH(Si(CH}_3)_3)_2$ <sup>52</sup>,  $\text{Cp}_2\text{MoCO}$ <sup>53</sup>, and  $\text{Cp}_2\text{WCO}$ <sup>54</sup> were prepared according to previously reported procedures. Benzaldehyde (Aldrich) was dried over 4Å molecular sieves.  $\text{CpCo(CO)}_2$  was obtained from Alfa and  $\text{CpRh(CO)}_2$  was obtained from Strem; both were used as received.  $\text{CpRh(}^{13}\text{CO)}_2$  and  $\text{Cp}_2\text{W(}^{13}\text{CO)}$  were prepared by photolysis of  $\text{CpRh(CO)}_2$  and  $\text{Cp}_2\text{WCO}$ , respectively, under 1 atmosphere of  $^{13}\text{CO}$  (Monsanto-Mound facility). If not otherwise specified, reactivity studies were carried out in NMR tubes and monitored by  $^1\text{H}$  NMR. For example, a typical experiment involved dissolving 20 mg of  $\text{Cp}^*_2\text{ScMe}$  in 0.5 ml  $\text{C}_6\text{D}_6$  in a septa capped tube and injecting 5  $\mu\text{l}$ . of benzaldehyde into the solution.

Elemental analyses were provided by the Caltech microanalytical service. Nuclear magnetic resonance spectra were recorded on Varian EM 390, Jeol FX90Q, Bruker WM 500, or Jeol GX400Q spectrometers. Infrared spectra were recorded on a Beckman 4240 spectrometer, and are reported from 2800-1000  $\text{cm}^{-1}$ . Relative intensities are abbreviated as follows: vs (very strong), s (strong), m (medium), w (weak), bd (broad), sh (shoulder).

**Table 4.**  $^1\text{H}$  and  $^{13}\text{C}$  NMR Data

<u>Compound</u>	<u>Assignment</u>	<u>Shift (ppm)<sup>b</sup></u>
$\text{Cp}^*_2\text{ScOCH}_3^{\text{h}}$	$\text{C}_5(\underline{\text{CH}}_3)_5$	1.97 s
	$\text{OCH}_3$	4.27 s
$\text{Cp}^*_2\text{Sc}(\text{CO})\text{C}_6\text{H}_4\text{CH}_3\text{-}p^{\text{g}}$	$\text{C}_5(\underline{\text{CH}}_3)_5$	1.90 s
	$\text{C}_6\text{H}_4\text{CH}_3$	7.08, 7.90 d (dd with $^{13}\text{CO}$ ) ( $J_{\text{HH}}=8$ Hz, $^3J_{\text{CH}}=16$ Hz)
	$\text{C}_6\text{H}_4\text{CH}_3$	2.08 s
	$\text{C}_5(\underline{\text{CH}}_3)_5$	11.3
	$\underline{\text{C}}_5(\text{CH}_3)_5$	117.5
	$(\underline{\text{CO}})\text{C}_6\text{H}_4\text{CH}_3\text{-}p$	324.7
	$(\text{CO})\underline{\text{C}}_6\text{H}_4\text{CH}_3\text{-}p$	143.8, 130.9, 130.6, 129.7
	$(\text{CO})\text{C}_6\text{H}_4\underline{\text{C}}\text{H}_3\text{-}p$	21.6
$\text{Cp}^*_2\text{ScOCH}_2\text{C}_6\text{H}_4\text{CH}_3\text{-}p^{\text{h}}$	$\text{C}_5(\underline{\text{CH}}_3)_5$	1.92 s
	$\text{OCH}_2\text{C}_6\text{H}_4\text{CH}_3\text{-}p$	5.60 s
	$\text{OCH}_2\text{C}_6\text{H}_4\text{CH}_3\text{-}p$	7.15-7.35 m
	$\text{OCH}_2\text{C}_6\text{H}_4\underline{\text{C}}\text{H}_3\text{-}p$	2.23 s
$\text{Cp}^*_2\text{ScCH}_3(\text{OCH}_2\text{CH}_2)^{\text{h}}$	$\text{C}_5(\underline{\text{CH}}_3)_5$	1.91 s
	$\text{ScCH}_3$	-0.52 s
	$(\text{OCH}_2\text{CH}_2)$	2.13 s
$\text{Cp}^*_2\text{ScOCH}_2\text{CH}_2\text{CH}_3^{\text{h}}$	$\text{C}_5(\underline{\text{CH}}_3)_5$	1.94 s
	$\text{OCH}_2\text{CH}_2\text{CH}_3$	4.34 t ( $^3J_{\text{HH}} = 7$ Hz)
	$\text{OCH}_2\text{CH}_2\underline{\text{C}}\text{H}_3$	0.76-1.12 m
$\text{Cp}_2\text{MoC}(\text{CH}_3)\text{OScCp}^*_2^{\text{c,d}}$	$\text{C}_5(\underline{\text{CH}}_3)_5$	1.89 s
	$\text{C}_5\text{H}_5$	4.62, 4.45 s
	$\text{Mo}=\text{C}(\text{CH}_3)$	2.08 s
	$\text{C}_5(\underline{\text{CH}}_3)_5$	11.4
	$\underline{\text{C}}_5(\text{CH}_3)_5$	125.4
	$\underline{\text{C}}_5\text{H}_5$	81.7, 79.5
	$\text{Mo}=\underline{\text{C}}(\text{CH}_3)$	292.4
	$\text{Mo}=\text{C}(\underline{\text{C}}\text{H}_3)$	48.1
$\text{Cp}_2\text{WC}(\text{H})\text{OScCp}^*_2^{\text{d,e}}$	$\text{C}_5(\underline{\text{CH}}_3)_5$	1.93 s
	$\text{C}_5\text{H}_5$	4.61, 4.53 s
	$\text{W}=\text{C}(\text{H})$	11.07 s
	$\underline{\text{C}}_5(\text{CH}_3)_5$	120.3 s
	$\text{C}_5(\underline{\text{CH}}_3)_5$	11.2 q ( $J_{\text{CH}}=125.1$ Hz)
	$\underline{\text{C}}_5\text{H}_5$	78.9, 75.6 d ( $J_{\text{CH}}=180.1$ Hz)
	$\text{W}=\underline{\text{C}}(\text{H})$	249.0 d ( $J_{\text{CH}}=123.6$ Hz)

$\text{Cp}_2\text{WC}(\text{CH}_3)\text{OScCp}^*2^{\text{e}}$	$\text{C}_5(\text{CH}_3)_5$	1.92 s
	$\text{C}_5\text{H}_5$	4.49, 4.43 s
	$\text{W}=\text{C}(\text{CH}_3)$	1.31 s
	$\text{C}_5(\underline{\text{C}}\text{H}_3)_5$	11.5
	$\underline{\text{C}}_5(\text{CH}_3)_5$	121.2
	$\underline{\text{C}}_5\text{H}_5$	78.4, 75.8
	$\text{W}=\underline{\text{C}}(\text{CH}_3)$	263.5
	$\text{W}=\text{C}(\underline{\text{C}}\text{H}_3)$	49.8
$\text{Cp}_2\text{WCOSc}(\text{Cl})\text{Cp}^*2^{\text{e}}$	$\text{C}_5(\text{CH}_3)_5$	1.94 s
	$\text{C}_5\text{H}_5$	4.20 s
	$\underline{\text{C}}_5(\text{CH}_3)_5$	121.4
	$\text{C}_5(\underline{\text{C}}\text{H}_3)_5$	11.9
	$\underline{\text{C}}_5\text{H}_5$	71.6
	$\text{W}-\underline{\text{C}}\text{O}$	245.9
$\text{Cp}(\text{CO})\text{CoC}(\text{H})\text{OScCp}^*2^{\text{e,f}}$	$\text{C}_5(\text{CH}_3)_5$	1.95 s
	$\text{C}_5\text{H}_5$	4.92 s
	$\text{Co}=\text{C}(\text{H})$	14.31 s
	$\text{C}_5(\underline{\text{C}}\text{H}_3)_5$	11.5 q ( $J_{\text{CH}}=125.5$ Hz)
	$\underline{\text{C}}_5(\text{CH}_3)_5$	120.5 s
	$\underline{\text{C}}_5\text{H}_5$	86.2 d ( $J_{\text{CH}}=174.5$ Hz)
	$\text{Co}=\underline{\text{C}}(\text{H})$	284.0 ( $J_{\text{CH}} = 150.1$ Hz)
$\text{Cp}(\text{CO})\text{CoC}(\text{CH}_3)\text{OScCp}^*2^{\text{e,f}}$	$\text{C}_5(\text{CH}_3)_5$	1.92 s
	$\text{C}_5\text{H}_5$	4.91 s
	$\text{Co}=\text{C}(\text{CH}_3)$	2.57 s
	$\text{C}_5(\underline{\text{C}}\text{H}_3)_5$	11.5
	$\underline{\text{C}}_5(\text{CH}_3)_5$	120.3
	$\underline{\text{C}}_5\text{H}_5$	85.6
	$\text{Co}=\underline{\text{C}}(\text{CH}_3)$	295.0
	$\text{Co}=\text{C}(\underline{\text{C}}\text{H}_3)$	52.6
$\text{Cp}(\text{CO})\text{CoC}(\text{N}(\text{CH}_3)_2)-\text{OScCp}^*2^{\text{d,e,f}}$	$\text{C}_5(\text{CH}_3)_5$	1.95 s
	$\text{C}_5\text{H}_5$	4.86 s
	$\text{N}(\text{CH}_3)_2$	2.94, 2.61 s, br
	$\text{C}_5(\underline{\text{C}}\text{H}_3)_5$	11.6
	$\underline{\text{C}}_5(\text{CH}_3)_5$	119.6
	$\underline{\text{C}}_5\text{H}_5$	83.8
	$\text{Co}=\text{C}(\text{N}(\underline{\text{C}}\text{H}_3)_2)$	43.0, 35.7
	$\text{Co}=\underline{\text{C}}(\text{N}(\text{CH}_3)_2)$	228.8
$\text{Cp}(\text{CO})\text{CoC}(\text{CH}_2\text{CH}_2\text{C}_6\text{H}_5)-\text{OScCp}^*2^{\text{d,e,f}}$	$\text{C}_5(\text{CH}_3)_5$	1.95 s
	$\text{C}_5\text{H}_5$	4.92 s
	$\text{CH}_2\text{CH}_2\text{C}_6\text{H}_5$	3.34, 3.30 m
	$\text{CH}_2\text{CH}_2\text{C}_6\underline{\text{H}}_5$	7.22, 7.23 m
	$\text{C}_5(\underline{\text{C}}\text{H}_3)_5$	11.6
	$\underline{\text{C}}_5(\text{CH}_3)_5$	120.4
	$\underline{\text{C}}_5\text{H}_5$	85.7

	$\text{Co}=\text{C}(\underline{\text{CH}_2\text{CH}_2-}\text{C}_6\text{H}_5)$	68.1, 33.5
	$\text{Co}=\text{C}(\text{CH}_2\text{CH}_2-\underline{\text{C}_6\text{H}_5})$	142.5, 128.9, 128.6, 126.2
	$\text{Co}=\underline{\text{C}}(\text{CH}_2\text{CH}_2-\text{C}_6\text{H}_5)$	297.6
$\text{Cp}(\text{CO})\text{RhC}(\text{CH}_3)\text{OScCp}^*_{2^{\text{e,h}}}$	$\text{C}_5(\underline{\text{CH}_3})_5$	1.90 s
	$\text{C}_5\text{H}_5$	5.43 s
	$\text{Rh}=\text{C}(\underline{\text{CH}_3})$	2.56 s
	$\text{C}_5(\underline{\text{C}}\text{H}_3)_5$	11.5
	$\underline{\text{C}_5}(\text{CH}_3)_5$	120.5
	$\underline{\text{C}_5}\text{H}_5$	89.5
	$\text{Rh}-\underline{\text{CO}}$	206.7 ( $J_{\text{Rh}-\text{C}}=113.9$ Hz)
	$\text{Rh}=\underline{\text{C}}(\text{CH}_3)$	279.1 ( $J_{\text{Rh}-\text{C}}=56.3$ Hz)
	$\text{Rh}=\text{C}(\underline{\text{C}}\text{H}_3)$	53.5

<sup>a</sup> Unless otherwise specified, spectra were obtained in benzene- $d_6$  at ambient temperature, 90 MHz. s = singlet, d = doublet, t = triplet, q = quartet, m = multiplet, br = broad. <sup>b</sup> Chemical shifts are referenced to internal  $\text{Si}(\text{CH}_3)_4$  or to solvent signals and indirectly referenced to  $\text{Si}(\text{CH}_3)_4$ . <sup>c</sup>  $^1\text{H}$  spectrum measured at 500 MHz. <sup>d</sup>  $^1\text{H}$  spectrum measured at 400 MHz. <sup>e</sup>  $^{13}\text{C}$  spectrum measured at 100.38 MHz. <sup>f</sup> Signals for the CO were not observed, presumably due to  $^{59}\text{Co}$  quadrupolar broadening. <sup>g</sup>  $^{13}\text{C}$  spectrum measured at 22.49 MHz. <sup>h</sup> Compounds were not isolated.

**Reaction of  $\text{Cp}^*_2\text{ScH}$ ,  $\text{H}_2$ , and  $\text{CO}$ .** 27 mg of  $\text{Cp}^*_2\text{ScCH}_2\text{C}_6\text{H}_5$  (0.07 mmol) were placed in a small, thick-walled, glass bomb and dissolved in 0.5 ml of toluene. The bomb was cooled to  $-196^\circ\text{C}$  and one atmosphere of  $\text{H}_2$  was admitted to the evacuated bomb. The reaction mixture was then warmed to room temperature and allowed to stir for one half hour. It was then cooled to  $-196^\circ\text{C}$  and evacuated. A mixture of 23 torr  $\text{CO}$  (volume of bomb = 13.56 ml, thus 0.07 mmol) and 675 torr  $\text{H}_2$  was then added to the bomb at  $-196^\circ\text{C}$ . The bomb was then warmed to room temperature, volatiles removed, and the product analyzed by  $^1\text{H}$  NMR.

**$\text{Cp}^*_2\text{Sc}(\text{CO})\text{C}_6\text{H}_4\text{CH}_3$ -*p*.** 300 mg (0.74 mmol) of  $\text{Cp}^*_2\text{ScC}_6\text{H}_4\text{CH}_3$ -*p* were dissolved in 25 ml of toluene. At  $-78^\circ\text{C}$ , with stirring, 326 torr x 42.2 ml (0.74 mmol) of  $\text{CO}$  were admitted to the solution, which immediately changed color from yellow to orange. The solution was allowed to stir at  $-78^\circ\text{C}$  for 30 minutes. With the solution at  $-78^\circ\text{C}$ , any remaining  $\text{CO}$  was removed; the solution was then allowed to warm to room temperature, and the toluene was removed under vacuum. 10 ml of petroleum ether was then vacuum transferred onto the product, the frit assembly cooled to  $-78^\circ\text{C}$ , and the product filtered. Orange crystals were collected in 55% yield (177 mg). Analysis: Calculated for  $\text{C}_{27}\text{H}_{37}\text{OSc}$ : C, 77.38%; H, 8.60%; Found: C, 77.14%; H, 8.60%. IR ( $\text{cm}^{-1}$ , Nujol): 1600(m), 1448(s), 1375(m), 1290(w), 1245(w), 1222(w), 1208(m), 1153(s), 1103(s), 1018(m).

**$\text{Cp}^*_2\text{ScOCH}_2\text{C}_6\text{H}_5\text{CH}_3$ -*p*.** 20 mg of  $\text{Cp}^*_2\text{Sc}(\text{CO})\text{C}_6\text{H}_4\text{CH}_3$ -*p* were placed in a sealable NMR tube and dissolved in  $\text{C}_6\text{D}_6$ . The tube was cooled to  $-196^\circ\text{C}$ , evacuated, filled with one atmosphere of  $\text{H}_2$ , and sealed. At  $25^\circ\text{C}$ , the reaction proceeded to completion (by  $^1\text{H}$  NMR) in 48 hours.

**Reaction of  $\text{CH}_2\text{O}$  with  $\text{Cp}^*_2\text{ScCH}_3$ .** 30 mg of  $\text{Cp}^*_2\text{ScCH}_3$  (0.09 mmol) was placed in a three necked round bottom flask equipped with  $180^\circ$  needle valve and a sidearm loaded with 4 mg paraformaldehyde (0.13 mmol formaldehyde). 15 ml of toluene were vacuum transferred onto the  $\text{Cp}^*_2\text{ScCH}_3$ . A dry ice/acetone bath was placed at the level

of the solution in the flask. The paraformaldehyde was vaporized with a heat gun and condensed, as the monomer, into the stirring solution. The solution was allowed to stir for 30 minutes at room temperature. The toluene was removed under vacuum and the product was analyzed by  $^1\text{H}$  NMR. The product was identified by comparison of its  $^1\text{H}$  NMR spectra to the  $^1\text{H}$  NMR spectra of a sample of  $\text{Cp}^*_2\text{ScOCH}_2\text{CH}_3$  prepared by an alternative method.<sup>37</sup>

**$\text{Cp}_2\text{W}=\text{C}(\text{CH}_3)(\text{OScCp}^*_2)$ .** 0.173 g of  $\text{Cp}^*_2\text{ScCH}_3$  (0.51 mmol) and 0.175 g  $\text{Cp}_2\text{WCO}$  (0.52 mmol) were dissolved in toluene (10 ml) and allowed to stir overnight. The color of the solution changes gradually from green to brown as the reaction progresses. The solvent was removed under reduced pressure, and n-pentane (3 ml) was distilled in. The flask and frit were cooled to  $-78^\circ\text{C}$  and filtered, yielding 205 mg of brown powder,  $\text{Cp}^*_2\text{ScOC}(\text{CH}_3)\text{WCp}_2$  (60%). IR( $\text{cm}^{-1}$ , Nujol) 2725(w), 1900(br), 1455(s), 1379(s), 1167(s), 1063(m), 1017(m).  $\text{Cp}_2\text{WH}_2$  impurity in  $\text{Cp}_2\text{WCO}$  prevented accurate elemental analysis.

**$\text{Cp}_2\text{W}=\text{C}(\text{H})(\text{OScCp}^*_2)$ .** 21 mg of  $\text{Cp}^*_2\text{ScH}(\text{THF})$  (0.053 mmol) and 18 mg (0.053 mmol) of  $\text{Cp}_2\text{WCO}$  were dissolved in  $\text{C}_6\text{D}_6$  in an NMR tube. The progress of the reaction was monitored by  $^1\text{H}$  NMR. The product was not isolated. Alternatively, the compound can be made by heating  $\text{Cp}^*_2\text{ScOC}(\text{CH}_3)\text{WCp}_2$  under 4 atm of  $\text{H}_2$  to  $80^\circ\text{C}$ . IR( $\text{cm}^{-1}$ ,  $\text{C}_6\text{D}_6$ ) 2723(w), 2220(w), 1905(s,  $\text{Cp}_2\text{WCO}$  starting material), 1863(m), 1566(s), 1429(m), 1387(m), 1200(s).

**$\text{Cp}_2\text{WCOScClCp}^*_2$ .** 21 mg (0.060 mmol) of  $\text{Cp}^*_2\text{ScCl}$  and 25 mg of  $\text{Cp}_2\text{WCO}$  (0.073 mmol) were dissolved in 0.5 ml of  $\text{C}_6\text{D}_6$  in an NMR tube. The product was not isolated. IR ( $\text{cm}^{-1}$ , soln.,  $\text{C}_6\text{D}_6$ ,  $\text{CaF}_2$  cells) 1905(s,  $\text{Cp}_2\text{WCO}$  starting material), 1835(s), 1424(br), 1378(w), 1340(w).

**$\text{Cp}_2\text{Mo}=\text{C}(\text{CH}_3)(\text{OScCp}^*_2)$ .** 20 mg (0.060 mmol) of  $\text{Cp}^*_2\text{ScCH}_3$  and 16 mg (0.063 mmol)  $\text{Cp}_2\text{MoCO}$  were dissolved in  $\text{C}_6\text{D}_6$  in an NMR tube. The product was not isolated.



IR ( $\text{cm}^{-1}$ , soln.,  $\text{C}_6\text{D}_6$ ,  $\text{CaF}_2$  cells) 1948(s,  $\text{Cp}_2\text{MoCO}$  starting material), 1175(s), 1104(s), 1060(m), 1035(m).

**$\text{Cp}(\text{CO})\text{Co}=\text{C}(\text{H})(\text{OScCp}^*_2)$**  195 mg (0.51 mmol) of  $\text{Cp}^*_2\text{ScH}(\text{THF})$  was dissolved in toluene (10 ml) and 64  $\mu\text{l}$  of  $\text{CpCo}(\text{CO})_2$  (95 mg, 0.53 mmol) was added to the solution. The orange solution was allowed to stir at room temperature overnight.

Volatiles were removed under reduced pressure, and n-pentane (2 ml) was vacuum transferred onto the residue. The flask and frit were cooled to  $-78^\circ\text{C}$  and filtered. 160 mg (55%) of yellow-orange, microcrystalline  $\text{Cp}^*_2\text{ScOCHCo}(\text{CO})\text{Cp}$  was obtained.

Analysis: Calculated for  $\text{C}_{27}\text{H}_{36}\text{O}_2\text{ScCo}$ : C, 65.32; H, 7.31. Found: C, 64.97; H, 7.15.

IR ( $\text{cm}^{-1}$ , Nujol) 2590(w), 1840(s), 1798(sh), 1342(sh), 1108(w), 1050(w), 1005(w).

**$\text{Cp}(\text{CO})\text{Co}=\text{C}(\text{CH}_3)(\text{OScCp}^*_2)$** . The procedure is the same as that for  $\text{Cp}^*_2\text{ScOCHCo}(\text{CO})\text{Cp}$  except that 503 mg (1.52 mmol) of  $\text{Cp}^*_2\text{ScCH}_3$  and 187  $\mu\text{l}$  of  $\text{CpCo}(\text{CO})_2$  (274 mg, 1.52 mmol) yield 545 mg (70%) of dark orange, microcrystalline  $\text{Cp}^*_2\text{ScOC}(\text{CH}_3)\text{Co}(\text{CO})\text{Cp}$ . Analysis: Calculated for  $\text{C}_{28}\text{H}_{38}\text{O}_2\text{ScCo}$ : C, 65.88; H, 7.50. Found: C, 65.64; H, 7.44. IR ( $\text{cm}^{-1}$ , Nujol) 2720(w), 2015(w), 1962(w), 1795(s), 1616(w), 1082(m), 1018(m).

**$\text{Cp}(\text{CO})\text{Co}=\text{C}(\text{CH}_2\text{CH}_2\text{C}_6\text{H}_5)(\text{OScCp}^*_2)$** . The procedure is the same as that for  $\text{Cp}(\text{CO})\text{Co}=\text{C}(\text{H})(\text{OScCp}^*_2)$  except that 208 mg of  $\text{Cp}^*_2\text{ScCH}_2\text{CH}_2\text{C}_6\text{H}_5$  (0.50 mmol) and 60  $\mu\text{l}$  of  $\text{CpCo}(\text{CO})_2$  (89 mg, 0.49 mmol) yield 153 mg (52%) of the red-orange  $\text{Cp}(\text{CO})\text{Co}=\text{C}(\text{CH}_2\text{CH}_2\text{C}_6\text{H}_5)(\text{OScCp}^*_2)$ . Analysis: Calculated for  $\text{C}_{35}\text{H}_{44}\text{O}_2\text{ScCo}$ : C, 69.99; H, 7.38. Found: C, 70.22; H, 7.62. IR ( $\text{cm}^{-1}$ , Nujol) 2718(w), 1805(s), 1757(sh), 1600(w), 1492(w), 1410(m), 1322(s), 1309(m), 1230(w), 1110(w), 1040(w), 1010(w).

**$\text{Cp}(\text{CO})\text{Co}=\text{C}(\text{NMe}_2)(\text{OScCp}^*_2)$** . The procedure is the same as that for  $\text{Cp}^*_2\text{ScOCHCo}(\text{CO})\text{Cp}$  except that 150 mg of  $\text{Cp}^*_2\text{ScN}(\text{CH}_3)_2$  (0.42 mmol) and 51  $\mu\text{l}$  (76 mg, 0.42 mmol) of  $\text{CpCo}(\text{CO})_2$  yield 132 mg of  $\text{Cp}^*_2\text{ScOC}(\text{N}(\text{CH}_3)_2)$ . Analysis:

Calculated for  $C_{29}H_{41}N_2ScCo$ : C, 64.56; H, 7.65; N, 2.60. Found: C, 65.47; H, 7.75; N 2.20. IR ( $cm^{-1}$ , Nujol) 2722(w), 2028(w), 1795(s), 1742(w), 1495(m), 1434(m), 1399(w), 1380(m), 1300(s), 1240(m), 1085(s), 1050(w), 1018(w).

**$Cp(CO)Rh=C(CH_3)(OScCp^*)_2$** . 19 mg of  $Cp^*ScCH_3$  and 77  $\mu l$  of 0.75M  $CpRh(CO)_2$  in  $C_6D_6$  were dissolved in 0.5 ml of  $C_6D_6$  in an NMR tube. The product was not isolated. IR ( $cm^{-1}$ , soln.,  $C_6D_6$ ,  $CaF_2$  cells) 2041(s,  $CpRh(CO)_2$  starting material), 1978(s), 1805(s), 1765(w), 1420(br).

### Crystal Structure Determination of $CpCo(\mu^2:\eta^1,\eta^1-$

$CO)(=C(CH_3)OScCp^*)_2$ . A single crystal (dimensions 0.21 x 0.43 x 0.76 mm), grown by slow cooling of a saturated solution of toluene was placed in a glass capillary and sealed under nitrogen. The capillary was mounted on a CAD4 diffractometer equipped with graphite monochromator and  $MoK\alpha$  radiation. The preliminary photographic workup indicated a symmetry no higher than  $\bar{1}$ ; we assigned space group  $P\bar{1}$  with  $Z=2$ . The least squares refinement of the orientation matrix with the setting angles of twenty-five reflections generated the following cell parameters:  $a = 8.592(4)\text{\AA}$ ,  $b = 10.923(2)\text{\AA}$ ,  $c = 14.648(2)\text{\AA}$ ,  $\alpha = 91.074(14)^\circ$ ,  $\beta = 100.84(2)^\circ$ ,  $\gamma = 100.77(3)^\circ$ ,  $V = 1324.35(66)\text{\AA}^3$ . Intensity data were collected by  $\theta - 2\theta$  scans of width  $2.00^\circ$  (plus dispersion) at  $6^\circ/\text{min}$  for the Ewald sphere ( $\pm h, \pm k, \pm l$ ) to  $2\theta = 50^\circ$  (13,156 reflections). The three check reflections indicated no decomposition. The data were averaged over  $\bar{1}$  symmetry (average goodness of fit = 1.19, 3,378 reflections; and  $R = 0.036$  for the 2,930 paired reflections), 1,185 reflections were deleted, and the remaining data were reduced to  $F_o^2$ . The form factors were taken from a standard reference<sup>55</sup>; those for Co and Sc were corrected for  $f'$  and  $f''$ .

The coordinates of the scandium and cobalt atoms were derived from the Patterson map, and the remainder of the structure from subsequent  $F_o$  and  $\Delta F$  Fourier maps. The hydrogen atoms were placed at idealized positions with  $B = 9.0 \text{ \AA}^2$  and were not refined.

The full matrix least squares refinement of atom coordinates and  $U_{ij}$ s of non-hydrogen atoms, the scale factor, and a term for isotropic secondary extinction ( $g = 1.6(2) \times 10^{-6}$ ) minimizing  $\sum w[(F_o)^2 - (F_c/k)^2]^2$  yielded a goodness of fit =  $\{\sum w[(F_o)^2 - (F_c/k)^2]/(n - p)\}^{1/2} = 3.51$  ( $n = 4,593$  reflections,  $p = 290$  parameters),  $R_F = \sum ||F_o| - F_c| / \sum |F_o| = 0.055$  (4,391 reflections,  $I > 0$ ), and  $R'_F = 0.046$  (3,724 reflections,  $I > 3\sigma$ ); the largest peak in the final  $\Delta F$  map was approximately  $0.5 \text{ e}/\text{\AA}^3$ . The labeling scheme is given in Figure 3, atom coordinates and  $U_{eq}$ s for non-hydrogen atoms in Table 4, bond lengths and angles are given in Table 5,  $U_{ij}$ s for non-hydrogen atoms in Table 6, atom coordinates for H-atoms in Table 7, and least square planes in Table 8.

**Figure 3.** Labeling Scheme for  $\text{Cp}^*_2\text{ScOC}(\text{CH}_3)\text{Co}(\text{CO})\text{Cp}$

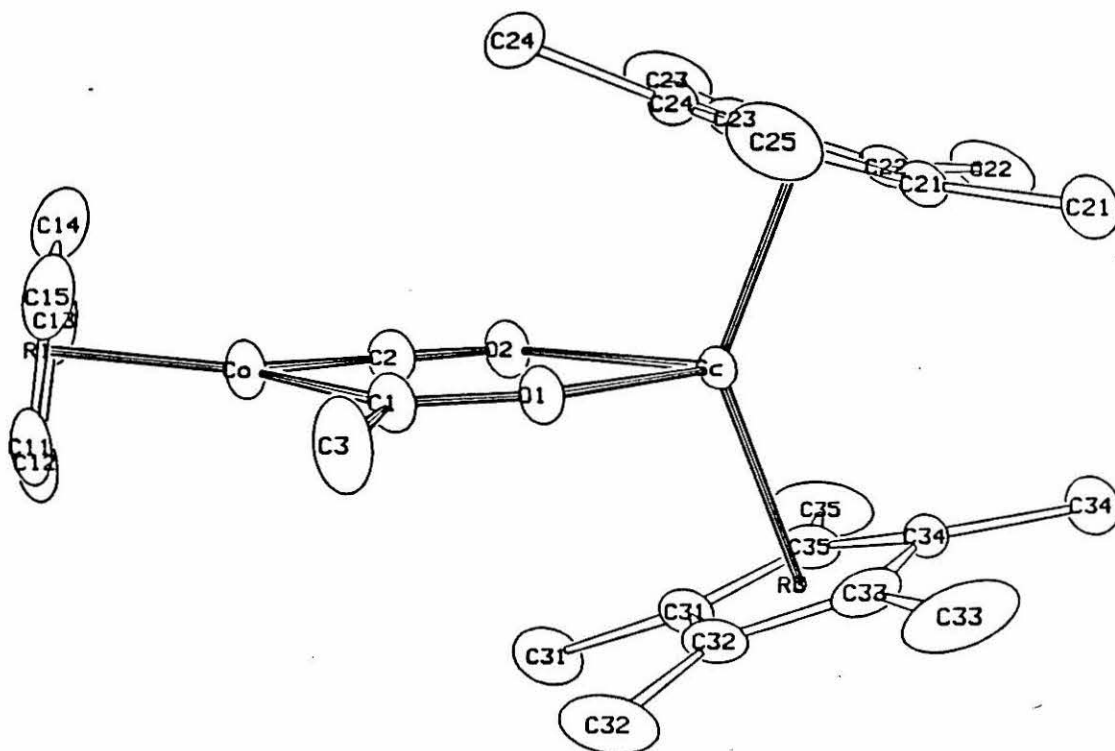


Table 4. Atom Coordinates and  $U_{ij}$ s ( $\times 10^4$ )

Atom	$x$	$y$	$z$	$U_{eq}$
Co	607.5(6)	-554.2(4)	-2335.5(4)	584(1)
Sc	3749.4(6)	2711.1(5)	-2583.8(4)	339(1)
C1	2705(4)	-240(3)	-2534(3)	560(9)
O1	3621(2)	803(2)	-2573(2)	481(5)
C2	727(4)	970(3)	-2397(3)	534(9)
O2	1062(3)	2082(2)	-2444(2)	543(6)
C3	3585(6)	-1320(4)	-2663(4)	961(16)
C11	-223(8)	-2480(4)	-2650(5)	1007(18)
C12	-1518(7)	-1889(5)	-2849(5)	1062(18)
C13	-1605(6)	-1307(5)	-1965(6)	1047(18)
C14	-388(8)	-1594(6)	-1310(4)	1058(18)
C15	463(7)	-2278(5)	-1710(5)	1054(18)
C21	6173(4)	3901(3)	-1479(2)	515(8)
C22	4883(4)	4498(3)	-1404(2)	526(9)
C23	3746(4)	3647(4)	-1023(2)	562(9)
C24	4362(4)	2549(3)	-862(2)	539(9)
C25	5848(4)	2721(3)	-1159(2)	545(9)
C21M	7806(5)	4505(5)	-1679(3)	893(14)
C22M	4805(7)	5855(4)	-1516(3)	988(16)
C23M	2253(6)	3972(5)	-760(3)	1043(16)
C24M	3623(7)	1450(4)	-380(3)	1005(16)
C25M	6953(6)	1777(5)	-1076(4)	1038(15)
C31	2179(4)	2681(3)	-4227(2)	553(9)
C32	3457(5)	2106(3)	-4282(2)	596(9)
C33	4894(4)	2985(5)	-4014(3)	702(12)
C34	4460(5)	4147(4)	-3807(2)	693(12)
C35	2768(5)	3929(3)	-3920(2)	558(9)
C31M	416(5)	2054(5)	-4533(3)	1044(17)
C32M	3360(8)	788(5)	-4637(3)	1191(18)
C33M	6561(6)	2787(8)	-4057(4)	1551(25)
C34M	5570(9)	5397(5)	-3710(3)	1503(24)
C35M	1734(8)	4879(5)	-3812(3)	1177(18)

Table 5. Bond Lengths and Angles

Sc	C21	2.506 (3)	O1	Sc	O2	80.49 (8)
Sc	C22	2.505 (3)	Sc	O1	C1	144.8 (2)
Sc	C23	2.486 (4)	Sc	O2	C2	110.9 (2)
Sc	C24	2.493 (3)	C3	C1	O1	110.7 (3)
Sc	C25	2.485 (3)	C1	Co	C2	85.1 (2)
Sc	C31	2.525 (4)	Co	C1	C3	120.9 (3)
Sc	C32	2.517 (4)	Co	C1	O1	128.5 (3)
Sc	C33	2.478 (4)	Co	C2	O2	169.9 (3)
Sc	C34	2.492 (4)				
Sc	C35	2.493 (4)				
Sc	O1	2.067 (2)				
Sc	O2	2.331 (2)				
Sc	R2	2.192				
Sc	R3	2.199				
C1	O1	1.268 (4)	C15	C11	C12	109.5 (6)
C1	C3	1.542 (6)	C13	C12	C11	104.8 (5)
C2	O2	1.202 (4)	C14	C13	C12	107.3 (5)
Co	C11	2.105 (6)	C15	C14	C13	109.8 (6)
Co	C12	2.117 (6)	C14	C15	C11	108.5 (6)
Co	C13	2.099 (6)	C25	C21	C22	108.4 (3)
Co	C14	2.112 (6)	C21M	C21	C22	126.8 (3)
Co	C15	2.103 (6)	C21M	C21	C25	123.7 (3)
Co	C1	1.850 (4)	C23	C22	C21	107.4 (3)
Co	C2	1.654 (3)	C22M	C22	C21	128.0 (3)
Co	R1	1.748	C22M	C22	C23	123.7 (3)
C11	C12	1.376 (9)	C24	C23	C22	107.7 (3)
C11	C15	1.388 (9)	C23M	C23	C22	123.8 (3)
C22	C22M	1.507 (6)	C23M	C23	C24	128.2 (3)
C12	C13	1.452 (9)	C25	C24	C23	107.4 (3)
C22	C23	1.419 (5)	C24M	C24	C23	125.5 (3)
C13	C14	1.367 (9)	C24M	C24	C25	126.9 (3)
C23	C24	1.406 (5)	C24	C25	C21	109.1 (3)
C14	C15	1.337 (9)	C25M	C25	C21	126.0 (3)
C23	C23M	1.507 (6)	C25M	C25	C24	124.7 (3)
C21	C22	1.407 (5)	C35	C31	C32	109.3 (3)
C24	C25	1.406 (5)	C31M	C31	C32	124.1 (3)
C21	C25	1.377 (5)	C31M	C31	C35	126.5 (3)
C24	C24M	1.502 (6)	C33	C32	C31	108.6 (3)
C21	C21M	1.518 (6)	C32M	C32	C31	126.7 (4)
C31	C32	1.377 (5)	C32M	C32	C33	124.6 (4)
C25	C25M	1.519 (6)	C34	C33	C32	107.2 (3)
C31	C35	1.397 (5)	C33M	C33	C32	126.2 (4)
C31	C31M	1.519 (6)	C33M	C33	C34	126.1 (4)
C32	C33	1.400 (6)	C35	C34	C33	107.2 (3)
C32	C32M	1.505 (7)	C34M	C34	C33	125.1 (4)
C33	C34	1.431 (6)	C34M	C34	C35	126.3 (4)
C33	C33M	1.500 (8)	C34	C35	C31	107.7 (3)
C34	C35	1.405 (5)	C35M	C35	C31	125.0 (4)
C34	C34M	1.500 (7)	C35M	C35	C34	127.1 (4)
C35	C35M	1.510 (7)				

Table 6. Gaussian Amplitudes ( $\times 10^4$ )

Atom	$U_{11}$	$U_{22}$	$U_{33}$	$U_{12}$	$U_{13}$	$U_{23}$
Co	515(3)	416(3)	761(4)	-88(2)	151(2)	28(2)
Sc	305(3)	295(3)	404(3)	31(2)	65(2)	-3(2)
C1	594(21)	337(18)	713(24)	43(16)	89(18)	14(16)
O1	412(11)	334(11)	700(15)	48(9)	140(11)	6(10)
C2	318(16)	599(23)	676(23)	24(15)	147(15)	-14(18)
O2	419(12)	426(13)	793(17)	56(10)	171(11)	-14(12)
C3	786(29)	388(21)	1796(52)	198(20)	392(32)	43(26)
C11	1172(44)	444(25)	1266(49)	-312(27)	363(39)	-22(27)
C12	811(35)	721(33)	1320(50)	-400(28)	-102(34)	182(34)
C13	632(30)	712(32)	1808(63)	-127(24)	498(38)	274(38)
C14	959(41)	1043(43)	1105(44)	-184(33)	395(37)	230(35)
C15	1035(40)	660(31)	1393(56)	-69(29)	245(41)	405(33)
C21	420(17)	589(21)	433(19)	-38(16)	-35(15)	-18(16)
C22	710(23)	366(17)	400(19)	84(16)	-117(17)	-62(14)
C23	450(18)	801(25)	412(19)	159(18)	13(15)	-207(18)
C24	657(22)	489(20)	385(19)	-38(17)	26(16)	66(15)
C25	524(20)	561(21)	499(21)	175(17)	-91(16)	-1(16)
C21M	532(23)	1157(38)	795(31)	-214(24)	20(21)	6(26)
C22M	1588(47)	436(22)	754(29)	291(27)	-311(30)	-163(20)
C23M	735(29)	1623(49)	796(32)	361(31)	138(25)	-505(31)
C24M	1373(44)	844(32)	599(27)	-228(30)	114(28)	209(23)
C25M	881(33)	1039(36)	1154(40)	570(29)	-266(29)	-99(30)
C31	480(19)	675(23)	442(20)	58(17)	-4(15)	-49(17)
C32	730(25)	662(23)	428(20)	240(20)	102(18)	-90(17)
C33	461(20)	1275(38)	444(22)	243(23)	189(17)	142(23)
C34	826(28)	676(25)	349(20)	-311(21)	-13(18)	92(18)
C35	758(25)	511(20)	418(20)	237(19)	30(17)	46(16)
C31M	595(26)	1566(49)	731(31)	-119(28)	-128(23)	-115(30)
C32M	1904(62)	954(36)	787(34)	591(40)	164(38)	-267(28)
C33M	711(33)	3354(98)	857(38)	813(47)	387(30)	383(49)
C34M	2041(64)	1235(44)	576(29)	-1016(43)	-94(34)	297(29)
C35M	1814(59)	1165(40)	710(31)	1041(43)	-94(34)	-16(28)

Table 7. Hydrogen Atom Coordinates ( $\times 10^4$ ) and Bs

Atom	<i>x</i>	<i>y</i>	<i>z</i>	<i>B</i>
H11	203	-2994	-3122	9.0
H12	-2249	-1874	-3487	9.0
H13	-2447	-799	-1865	9.0
H14	-134	-1313	-609	9.0
H15	1463	-2617	-1381	9.0
H31	2824	-2121	-2629	9.0
H32	3944	-1284	-3281	9.0
H33	4603	-1236	-2158	9.0
H211	8232	3871	-2003	9.0
H212	8573	4814	-1094	9.0
H213	7665	5245	-2084	9.0
H221	5752	6277	-1768	9.0
H222	4801	6259	-898	9.0
H223	3768	5914	-1955	9.0
H231	1692	3234	-478	9.0
H232	2558	4702	-300	9.0
H233	1517	4174	-1327	9.0
H241	4333	815	-371	9.0
H242	3569	1701	274	9.0
H243	2498	1081	-724	9.0
H251	7937	2168	-1314	9.0
H252	7305	1576	-427	9.0
H253	6389	983	-1464	9.0
H311	-259	2676	-4418	9.0
H312	175	1800	-5214	9.0
H313	146	1308	-4170	9.0
H321	2196	390	-4758	9.0
H322	4042	332	-4153	9.0
H323	3757	752	-5226	9.0
H331	6561	1888	-3954	9.0
H332	7403	3329	-3559	9.0
H333	6839	2984	-4677	9.0
H341	4946	6016	-3533	9.0
H342	5897	5637	-4310	9.0
H343	6519	5448	-3207	9.0
H351	785	4430	-3577	9.0
H352	1371	5239	-4433	9.0
H353	2328	5582	-3359	9.0



**Table 8.** Selected Least-Squares Planes

Plane 1			
Atom	$\Delta^a$		
C11 <sup>b</sup>	-.004		
C12 <sup>b</sup>	-.000		
C13 <sup>b</sup>	0.005		
C14 <sup>b</sup>	-.008		
C15 <sup>b</sup>	0.007		
Co	1.748		
Plane 2		Plane 3	
Atom	$\Delta^a$	Atom	$\Delta^a$
C21 <sup>b</sup>	-.003	C31 <sup>b</sup>	-.006
C22 <sup>b</sup>	-.002	C32 <sup>b</sup>	-.003
C23 <sup>b</sup>	0.005	C33 <sup>b</sup>	0.010
C24 <sup>b</sup>	-.007	C34 <sup>b</sup>	-.014
C25 <sup>b</sup>	0.006	C35 <sup>b</sup>	0.012
Sc	2.191	Sc	2.198
C21M	-.263	C31M	-.126
C22M	-.235	C32M	-.105
C23M	-.106	C33M	-.109
C24M	-.135	C34M	-.329
C25M	-.054	C35M	-.046
Plane 4			
Atom	$\Delta^a$		
Co <sup>b</sup>	-.068		
C1 <sup>b</sup>	-.010		
C2 <sup>b</sup>	0.021		
O1 <sup>b</sup>	-.044		
O2 <sup>b</sup>	0.061		
C3 <sup>b</sup>	0.065		
Sc <sup>b</sup>	-.025		

<sup>a</sup>Distance from least-squares plane (Å).<sup>b</sup>Atoms defining plane, unit weights.

## REFERENCES

\*Parts of this work have previously been reported: St.Clair, M.A.; Santarsiero, B.D.; Bercaw, J.E. *Organometallics*, **1989**, *8*, 17-22.

1. Collman, J.P.; Hegedus, L.S.; Norton, J.R.; Finke, R.G. "Principles and Applications of Organotransition Metal Chemistry"; University Science Books: Mill Valley, California, 1987.
2. Herrmann, W.A. *Angew. Chem., Intl. Ed. Engl.* **1982**, *21*, 117-130.
3. Kuhlmann, E.J.; Alexander, J. *J. Coord. Chem. Rev.* **1980**, *33*, 195-225. Other reactions besides insertion may occur as well. See, for example, Toreki, R.; LaPointe, R.E.; Wolczanski, P.T. *J. Am. Chem. Soc.* **109**, 1987, 7558-7560.
4. Lauher, J.W.; Hoffman, R. *J. Am. Chem. Soc.* **1976**, *98*, 1729-1742.
5. Hofman, P.; Stauffert, P.; Tatsumi, K.; Nakamura, A.; Hoffmann, R. *Organometallics* **1984**, *4*, 404-406.
6. Rappe, A.K. *J. Am. Chem. Soc.* **1987**, *109*, 5605-5613. Rappe's calculation does put the C-O bond distance of the acyl at 1.27Å; other early transition metal  $\eta^2$  acyls that have been structurally characterized have not exhibited lengthened C-O bonds.
7. Manriquez, J.M.; McAlister, D.R.; Sanner, R.D.; Bercaw, J.E. *J. Am. Chem. Soc.* **1978**, *100*, 2716-2724.
8. Fagan, P.J.; Manriquez, J.M.; Marks, T.J.; Day, V.W.; Vollmer, S.J.; Day, C.S. *J. Am. Chem. Soc.* **1980**, *102*, 7112-7114.
9. Thompson, M.E.; Bercaw, J.E. *Pure & Appl. Chem.* **1984**, *56*, 1-11.
10. Butts, S.B.; Holt, E.M.; Strauss, S.H.; Alcock, N.W.; Stimson, R.E.; Shriver, D.F. *J. Am. Chem. Soc.* **1979**, *101*, 5864-5866.; *ibid.* **1980**, *102*, 5093-5100.

11. Collman, J.P.; Finke, R.G.; Cawse, J.N.; Brauman, J.I. *J. Am. Chem. Soc.* **1978**, *100*, 4766-4772.
12. Gutsche, C.D. "The Chemistry of Carbonyl Compounds"; Prentice-Hall: Englewood Cliffs, New Jersey, 1967; p. 74.
13. Such reactivity has been observed in the reactions of metal acyls with a.) aluminum and b.) zirconium alkyls. a.) Waymouth, R.M.; Grubbs, R.H. *Organometallics* **1988**, *7*, 1631-1635. b.) reference 39.
14. Masters, C.; van der Woude, C.; van Doorn, J.A. *J. Am. Chem. Soc.* **1979**, *101*, 1633-1634.
15. a.) Fischer, E.O., *Adv. Organomet. Chem.*, **1976**, *14*, 1-32. b.) Fischer, E.O.; Kreissl, F.R.; Winkler, E. *Chem. Ber.*, **1972**, *105*, 588-598.
16. a.) Macomber, D. W.; Rogers, R. D. *Organometallics* **1985**, *4*, 1485-1487. b.) Lappert, M. F.; Pyl, P. L. *J. Chem. Soc., Dalton Trans.* **1977**, 2172-2180.
17. a.) Erker, G; Dorf, U.; Benn, R.; Reinhardt, R. *J. Am. Chem. Soc.* **1984**, *106*, 7649-7650. b.) Erker, G.; Lecht, R.; Petersen, J.L.; Bönneman, H. *Organometallics* **1987**, *6*, 1962-1967. c.) Erker, G.; Lecht, R.; Kruger, C.; Tsay, Y.; Bönneman, H. *J. Organomet. Chem.* **1987**, *326*, C75-C78. d.) Metallacyclic carbenes have been proposed as intermediates in the reaction of "Cp<sub>2</sub>TiCH<sub>2</sub>" with M(CO)<sub>6</sub>. Anslyn, E.; Grubbs, R.G. *Organometallics*, **1988**, *7*, 2137-2145.
18. Mashima, K.; Jyodoi, K.; Ohyoshi, A.; Takaya, H. *J. Chem. Soc., Chem. Commun.* **1986**, 1145-1146.
19. a.) Petz, W. *J. Organomet. Chem.* **1974**, *72*, 369-375. b.) Petz, W.; Schmid, G. *Angew. Chem, Intl. Ed.* **1972**, *11*, 934-935.

20. a.) Wolczanski, P.T.; Threlkel, R.S.; Bercaw, J.E. *J. Am. Chem. Soc.* **1979**, *101*, 218-220. b.) Threlkel, R. S., Bercaw, J. E. *J. Am. Chem. Soc.*, **1981**, *103*, 2650-2659.
21. Thompson, M.E.; Bercaw, J.E. unpublished work.
22. a.) Fagan, P.J.; Moloy, K.G.; Marks, T.J. *J. Am. Chem. Soc.* **1981**, *103*, 6959-6962. b.) Fagan, P.J.; Maatta, E.A.; Marks, T.J. In "Catalytic Activation of Carbon Monoxide"; Ford, P.C., ed.; American Chemical Society: Washington, D.C.,1981; Chapter 4.
23. a.) Marsella, J.A.; Caulton, K.G. *J. Am. Chem. Soc.* **1980**, *102*, 1747-1748. b.) Marsella, J.A.; Huffman, J.C.; Caulton, K.G. In "Catalytic Activation of Carbon Monoxide"; Ford, P.C., ed.; American Chemical Society: Washington, D.C.,1981; Chapter 3.
24. Thompson, M.E.; Baxter, S.M.; Bulls, A.R.; Burger, B.J.; Nolan, M.C.; Santarsiero, B.D.; Schaefer, W.P.; Bercaw, J.E. *J. Am. Chem. Soc.* **1987**, *109*, 203-219.
25. Threlkel, R.S.; Bercaw, J.E. *J. Am. Chem. Soc.* **1981**, *103*, 2650-2659.
26. Marsella, J.A.; Curtis, C.J.; Bercaw, J.E.; Caulton, K.G. *J. Am. Chem. Soc.* **1980**, *102*, 7244-7246.
27. Wolczanski, P.T.; Bercaw, J.E. *Acc. Chem. Res.*, **1980**, *13*, 121-127.
28. Evans, W.J.; Wayda, A.L.; Hunter, W.E.; Atwood, J.L. *J. Chem. Soc., Chem. Commun.* **1981**, 706-708.
29. Fachinetti, G.; Fochi, G.; Floriani, C. *J. Chem. Soc., Dalton Trans.* **1977**, 2297-2302.
30. Fachinetti, G.; Fochi, G.; Floriani, C. *J. Chem. Soc., Dalton Trans.* **1977**, 1946-1950.
31. Klei, E.; Teuben, J.H. *J. Organomet. Chem.*, **1981**, *222*, 79-88.

32. Fagan, P.J.; Manriquez, J. M.; Marks, T.J.; Day, V.W.; Vollmer, S.H.; Day, C.S. *J. Am. Chem. Soc.* **1980**, *102*, 5393-5396.
33. Bercaw, J.E.; Davies, D.L.; Wolczanski, P.T. *Organometallics* **1986**, *5*, 443-450.
34. Bulls, A. R., Manriquez, J. M., Thompson, M. E., Bercaw, J. E. *Polyhedron* **1988**, *7*, 1409-1428.
35. See, for example: Connor, J.A.; Fischer, E.O. *J. Chem. Soc. A* **1969**, 578-584.
36. Barger, P.T.; Bercaw, J.E. *Organometallics* **1984**, *3*, 278-284.
37. Burger, B.J., Ph.D dissertation, California Institute of Technology, Pasadena, California, 1987.
38. a.) Fischer, E.O.; Beck, H.J.; Kreiter, C.G.; Lynch, J.; Muller, J; Winkler, E. *Chem. Ber.* **1972**, *105*, 162-172. b.) Fischer, E.O.; Kreissl, F.R.; Winkler, E.; Kreiter, C.G. *Chem. Ber.* **1972**, *105*, 588-598.
39. a.) Edidin, R. T.; Longato, B.; Martin, B. D.; Matchett, S. A.; Norton, J. R. "Organometallic Compounds"; Shapiro, B. L. Ed.; Texas A&M University Press: College Station 1983; p 260-280. b.) Longato, B.; Norton, J. R.; Huffman, J. C.; Marsella, J. A.; Caulton, K. G. *J. Am. Chem. Soc.* **1981**, *103*, 209-210; **1982**, *104*, 6360-6368.
40. Merola, J.S.; Gentile, R.A.; Ansell, G.B.; Modrick, M.A.; Zentz, S. *Organometallics*, **1982**, *1*, 1731-1733.
41. Hamilton, D.M.; Willis, W.S.; Stucky, G.D. *J. Am. Chem. Soc.* **1981**, *103*, 4255-4256.
42. Longato, B.; Martin, B.D.; Norton, J.R.; Anderson, O.P. *Inorg. Chem.*, **1985**, *24*, 1389-1394.
43. Tilley, T.D.; Andersen, R.A. *J. Chem. Soc., Chem. Comm.* **1981**, 985-986.
44. Berry, D.B.; Bercaw, J.E. *Polyhedron* **1988**, *7*, 759-766.
45. St.Clair, M.A.; Santarsiero, B.D. *Acta Crystallographica, Section C*, in press.

46. Beagley, B.; Parrott, C.T.; Ulbrecht, V.; Young, G.G. *J. Mol. Struct.* **1979**, *52*, 47-52.
47. Kemmitt, R.D.W.; Russell, D.R. In "Comprehensive Organometallic Chemistry"; Wilkinson, G., Ed.; Pergamon Press: New York, 1982, Chapter 34.
48. Carre, F.; Cerveau, G.; Colomer, E.; Corriu, R.J.P.; Colin Young, J.; Ricard, L.; Weiss, R. *J. Organomet. Chem.* **1979**, *179*, 215-226.
49. Coleman, A.W.; Hitchcock, P.B.; Lappert, M.F.; Maskell, R.K.; Muller, J. *J. Organomet. Chem.* **1983**, *250*, C9-C14.
50. "Vacuum Line Techniques for Handling Air-Sensitive Organometallic Compounds", Burger, B. J.; Bercaw, J. E. in "New Developments in the Synthesis, Manipulation and Characterization of Organometallic Compounds" Wayda, A. L., Darensbourg, M. Y. eds., *ACS Symposium Series* **1987** *357*, 79-98.
51. Marvich, R.H.; Brintzinger, H.H. *J. Am. Chem. Soc.* **1971**, *93*, 2046-2048.
52. Bunel, E., Ph.D. dissertation, California Institute of Technology, Pasadena, California, 1988.
53. Thomas, J.L. *J. Am. Chem. Soc.* **1973**, *95*, 1838-1848.
54. Green, M.L.H.; Francis, B.R.; Luong-thi, T.; Moser, G.A. *J. Chem. Soc., Dalton Trans.* **1976**, 1339-1345.
55. "International Tables for X-ray Crystallography"; Kynoch Press: Birmingham, 1974; Vol. IV, Table 2.2B, pp. 99-101.

## Chapter 2

### Insertion of CO<sub>2</sub> Into Cp<sup>\*</sup><sub>2</sub>Sc-R Bonds

## INTRODUCTION

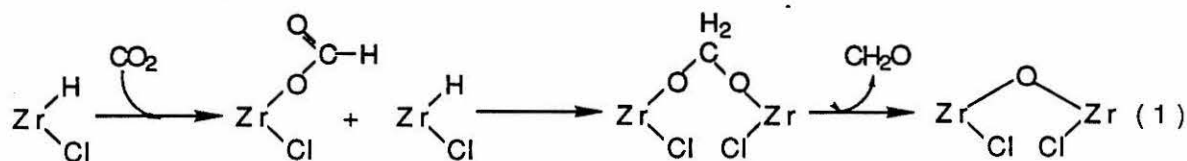
The fixation of carbon dioxide, and its role as a source of carbon for more useful organic molecules, has been a topic of considerable interest in the past decade. Of particular interest is the use of CO<sub>2</sub> in C-C bond forming reactions. As the stable thermodynamic end product of many combustion and respiration reactions, CO<sub>2</sub> is likely to require a significant input of energy in order to convert it to a more desirable molecule. The reactivity of CO<sub>2</sub> can be enhanced substantially, however, by coordination to a transition metal.<sup>1</sup>

As the oxygen in CO<sub>2</sub> is a weak Lewis base and the carbon is somewhat Lewis acidic, there are a number of possible ways for the molecule to bind to a transition metal. While relatively few molecules incorporate CO<sub>2</sub> as an intact ligand, nearly all of the transition metals undergo some type of insertion of CO<sub>2</sub> into metal-carbon or metal-hydrogen bonds. The most common reaction pathway observed is formation of a carboxylate complex, with C-C (or C-H) and M-O bond formation.<sup>2</sup> This is especially true for the early transition metals and f-block elements, in which the oxophilicity of the metal center would be expected to result in strong M-O bonds. While these strong bonds make the early transition metals unlikely candidates for CO<sub>2</sub> catalysis, there have been a number of interesting transformations and a surprising number of coordination modes of CO<sub>2</sub> found in reactions with organometallic compounds of these elements.

Much of the chemistry observed for the reactions of CO<sub>2</sub> with early transition metal organometallics is dependent on whether or not there are d electrons available to carry out reduction chemistry. Though d<sup>1</sup> Cp<sub>2</sub>Ti-R reacts with CO<sub>2</sub> in a straight forward manner to give the carboxylate<sup>3</sup>, the patent literature reports the reaction of Cp<sub>2</sub>Ti(CH<sub>2</sub>)<sub>3</sub>NBu(CH<sub>2</sub>)<sub>2</sub>NBu(CH<sub>2</sub>)<sub>3</sub>TiCp<sub>2</sub> with CO<sub>2</sub> to give (Cp<sub>2</sub>Ti)<sub>2</sub>(C<sub>2</sub>O<sub>4</sub>) via a reductive coupling of CO<sub>2</sub><sup>4</sup>. (Cp<sub>2</sub>TiCl)<sub>2</sub> deoxygenates CO<sub>2</sub> to give CO and the oxo-bridged Cp<sub>2</sub>TiCl dimer, while Cp<sub>2</sub>Ti(CO)<sub>2</sub> disproportionates CO<sub>2</sub> to CO<sub>3</sub><sup>2-</sup> and CO.<sup>5</sup> Cp<sub>2</sub>Zr(CO)<sub>2</sub> deoxygenates CO<sub>2</sub> to CO and yields a cyclic Cp<sub>2</sub>ZrO trimer.<sup>5</sup>



Among  $d^0$  complexes, perhaps the most interesting example of  $\text{CO}_2$  activation is the reaction of two equivalents of  $\text{Cp}_2\text{ZrHCl}$  with  $\text{CO}_2$  to yield formaldehyde and the oxo bridged  $\text{Cp}_2\text{ZrCl}$  dimer (1).<sup>6</sup> The reaction presumably proceeds via initial insertion of



$\text{CO}_2$  into the  $\text{Zr-H}$  bond, followed by intermolecular reduction of the formate species by a second equivalent of  $\text{Cp}_2\text{ZrHCl}$  to give a bridging dioxomethylene unit. This can then lose formaldehyde and form the bridged oxo unit. Less exotic transformations yielding carboxylates occur with the insertion of  $\text{CO}_2$  into one of the  $\text{Ti-C}$  bonds of  $\text{Cp}_2\text{Ti}(\text{CH}_3)_2$ , which may occur thermally<sup>7</sup> or with photochemical activation<sup>8</sup>; and with the insertion of  $\text{CO}_2$  into both actinide- $\text{R}$  bonds of  $\text{Cp}^*_2\text{MR}_2$  ( $\text{M} = \text{U}, \text{Th}$ ;  $\text{R} = \text{H}, \text{CH}_3$ )<sup>9</sup>. Given the diversity of reactivity observed for these types of complexes, it was of interest to investigate the reaction of  $\text{Cp}^*_2\text{Sc-R}$  complexes with  $\text{CO}_2$ .

## RESULTS AND DISCUSSION

$\text{CO}_2$  reacts with  $\text{Cp}^*_2\text{ScH}(\text{THF})$  to give a white insoluble gel. When five equivalents of  $\text{CO}_2$  were placed over a benzene solution and allowed to stir at room temperature for 30 minutes, five equivalents of gas were then collected, through  $0^\circ\text{C}$  traps, with a Toepler pump.  $^1\text{H}$  NMR of the benzene-soluble products of the reaction showed decomposition had occurred. No signals other than residual solvent peaks were observed in a subsequent  $\text{THF-}d_8$  extract. It seems plausible, based on the chemistry cited above, that O abstraction from  $\text{CO}_2$  could be taking place to give  $\text{CO}$  and some type of oxo-bridged Sc polymer. However, the  $^1\text{H}$  NMR of the benzene-soluble fraction indicates that a number of products are being formed, and the reaction was not

investigated further. Similarly, reaction of  $\text{Cp}^*_2\text{ScCH}_3$  with  $\text{CO}_2$  leads to a number of decomposition products, regardless of the conditions used.

As observed for the insertion of  $\text{CO}^{10}$ , insertion of  $\text{CO}_2$  into a Sc-aryl C bond is clean and facile. One equivalent of  $\text{CO}_2$  reacts with  $\text{Cp}^*_2\text{ScC}_6\text{H}_4\text{CH}_3\text{-}p$  at  $-78^\circ\text{C}$  to give the carboxylate  $\text{Cp}^*_2\text{Sc}(\text{O}_2\text{C})\text{C}_6\text{H}_4\text{CH}_3\text{-}p$  in good yield. The carboxylate can also be synthesized by reacting  $p\text{-CH}_3\text{C}_6\text{H}_4\text{COOH}$  with  $\text{Cp}^*_2\text{ScH}(\text{THF})$ . Similarly,  $\text{CS}_2$  also reacts with  $\text{Cp}^*_2\text{ScC}_6\text{H}_4\text{CH}_3\text{-}p$ , albeit more slowly, to give the thiocarboxylate  $\text{Cp}^*_2\text{Sc}(\text{S}_2\text{C})\text{C}_6\text{H}_4\text{CH}_3\text{-}p$ . The carboxylate is unreactive toward excess  $\text{CO}_2$ , and does not react with added  $\text{Cp}^*_2\text{ScH}(\text{THF})$ . The latter lack of reactivity may simply be due to unfavorable steric interactions; alternatively, an  $\eta^1$  carboxylate may be necessary to observe the type of reduction observed in the  $[\text{Cp}_2\text{Zr}]$  system<sup>11</sup>. The Sc carboxylate is even moderately stable to air and water.

The  $^1\text{H}$  NMR of the carboxylate is unexceptional, showing a typical di-substituted aryl pattern with  $J_{\text{HH}} = 8$  Hz. On labelling with  $^{13}\text{CO}_2$ , an additional  $^2J_{\text{CH}}$  coupling of 16 Hz is observed for the ortho hydrogens. The  $^{13}\text{C}$  NMR of the compound shows that the carboxylate resonance at 175.0 ppm is essentially unperturbed relative to benzoic acid, in which the carboxylic acid carbon is found at 172.6 ppm<sup>12</sup>. By analogy to  $\text{Cp}_2\text{Ti}(\text{O}_2\text{C})\text{C}_6\text{H}_5$ <sup>13</sup>, the IR band at  $1425\text{ cm}^{-1}$  can be assigned as the symmetric carboxyl stretching vibration ( $\nu_2$ ), and either  $1490\text{ cm}^{-1}$  or  $1530\text{ cm}^{-1}$  as the asymmetric vibration. As some early transition metal and lanthanide carboxylates bridge two metal centers<sup>14</sup>, a key piece of evidence in establishing the bonding mode is a molecular weight determination. An osmometric molecular weight determination unambiguously shows that, in cyclopentane,  $\text{Cp}^*_2\text{Sc}(\text{O}_2\text{C})\text{C}_6\text{H}_4\text{CH}_3\text{-}p$  is a monomer.

To complete the characterization, an x-ray crystal structure determination was undertaken. An ORTEP drawing of the molecule is shown in Figure 1, and a view of the carboxylate ligand is shown in Figure 2. The ring centroids and the two oxygen atoms are arranged in a pseudo-tetrahedral arrangement around Sc. The carboxylate acts as a

**Figure 1.** An ORTEP drawing of  $\text{Cp}^*_2\text{Sc}(\text{O}_2\text{C})\text{C}_6\text{H}_4\text{CH}_3\text{-}p$

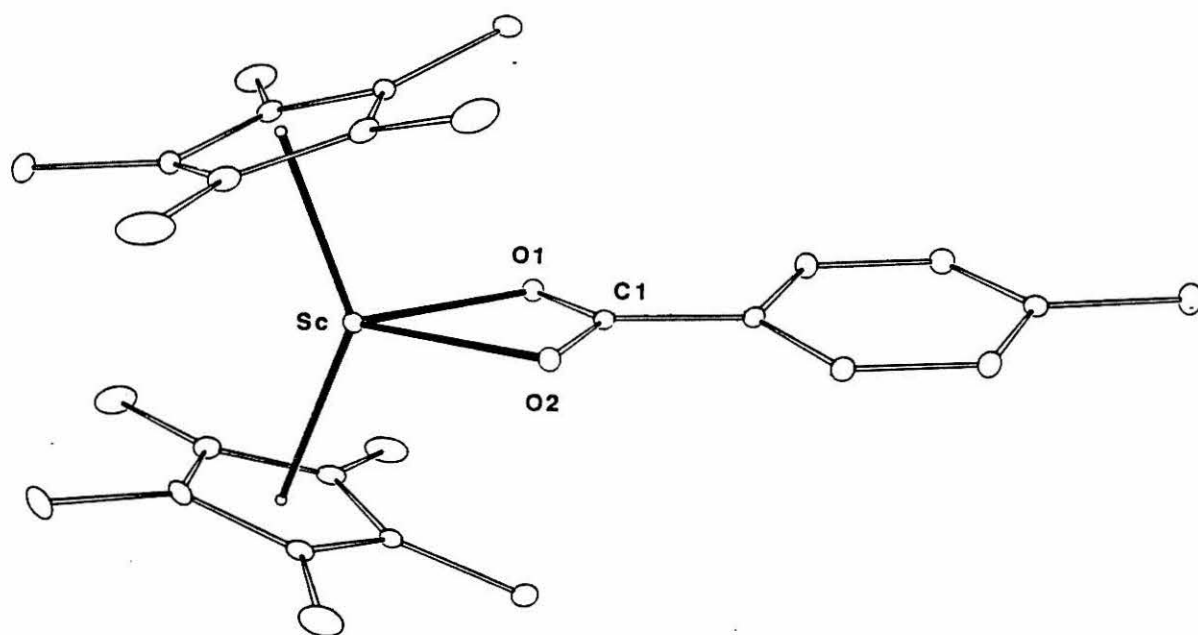
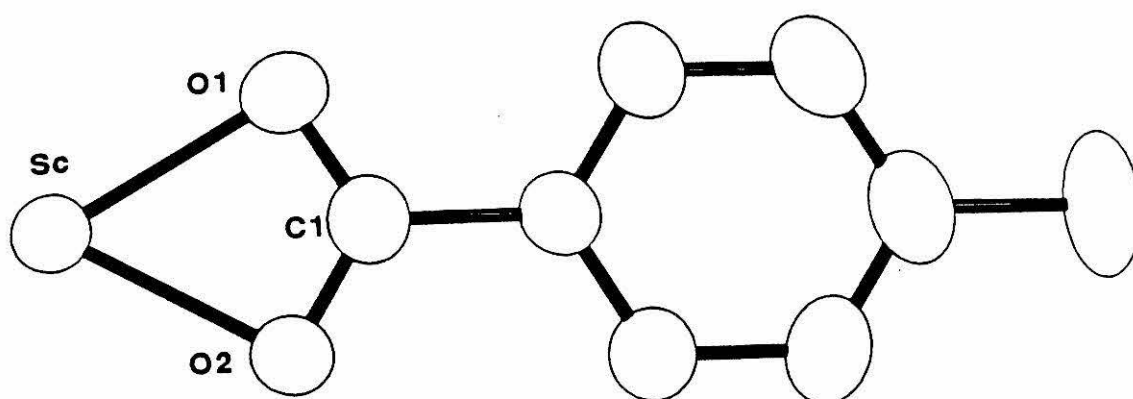


**Figure 2.** Skeletal view of  $\text{Cp}^*_2\text{Sc}(\text{O}_2\text{C})\text{C}_6\text{H}_4\text{CH}_3$ -*p* with  $\text{Cp}^*$ 's removed for clarity



bidentate chelating ligand in the center of the wedge formed by the two  $\text{Cp}^*$  rings. This 16-electron, relatively sterically saturated configuration explains the molecule's stability. The average Sc-O bond length of 2.172Å is slightly shorter than that found in  $\text{Cp}(\text{CO})\text{CoC}(\text{CH}_3)\text{OScCp}^*_2$  (2.199Å). A useful comparison can be made to the similar  $d^1$  complex  $\text{Cp}_2\text{Ti}(\text{O}_2\text{C})\text{C}_6\text{H}_5$ .<sup>15</sup> The average Ti-O bond length of 2.147Å and the O-Ti-O angle of 60.7° are in close agreement with the analogous measurements in the  $d^0$  Sc compound. Interestingly, both of these molecules have a twist about the C1-C2 bond: 10° in the Sc case, and 12° in the Ti case. The centroid-Sc-centroid angle (142.3°), C-C bond distances and angles, and C-H bond lengths and angles are similar to those found in other structurally characterized  $[\text{Cp}^*_2\text{Sc}]$  compounds.<sup>16</sup>

## CONCLUSION

$\text{CO}_2$  reacts readily with  $\text{Cp}^*_2\text{Sc-R}$  ( $\text{R} = \text{H}, \text{CH}_3, \text{C}_6\text{H}_4\text{CH}_3\text{-}p$ ). However, as is the case with the reaction of these complexes with CO, compounds that may be fully characterized are formed only when the R is an aryl group. Insertion of  $\text{CO}_2$  into the Sc-C bond of  $\text{Cp}^*_2\text{ScC}_6\text{H}_4\text{CH}_3\text{-}p$  occurs readily to form a new C-C bond. The product,  $\text{Cp}^*_2\text{Sc}(\text{O}_2\text{C}(\text{C}_6\text{H}_4\text{CH}_3\text{-}p))$ , was characterized by spectroscopic and x-ray crystallographic means.

## EXPERIMENTAL

### General Considerations

All manipulations of air- and/or water-sensitive materials were carried out using high vacuum techniques or in a dry box under an atmosphere of dinitrogen as described elsewhere.<sup>17</sup> Solvents were dried and purified by prolonged reflux over a suitable drying agent followed by distillation under an atmosphere of dinitrogen. Ethereal solvents were stored over sodium benzophenone ketyl, and hydrocarbon solvents were stored over titanocene<sup>18</sup>. Molecular weights were determined using a Signer molecular weight apparatus.<sup>19</sup> *p*-toluic acid (Aldrich) was used as received. CO<sub>2</sub> (Matheson) was frozen at -196°C and pumped on to remove oxygen, and then admitted to the reaction vessel from a trap at -78°C to prevent the transfer of residual water. CS<sub>2</sub> was dried over molecular sieves and vacuum transferred into the reaction vessel. Cp<sup>+</sup><sub>2</sub>ScH(THF)<sup>16a</sup>, Cp<sup>+</sup><sub>2</sub>ScCH<sub>3</sub><sup>16a</sup>, and Cp<sup>+</sup><sub>2</sub>ScC<sub>6</sub>H<sub>4</sub>CH<sub>3</sub>-*p*<sup>16a</sup> were prepared as previously reported. If not otherwise specified, reactivity studies were conducted by placing equimolar amounts of the specified reagents in an NMR tube, dissolving them in C<sub>6</sub>D<sub>6</sub>, and monitoring the reaction by <sup>1</sup>H NMR.

Elemental analyses were provided by the Caltech microanalytical service. Nuclear magnetic resonance spectra were recorded on Varian EM 390, Jeol FX90Q, Bruker WM 500, or Jeol GX400Q spectrometers. Infrared spectra were recorded on a Beckman 4240 spectrometer, and are reported from 2800-1000 cm<sup>-1</sup>. Relative intensities are abbreviated as follows: vs (very strong), s (strong), m (medium), w (weak), bd (broad), sh (shoulder).

Table 1.  $^1\text{H}$  and  $^{13}\text{C}$  NMR Data<sup>a,b</sup>

Compound	Assignment	Shift (ppm)
$\text{Cp}^*_2\text{Sc}(\text{O}_2\text{C})\text{C}_6\text{H}_4\text{CH}_3\text{-}p^c$	$[(\text{CH}_3)_5\text{C}_5]$	1.94 s
	$\text{C}_6\text{H}_4\text{CH}_3$	2.05 s
	$\text{C}_6\text{H}_4\text{CH}_3$	8.30, 6.95 d; dd with $^{13}\text{CO}_2$ ( $J_{\text{HH}} = 8 \text{ Hz}$ , $^2J_{\text{CH}} = 16 \text{ Hz}$ )
	$[(\text{OCH}_3)_5\text{C}_5]$	10.99
	$[(\text{CH}_3)_5\text{O}_5]$	119.46
	$\text{C}_6\text{H}_4\text{CH}_3$	21.43
	$\text{C}_6\text{H}_4\text{CH}_3$	138.54, 129.66, 129.27, 119.41
	$\text{Sc}(\text{O}_2\text{C})$	174.99
$\text{Cp}^*_2\text{Sc}(\text{S}_2\text{C})\text{C}_6\text{H}_4\text{CH}_3\text{-}p^d$	$[(\text{CH}_3)_5\text{C}_5]$	1.86 s
	$\text{C}_6\text{H}_4\text{CH}_3$	2.18 s
	$\text{C}_6\text{H}_4\text{CH}_3$	8.32, 6.96 d( $J_{\text{HH}} = 8 \text{ Hz}$ )

<sup>a</sup> Unless otherwise specified, spectra were obtained in benzene- $d_6$  at ambient temperature, 90 MHz. s = singlet, d = doublet. <sup>b</sup> Chemical shifts are referenced to internal  $\text{Si}(\text{CH}_3)_4$  or to solvent signals and indirectly referenced to  $\text{Si}(\text{CH}_3)_4$ . <sup>c</sup>  $^{13}\text{C}$  spectrum measured at 100.38 MHz. <sup>d</sup> Compound was not isolated.

**$\text{Cp}^*_2\text{Sc}(\text{O}_2\text{C})\text{C}_6\text{H}_4\text{CH}_3\text{-}p$ .** 25 ml of toluene were vacuum transferred onto 250 mg (0.61 mmol) of  $\text{Cp}^*_2\text{ScC}_6\text{H}_4\text{CH}_3\text{-}p$  in a swivel frit assembly. 338 torr x 33.5 ml (0.61 mmol) of  $\text{CO}_2$  was admitted to the solution, which was then stirred at  $-78^\circ\text{C}$  for 30 minutes. The solvent was then removed under vacuum, and 8 ml of petroleum ether distilled in. The frit assembly was cooled to  $-78^\circ\text{C}$ , and the product was filtered. Yield was 139 mg (50%) of a yellow-white crystalline material. Analysis- Calculated for  $\text{C}_{27}\text{H}_{37}\text{O}_2\text{Sc}$ : C, 74.39%; H, 8.29%; Found: C, 74.39%; H, 8.37%. IR: 2725(w), 1960(w), 1620(m), 1575(m), 1530(m), 1490(s), 1425(s), 1295(m), 1175(m), 1110(m), 1038(m). Molecular weight - calculated: 450.56; found: 408.  $\text{Cp}^*_2\text{Sc}(\text{O}_2\text{C})\text{C}_6\text{H}_4\text{CH}_3\text{-}p$  was also synthesized by dissolving 20 mg (0.05 mmol)  $\text{Cp}^*_2\text{ScH}(\text{THF})$  and 7 mg (0.05 mmol) *p*-toluic acid in  $\text{C}_6\text{D}_6$ .

**Cp<sup>+</sup><sub>2</sub>Sc(S<sub>2</sub>C)C<sub>6</sub>H<sub>4</sub>CH<sub>3</sub>-p** 20 mg (0.05 mmol) of Cp<sup>+</sup><sub>2</sub>Sc(S<sub>2</sub>C)C<sub>6</sub>H<sub>4</sub>CH<sub>3</sub>-p were placed in a sealable NMR tube with 0.25 ml of C<sub>6</sub>D<sub>6</sub>. After evacuating the tube, 0.25 ml of CS<sub>2</sub> (4.1 mmol) was vacuum transferred into the tube. The tube was sealed, and the reaction was monitored by <sup>1</sup>H NMR. After two days at room temperature, the <sup>1</sup>H NMR spectra closely resembled that of the analogous CO<sub>2</sub> insertion product.

**X-ray crystal structure determination of Cp<sup>+</sup><sub>2</sub>Sc(O<sub>2</sub>C)C<sub>6</sub>H<sub>4</sub>CH<sub>3</sub>-p.**

A single crystal (dimensions 0.2 x 0.3 x 0.5 mm), grown by slow cooling of a saturated solution of n-pentane, was placed in a glass capillary and sealed under nitrogen. The capillary was mounted on a CAD4 diffractometer equipped with graphite monochromator and MoK $\alpha$  radiation. The preliminary photographic workup indicated space group P2<sub>1</sub>/c (systematic absences: h0l for l odd, 0k0 for k odd) with Z=4. The least squares refinement of the orientation matrix with the setting angles of twenty-five reflections generated the following cell parameters: a = 16.712(3)Å, b = 10.355(2)Å, c = 15.310(2)Å,  $\beta$  = 99.77(1)°, V = 2611.0(8)Å<sup>3</sup>. Intensity data were collected by  $\theta$  - 2 $\theta$  scans of width 1.00° (plus dispersion) at 4°/min for (-h,  $\pm$ k,  $\pm$ l) to 2 $\theta$  = 40° (3,742 reflections). The four check reflections indicated no decomposition. F<sub>o</sub>s were scaled by Wilson plot, and all reflections were reduced to F<sub>o</sub><sup>2</sup>. The form factors were taken from the International Tables for X-Ray Crystallography, IV, Table 2.2B, pp. 99-101.

The coordinates of the scandium atom were derived from the Patterson map, and the remainder of the structure from subsequent F<sub>o</sub> and  $\Delta F$  Fourier maps. The methyl hydrogen atoms were determined from difference density maps, and the phenyl H-atoms were placed at idealized positions assuming trigonal planar geometry, and C-H bond distance = 1.00Å, and isotropic B = 12.0 Å<sup>3</sup>. No H atoms were refined. The full matrix least squares refinement of atom coordinates and U<sub>ij</sub>s of non-hydrogen atoms, the scale factor, and a term for isotropic secondary extinction ( $g = 0.24(5) \times 10^{-6}$ ) minimizing  $\sum w[(F_o)^2 - (F_c/k)^2]^2$  yielded a goodness of fit =  $\{\sum w[(F_o)^2 - (F_c/k)^2]^2 / (n - p)\}^{1/2} =$



1.79 ( $n = 3,742$  reflections,  $p = 281$  parameters),  $R_F = \sum ||F_o| - F_c| / \sum |F_o| = 0.077$  (2,395 reflections,  $I > 0$ ), and  $R'_F = 0.050$  (2,194 reflections,  $I > 3\sigma$ ); the largest peak in the final  $\Delta F$  map was approximately  $0.3 \text{ e}/\text{\AA}^3$ . The labeling scheme is given in Figure 3, atom coordinates and Ueqs for non-hydrogen atoms are given in Table 2, Gaussian amplitudes in Table 3, H atom coordinates in Table 4, and bond lengths and angles are given in Table 5.

Figure 3. Labeling Scheme for  $\text{Cp}^*_2\text{Sc}(\text{O}_2\text{C})\text{C}_6\text{H}_4\text{CH}_3$ -*p*

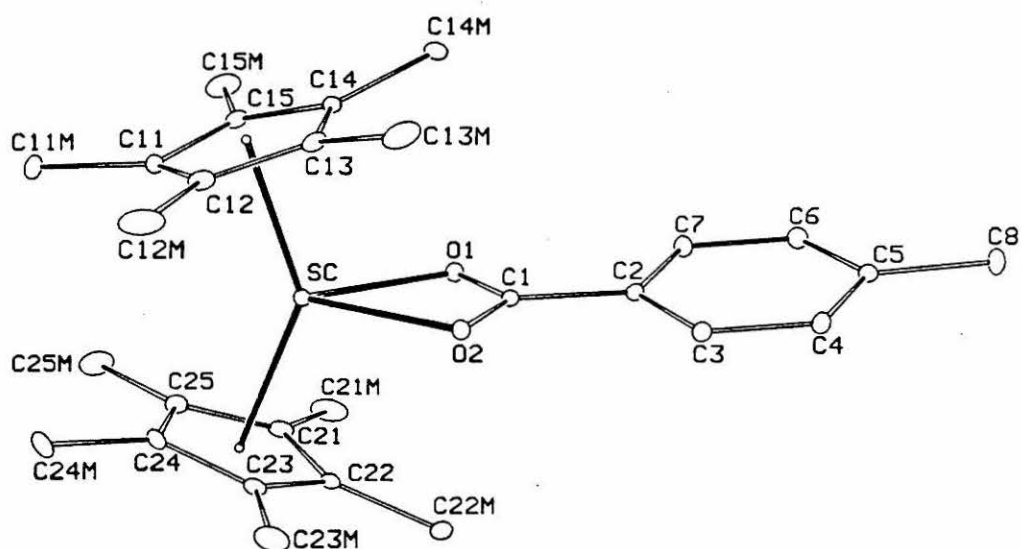


Table 2. Atom Coordinates ( $\times 10^4$ )

Atom	$x$	$y$	$z$	$U_{eq}$ or $B$
Sc	2875(.5)	213(.9)	2143(.6)	454(3)
O1	1886(2)	-764(3)	2618(2)	529(10)
O2	2628(2)	663(3)	3460(2)	532(10)
C1	2063(3)	-175(5)	3348(4)	478(16)
C2	1615(3)	-472(5)	4091(4)	470(16)
C3	1751(3)	261(5)	4856(4)	601(16)
C4	1351(4)	-41(6)	5558(3)	699(18)
C5	831(4)	-1082(6)	5503(4)	652(20)
C6	684(3)	-1789(6)	4723(5)	731(19)
C7	1088(4)	-1487(6)	4022(4)	649(18)
C8	412(3)	-1421(6)	6277(4)	1010(20)
C11	4057(4)	-832(7)	1641(4)	637(19)
C12	4359(3)	-235(6)	2451(6)	703(24)
C13	4022(4)	-872(7)	3104(4)	636(20)
C14	3528(3)	-1837(6)	2710(5)	564(18)
C15	3529(3)	-1812(6)	1804(4)	565(19)
C21	1737(4)	1096(6)	1062(5)	662(22)
C22	1862(4)	1957(6)	1767(4)	600(20)
C23	2623(5)	2519(5)	1796(4)	663(22)
C24	2973(4)	2035(7)	1100(6)	766(23)
C25	2411(6)	1144(7)	644(4)	779(26)
C11M	4391(4)	-701(7)	793(4)	1470(26)
C12M	4978(4)	800(6)	2624(6)	1743(44)
C13M	4222(4)	-626(7)	4089(4)	1363(29)
C14M	3097(4)	-2822(6)	3185(5)	1162(24)
C15M	3088(4)	-2758(6)	1141(4)	1193(25)
C21M	988(4)	306(6)	780(4)	1269(26)
C22M	1278(4)	2311(5)	2371(4)	1016(21)
C23M	3023(4)	3505(6)	2446(4)	1237(29)
C24M	3716(4)	2550(7)	780(5)	1488(27)
C25M	2448(5)	491(8)	-230(4)	1654(40)

$$^a U_{eq} = \frac{1}{3} \sum_i \sum_j [U_{ij} (a_i^* a_j^*) (\vec{a}_i \cdot \vec{a}_j)]$$

\*Isotropic displacement parameter,  $B$

Table 3. Gaussian Amplitudes ( $\times 10^4$ )

Atom	$U_{11}$	$U_{22}$	$U_{33}$	$U_{12}$	$U_{13}$	$U_{23}$
Sc	515(7)	434(7)	424(6)	-25(6)	108(5)	5(6)
O1	578(25)	538(26)	473(25)	-40(19)	93(20)	-44(20)
O2	585(25)	516(25)	522(24)	-109(20)	168(20)	-49(19)
C1	480(39)	455(42)	522(39)	61(35)	149(35)	44(37)
C2	415(36)	473(41)	546(42)	20(33)	148(32)	-6(34)
C3	617(40)	605(42)	616(40)	1(34)	209(34)	-19(38)
C4	772(46)	768(52)	623(41)	89(42)	305(35)	15(40)
C5	628(47)	609(50)	788(53)	153(38)	319(41)	201(42)
C6	746(45)	636(46)	875(51)	-93(35)	323(42)	43(43)
C7	662(44)	665(47)	667(45)	-96(37)	247(36)	14(36)
C8	1015(49)	1222(56)	980(50)	152(43)	706(42)	289(43)
C11	648(47)	653(48)	671(51)	123(37)	286(41)	148(41)
C12	339(38)	513(45)	1218(61)	-117(34)	19(41)	-73(49)
C13	628(46)	720(50)	516(47)	185(38)	-33(38)	-199(41)
C14	647(44)	448(42)	644(49)	88(35)	246(38)	85(40)
C15	590(43)	543(45)	535(48)	90(35)	21(36)	-182(38)
C21	662(53)	473(46)	766(52)	48(41)	-124(45)	74(41)
C22	659(50)	423(42)	760(51)	86(38)	241(40)	167(38)
C23	879(57)	381(42)	730(53)	-16(41)	143(44)	74(35)
C24	738(55)	735(55)	888(61)	103(45)	314(50)	432(47)
C25	1110(68)	791(58)	420(47)	372(52)	87(47)	152(41)
C11M	1785(70)	1659(74)	1294(61)	896(57)	1203(57)	736(54)
C12M	550(45)	775(55)	3731(118)	-216(42)	-135(56)	-9(64)
C13M	1515(63)	1750(74)	619(46)	844(54)	-405(42)	-424(48)
C14M	1225(54)	697(48)	1780(72)	359(43)	875(51)	599(47)
C15M	1286(56)	1006(58)	1130(59)	270(45)	-246(47)	-562(47)
C21M	995(51)	900(54)	1617(66)	-17(48)	-619(48)	127(50)
C22M	1128(53)	812(50)	1255(56)	454(42)	627(46)	342(41)
C23M	1617(68)	596(47)	1403(70)	-307(47)	-15(53)	-93(46)
C24M	1258(59)	1374(67)	2068(83)	287(52)	960(59)	1111(60)
C25M	2728(93)	1706(79)	466(45)	1203(71)	95(51)	55(49)

The form of the displacement factor is:

$$\exp -2\pi^2(U_{11}h^2a^{*2} + U_{22}k^2b^{*2} + U_{33}\ell^2c^{*2} + 2U_{12}hka^*b^* + 2U_{13}h\ell a^*c^* + 2U_{23}k\ell b^*c^*)$$

Table 4. H Atom Coordinates ( $\times 10^4$ )

Atom	<i>x</i>	<i>y</i>	<i>z</i>	<i>B</i>
H81	850	-1760	6810	12.0
H82	-20	-2120	6130	12.0
H83	120	-650	6490	12.0
H111	4680	-1510	710	12.0
H112	4755	75	758	12.0
H113	3926	-594	231	12.0
H121	5510	560	3030	12.0
H122	4770	1590	2910	12.0
H123	5160	1110	2050	12.0
H131	4710	-1190	4350	12.0
H132	3760	-900	4420	12.0
H133	4360	290	4260	12.0
H141	3400	-3610	3300	12.0
H142	2540	-3130	2810	12.0
H143	2950	-2520	3760	12.0
H151	3360	-3620	1130	12.0
H152	3030	-2420	480	12.0
H153	2510	-2920	1240	12.0
H211	610	720	240	12.0
H212	630	180	1270	12.0
H213	1110	-620	600	12.0
H221	1130	3260	2390	12.0
H222	740	1830	2160	12.0
H223	1460	2030	3020	12.0
H231	3010	4350	2140	12.0
H232	3590	3280	2720	12.0
H233	2700	3620	2980	12.0
H241	3640	3490	600	12.0
H242	3830	2040	230	12.0
H243	4220	2450	1240	12.0
H251	2050	920	-740	12.0
H252	2320	-470	-220	12.0
H253	3020	530	-380	12.0
H3	2152	1033	4906	12.0
H4	1419	490	6139	12.0
H6	271	-2578	4665	12.0
H7	970	-2016	3435	12.0

Table 5. Bond Lengths and Angles

Distance(Å)			Angle(°)			
Sc	-O1	2.167(3)	O2	-Sc	-O1	60.9(1)
Sc	-O2	2.176(3)	CP2	-Sc	-CP1	142.3(0)
Sc	-C11	2.485(7)	C1	-O1	-Sc	89.6(3)
Sc	-C12	2.488(7)	C1	-O2	-Sc	89.0(3)
Sc	-C13	2.478(7)	O2	-C1	-O1	120.4(5)
Sc	-C14	2.475(6)	C2	-C1	-O1	120.0(5)
Sc	-C15	2.460(6)	C2	-C1	-O2	119.6(5)
Sc	-C21	2.475(7)	C7	-C2	-C1	120.0(5)
Sc	-C22	2.476(6)	C7	-C2	-C3	120.0(5)
Sc	-C23	2.467(7)	C4	-C3	-C2	119.9(5)
Sc	-C24	2.494(8)	C5	-C4	-C3	120.6(5)
Sc	-C25	2.489(8)	C6	-C5	-C4	118.9(6)
Sc	-CP1	2.178(1)	C8	-C5	-C4	120.2(5)
Sc	-CP2	2.178(1)	C8	-C5	-C6	120.9(5)
O1	-C1	1.264(6)	C7	-C6	-C5	120.3(6)
O2	-C1	1.272(6)	C6	-C7	-C2	120.2(5)
C1	-C2	1.496(8)	C15	-C11	-C12	107.9(6)
C2	-C3	1.382(7)	C11M-C11	-C12		126.4(6)
C2	-C7	1.364(8)	C11M-C11	-C15		124.0(6)
C3	-C4	1.394(8)	C13	-C12	-C11	107.2(6)
C4	-C5	1.378(9)	C12M-C12	-C11		127.9(6)
C5	-C6	1.386(9)	C12M-C12	-C13		124.7(6)
C5	-C8	1.516(9)	C14	-C13	-C12	108.5(6)
C6	-C7	1.398(8)	C13M-C13	-C12		126.0(6)
C11	-C12	1.401(9)	C13M-C13	-C14		125.3(6)
C11	-C15	1.395(9)	C15	-C14	-C13	108.9(6)
C11	-C11M	1.504(9)	C14M-C14	-C13		125.7(6)
C12	-C13	1.394(9)	C14M-C14	-C15		125.3(5)
C12	-C12M	1.481(10)	C14	-C15	-C11	107.5(5)
C13	-C14	1.369(9)	C15M-C15	-C11		127.1(6)
C13	-C13M	1.511(9)	C15M-C15	-C14		125.2(5)
C14	-C15	1.387(8)	C25	-C21	-C22	108.0(6)
C14	-C14M	1.505(9)	C21M-C21	-C22		125.6(6)
C15	-C15M	1.510(9)	C21M-C21	-C25		126.3(6)
C21	-C22	1.390(9)	C23	-C22	-C21	107.9(6)
C21	-C25	1.387(10)	C22M-C22	-C21		127.5(6)
C21	-C21M	1.497(9)	C22M-C22	-C23		124.4(6)
C22	-C23	1.393(9)	C24	-C23	-C22	109.0(6)
C22	-C22M	1.500(9)	C23M-C23	-C22		127.3(6)
C23	-C24	1.392(10)	C23M-C23	-C24		123.7(6)
C23	-C23M	1.501(9)	C25	-C24	-C23	106.5(6)
C24	-C25	1.414(11)	C24M-C24	-C23		126.7(7)
C24	-C24M	1.507(10)	C24M-C24	-C25		125.7(7)
C25	-C25M	1.509(11)	C24	-C25	-C21	108.5(7)
			C25M-C25	-C21		123.4(7)
			C25M-C25	-C24		127.4(7)

## REFERENCES

1. For a recent review of the reactivity of CO<sub>2</sub> with transition metal complexes, see Braunstein, P.; Matt, D.; Nobel, D. *Chem. Rev.* **1988**, *88*, 747-764.
2. Behr, A. *Angew. Chem., Intl. Ed. Engl.* **1988**, *27*, 661-678.
3. a.) Klei, E.; Telgen, J.H.; Teuben, J.H. *J. Organomet. Chem.* **1981**, *209*, 297-307.  
b.) Klei, E.; Teuben, J.H. *J. Organomet. Chem.* **1981**, *222*, 79-88.
4. Froelich, H.O.; Schreer, H. Ger. (East) DD 219 488, 1985; *Chem. Abstr.* **1985**, *103*, 196262z.
5. Fachinetti, G.; Floriani, C.; Chiesi-Villa, A.; Guastini, C. *J. Am. Chem. Soc.* **1979**, *101*, 1767-1775.
6. a.) Fachinetti, G.; Floriani, C.; Roselli, A.; Pucci, S. *J. Chem. Soc., Chem. Commun.* **1978**, 269-270. b.) Gambarotta, S.; Strologo, S.; Floriani, C.; Chiesi-Villa, A.; Guastini, C. *J. Am. Chem. Soc.* **1985**, *107*, 6278-6282.
7. Kolomnikov, I.S.; Lobeeva, T.S.; Vol'pin, M.E. *Zh. Obschch. Khim. (Eng. Trans.)*, **1972**, *42*, 2229-2232.
8. Johnston, R.F.; Cooper, J.C. *Organometallics* **1987**, *6*, 2448-2449.
9. Moloy, K.G.; Marks, T.J. *Inorg. Chim. Acta* **1985**, *110*, 127-131.
10. See Chapter 1 of this thesis.
11. See reference 6 and Cutler, A.; Raja, M.; Todaro, A. *Inorg. Chem.* **1987**, *26*, 2877-2881.
12. Johnson, L.F.; Jankowski, W.C. "Carbon-13 NMR Spectra: A Collection of Assigned, Coded, and Indexed Spectra"; Wiley-Interscience: New York, 1972; p. 230.
13. Coutts, R.S.P.; Wailes, P.C. *Aust. J. Chem.* **1967**, *20*, 1579-1585.

14. See, for example,  $[\text{CpYb}(\text{O}_2\text{Ct-Bu})]_n$ . Tilley, T.D.; Andersen, R.A.; Zalkin, A.; Templeton, D.H. *Inorg. Chem.* **1982**, *21*, 2644-2647.
15. Clauss, A.W.; Wilson, S.R.; Buchanan, R.M.; Pierpont, C.G.; Hendrickson, D.N. *Inorg. Chem.* **1983**, *22*, 628-636.
16. a.)  $\text{Cp}^*_2\text{ScCH}_3$ ,  $\text{Cp}^*_2\text{Sc}(\text{NC}_5\text{H}_5)$ : Thompson, M.E.; Baxter, S.M.; Bulls, A.R.; Burger, B.J.; Nolan, M.C.; Santarsiero, B.D.; Schaefer, W.P.; Bercaw, J.E. *J. Am. Chem. Soc.* **1987**, *109*, 203—219. b.)  $\text{Cp}(\text{CO})\text{CoC}(\text{CH}_3)\text{OScCp}^*_2$ : St.Clair, M.A.; Santarsiero, B.D.; Bercaw, J.E. *Organometallics* **1989**, *8*, 17-22. c.)  $(\text{Cp}^*_2\text{ScC})_2$ : St.Clair, M.A.; Schaefer, W.P.; Bercaw, J.E., manuscript in preparation.
17. "Vacuum Line Techniques for Handling Air-Sensitive Organometallic Compounds", Burger, B. J.; Bercaw, J. E. in "New Developments in the Synthesis, Manipulation and Characterization of Organometallic Compounds" Wayda, A. L., Darensbourg, M. Y. eds., *ACS Symposium Series* **1987** 357, 79-98.
18. Marvich, R.H.; Brintzinger, H.H. *J. Am. Chem. Soc.* **1971**, *93*, 2046-2048.
19. Clark, E.P. *Ind. Eng. Chem., Anal. Ed.* **1941**, *13*, 820.

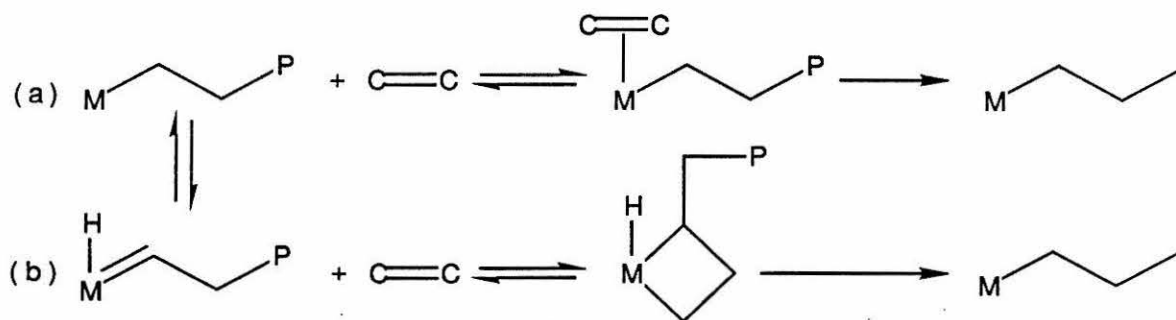


## Chapter 3

### Reaction of Acetylenes with $\text{Cp}^*_2\text{ScR}$

## INTRODUCTION

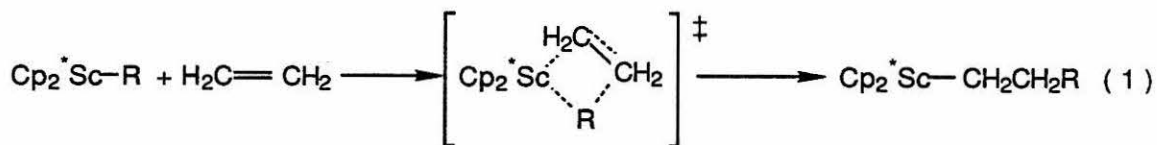
Ziegler-Natta polymerization of olefins is one of the most industrially important carbon-carbon bond forming reactions in use today. Millions of tons of polyethylene and polystyrene are produced each year using these catalysts. The intimate mechanism of these reactions, however, remains in doubt. Two mechanisms are generally proposed as possibilities: the "Cossee" mechanism (a) and the "Green-Rooney" mechanism (b).<sup>1</sup>



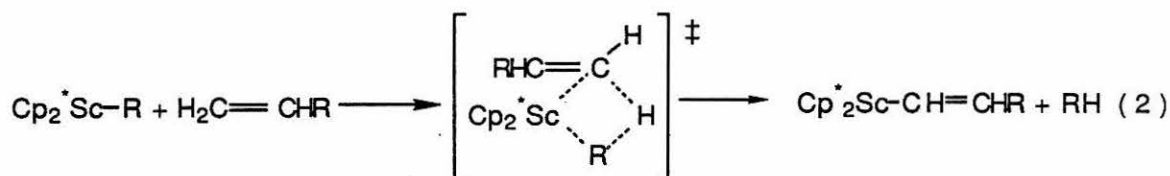
**Scheme 1.**

Schematics of these proposed mechanisms are shown in Figure 1. As the catalysts used in industry are generally heterogeneous, it is difficult to ascertain the nature of the reactive species involved in the reaction, and thus difficult to distinguish between the two mechanisms. As a result, a great deal of effort has been spent in finding homogeneous systems that perform the chemistry of interest, but are also amenable to characterization and spectroscopic observation.  $Cp^*_2Sc-R$  ( $Cp^* = C_5(CH_3)_5^-$ ;  $R =$  alkyl) has proved to be such a system. A number of  $Cp^*_2Sc-R$  derivatives are catalysts for the polymerization of ethylene under mild conditions.<sup>2</sup> The system has been investigated in detail, including studies of how the rate of insertion and the product distribution vary with different  $R$  groups.<sup>3</sup> These studies of the catalytic system, along with stoichiometric model reactions, have yielded a detailed picture of the mechanism of

polymerization of ethylene by  $\text{Cp}^*_2\text{Sc-R}$ . It appears that insertion of ethylene in these



complexes occurs via a highly ordered four-center transition state (the Cossee mechanism), with a significant dependence of rate of initiation (and, thus, molecular weight distribution) on the nature of the Sc-R interaction. Insertion is generally not observed for other  $\alpha$ -olefins, with the exception of the reaction of  $\text{Cp}^*_2\text{Sc-Me}$  with propylene, in which a single insertion is observed. Other  $\alpha$ -olefins (larger than propylene) react with  $\text{Cp}^*_2\text{Sc-R}$  via  $\sigma$ -bond metathesis to yield alkenyl compounds.

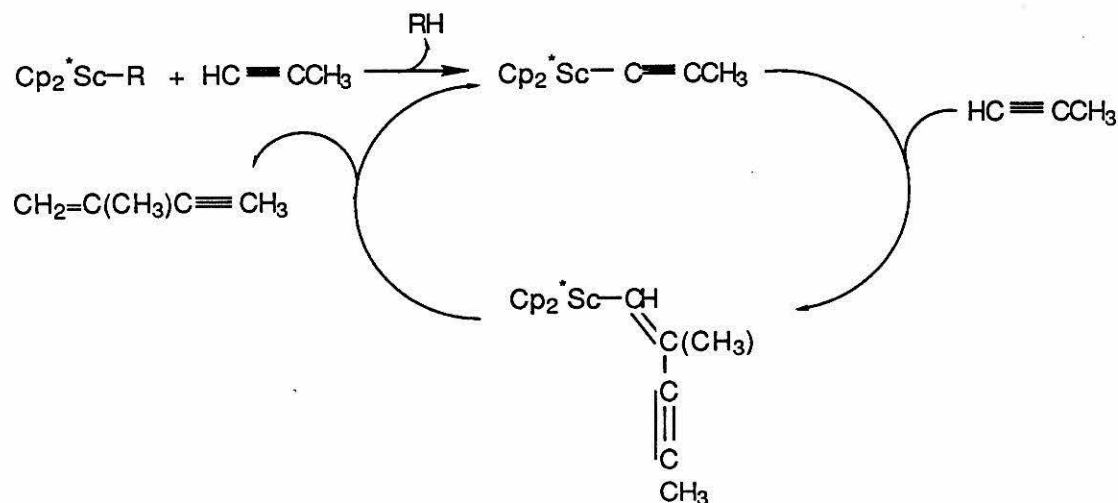


This mode of reactivity, which seems to be pervasive in the chemistry of these compounds, involves: i.) approach of the C-H (or H-H) bond to the  $1a_1$  orbital on Sc; ii.) formation of a four-centered transition state, as illustrated above for H- $\text{sp}^2$  C  $\sigma$ -bond metathesis; and iii.) loss of the new C-H (or H-H) bond from the complex. This picture fits the observed reactivities of  $\text{sp}^3$  C-H <  $\text{sp}^2$  C-H <  $\text{sp}$  C-H < H-H, as increasing non-directional s character improves the bonding in the transition state. In general, unless the substrate is small enough to fit in the wedge and allow the metal center to interact with the  $\pi$  system, the Sc will react via  $\sigma$ -bond metathesis.<sup>2</sup>

Ziegler-Natta catalysts are also widely used for the polymerization of alkynes. Interest in the polymerization of acetylenes has increased significantly since 1971, when Shirikawa and Ikeda showed that the Ziegler catalyst  $\text{Ti}(\text{OBu})_4/\text{AlEt}_3$  could be used to polymerize acetylene into free standing films of polyacetylene, which could then be doped to form a conducting polymer.<sup>4</sup> Most Ziegler catalysts also yield benzene,

cyclooctatetraene, styrene, and similar products, with polyacetylene often obtained only as a by-product. Mechanistic study of these systems has been hampered by the paramagnetism of the active species, oligomerization in solution, and the speed with which they polymerize their substrates.<sup>5</sup> A recent NMR study carried out by Yannoni and Katz does indicate that the  $\text{Ti}(\text{OBu})_4/\text{AlEt}_3$  catalyst polymerizes acetylene via simple insertion and not by metallacycle formation.<sup>6</sup> This result points to the Cossee mechanism as the most likely pathway for this early transition metal catalyzed polymerization.

Previous work in these labs has shown that propyne reacts rapidly with  $\text{Cp}^*_2\text{Sc-R}$  to give  $\text{RH}$  and  $\text{Cp}^*_2\text{Sc-C}\equiv\text{C-Me}$ .<sup>2</sup> Insertion into the  $\text{Sc-C}$  bond in  $\text{Cp}^*_2\text{Sc-C}\equiv\text{C-CH}_3$  is then observed. In the presence of excess propyne,  $\sigma$ -bond metathesis subsequently occurs to give the enyne and  $\text{Cp}^*_2\text{Sc-C}\equiv\text{C-Me}$ , thus completing a catalytic cycle for the dimerization of propyne to yield 2-methyl-1-pentene-3-yne. Interestingly,



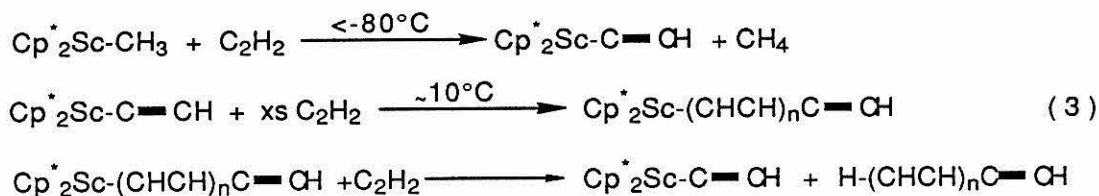
**Scheme 2.**

calculations by Rappe on a model of this system,  $\text{Cl}_2\text{Sc-R}$  ( $\text{R} = \text{H, Me}$ ) +  $\text{C}_2\text{H}_2$ , indicate that for  $\text{R}=\text{H}$ , insertion to give the vinyl compound initially should be favored over  $\sigma$ -bond metathesis to form the acetylide by over 20 kcal/mole. In large part, this

difference in enthalpy is attributed to stabilization gained by formation of a  $\pi$  complex of the acetylene with Sc. In contrast, when  $R=CH_3$ , acetylide formation is slightly favored.<sup>7</sup> As mentioned above, experimentally only acetylide formation is observed. Bergman and Hoffman have suggested that the differences between the two pathways may be dynamic in nature, with the coordination/insertion pathway demanding a very specific orientation, while the direct interaction of a C-H bond with an M-R bond may be more flexible conformationally.<sup>8</sup> Given the variety of reactivities seen in this system, and current interest in synthesis of polyacetylene, we decided to investigate the reactivity of  $C_2H_2$  with a number of  $Cp^*_2Sc$  derivatives. The possibility of C-C bond activation via  $\sigma$ -bond metathesis was also explored. The results of these investigations are reported herein.

## RESULTS AND DISCUSSION

The addition of excess acetylene to a frozen benzene solution of  $Cp^*_2Sc-CH_3$  in an NMR tube yields, on thawing, a black precipitate,  $CH_4$ , and a single organometallic species identified as  $Cp^*_2Sc-C\equiv C-H$ . (In a separate Toepler experiment, the amount of  $CH_4$  given off was found to be 0.95 equivalents (relative to Sc).) Vinylic signals (from  $\delta = 5-6$ ) are also observed in the  $^1H$  NMR, indicating the presence of soluble oligomers of acetylene in addition to the polyacetylene observed as a precipitate. However, in contrast to other Ziegler catalysts, no cyclotrimerization is observed by  $^1H$  NMR for the permethylscandocene system. A variable temperature  $^1H$  NMR study of the reaction



revealed that at  $-80^{\circ}\text{C}$ ,  $\sigma$ -bond metathesis had already occurred to give the acetylide complex. The rate of  $\sigma$  bond metathesis of the  $\text{Sc-C}(\text{sp}^3)$  bond by  $\text{C}_2\text{H}_2$  ( $t_{1/2} < 5$  min at  $-80^{\circ}\text{C}$ ) is comparable to the rate of the H/D exchange reaction of  $\text{Cp}^*_2\text{Sc-H}$  with  $\text{D}_2$ , which occurs quickly at  $-95^{\circ}\text{C}$ .<sup>2</sup> As the solution was warmed, no further reaction occurred until  $10^{\circ}\text{C}$ , at which point free  $\text{C}_2\text{H}_2$  was consumed and vinyl signals began to appear. While insertion of ethylene into  $\text{Sc-C}(\text{sp}^3)$  bonds occurs at a measurable rate at  $-80^{\circ}\text{C}$ ,<sup>3</sup> insertion of acetylene is not observed into the  $\text{Sc-C}(\text{sp})$  bond until  $10^{\circ}\text{C}$ . This is consistent with the finding that the  $\text{Sc-C}(\text{sp})$  bond is at least 45 kcal/mole stronger than the  $\text{Sc-C}(\text{sp}^3)$  bond.<sup>9</sup> Termination presumably occurs via  $\sigma$ -bond metathesis to give  $\text{Cp}^*_2\text{Sc-C}\equiv\text{C-H}$  and a terminal vinyl on the chain.

Polyacetylene formed in this reaction is globular in nature and varies in color depending on the conditions of polymerization. Reaction of  $\text{C}_2\text{H}_2$  with  $\text{Cp}^*_2\text{ScMe}$  generally gave a black precipitate, while  $\text{Cp}^*_2\text{ScH}(\text{THF})$  gave a reddish-black precipitate. No conditions were found, however, that resulted in formation of a film. Indeed, the only condition under which significant amounts of insoluble polyacetylene were formed was when the acetylene was condensed into a sealable NMR tube, sealed, inverted, and allowed to react with the catalyst solution as it thawed. Under other conditions, termination by  $\sigma$ -bond metathesis seems to be competitive with insertion into the  $\text{Sc-vinyl}$  bond, leading to oligomerization rather than longer-chain polymers. In addition, it is believed that in the  $\text{Ti}(\text{OBu})_4/\text{AlEt}_3$  catalytic system the sites involved in polymerization are actually clusters, thus allowing the initiation of several polyacetylene chains within close proximity. This may facilitate the formation of a film, as the polymer chains can then co-crystallize.<sup>5</sup> This is in contrast to the  $\text{Sc}$  system, in which the catalyst site is strictly monomeric due to the steric bulk of the  $\text{Cp}^*$  ligands. The apparent catalyst for this reaction,  $\text{Cp}^*_2\text{Sc-C}\equiv\text{C-H}$ , has been well characterized by

$^1\text{H}$  and  $^{13}\text{C}$  NMR and IR, but cannot be isolated (vide infra). The spectroscopic data shown in Table 1 provide some interesting comparisons.

**Table 1.** Spectroscopic Data on the  $\text{C}\equiv\text{C}\text{-H}$  Unit

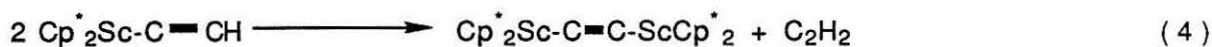
	$\nu(\text{C}\equiv\text{C})$	$J_{\text{C}\alpha\text{-C}\beta}$	Reference
$\text{C}_2\text{H}_2$	1974	172	10
$\text{Cp}^*_2\text{ScCCH}$	2267	87	this work
$\text{Cp}(\text{CO})_2\text{FeCCH}$	1925	-	11
$\text{Cp}_3\text{UCCH}$	2062	-	12
$t\text{-}[(\text{PEt}_3)_2\text{Pt}(\text{CCH})_2]$	1960	-	13
$(\text{nBu})_3\text{SnCCH}$	2010	122	14

The spectroscopic data is of some use in assessing the nature of the  $\text{C}\equiv\text{C}$  bond. The observed  $J_{\text{C}\alpha\text{-C}\beta}$  value is comparable to that of ethylene (67.6 Hz). An increase in the s character of the  $\text{Sc-C}$  bond and a corresponding smaller s character in the  $\text{CC}$  bond may account for the small coupling constant. While the effects are not as large, similar decreases in the  $J_{\text{C-C}}$  are observed upon substitution of tri-alkyl tin for alkyl groups on substituted acetylenes and were attributed to  $p\pi\text{-}d\pi$  bonding between the Sn and the acetylenic C (and thus, presumably also greater s character).<sup>14</sup> A somewhat more reliable indicator of bond strength,  $\nu(\text{C}\equiv\text{C})$ , indicates triple bond character for the  $\text{CC}$  bond in  $\text{Cp}_3\text{UCCH}$ . This is confirmed by the crystal structure of the compound, which shows a  $\text{C}\equiv\text{C}$  distance of 1.27 Å.<sup>15</sup> The  $\nu(\text{C}\equiv\text{C})$  for  $\text{Cp}^*_2\text{Sc-C}\equiv\text{C-H}$  is quite high; this would seem to be in accord with Rappe's calculations on  $\text{Cl}_2\text{Sc-C}\equiv\text{C-H}$ , which predict a  $\text{C}\equiv\text{C}$  bond distance of 1.22 Å.<sup>7</sup>

Acetylene was also reacted with a variety of other  $\text{Cp}^*_2\text{Sc-R}$  derivatives.  $\text{Cp}^*_2\text{ScNMe}_2$  reacts via  $\sigma$ -bond metathesis to give  $\text{Cp}^*_2\text{Sc-C}\equiv\text{C-H}$  and  $\text{H-NMe}_2$ . This reactivity has also been observed for zirconocene and hafnocene compounds, and is used

as a preparation of the bis-alkynyl compounds in those systems.<sup>16</sup> Acetylene reacts with other  $\text{Cp}^*_2\text{ScR}$  ( $\text{R} = \text{C}_6\text{H}_5$ ,  $\text{CMe}=\text{CMe}_2$ ,  $\text{CH}_2\text{Si}(\text{CH}_3)_3$ ) to give  $\text{Cp}^*_2\text{Sc-C}\equiv\text{C-H}$  and the corresponding  $\text{RH}$ . In the presence of excess acetylene, polyacetylene and oligomers are then formed. One equivalent of  $\text{C}_2\text{H}_2$  reacts with  $\text{Cp}^*_2\text{Sc-C}\equiv\text{C-Me}$  to give an approximately 50:50 mixture of  $\text{Cp}^*_2\text{Sc-C}\equiv\text{C-H}$  and  $\text{Cp}^*_2\text{Sc-C}\equiv\text{C-Me}$ . Though the organometallic starting material remains unchanged,  $\text{C}_2\text{H}_2$  reacts with  $\text{Cp}^*_2\text{ScCl}$  to give polyacetylene. In a control experiment in which acetylene was purified in the same manner, placed in an NMR tube at the same concentration, and heated at the same temperature no polymerization was observed.

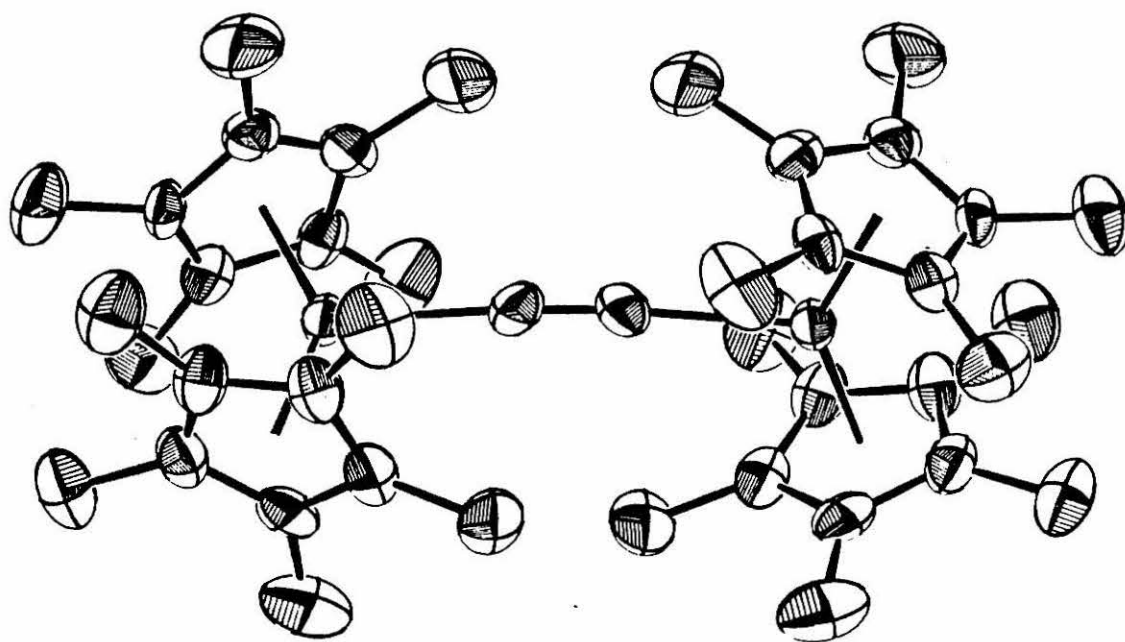
The final organometallic product of the reaction of acetylene with  $\text{Cp}^*_2\text{ScR}$  was also of interest. The product of  $\sigma$ -bond metathesis,  $\text{Cp}^*_2\text{Sc-C}\equiv\text{C-H}$ , which is initially the only organometallic compound observed in solution, reacts over a period of several hours to give a different product. Only a single  $\text{Cp}^*$  signal is observed in the  $^1\text{H}$  NMR. A molecular weight determination indicated that the product was a dimer. No stretches were observed in the characteristic  $\text{C}\equiv\text{C}$  region of the infrared spectrum; however, an intense Raman absorption at  $1899\text{ cm}^{-1}$  signaled the presence of a symmetric  $\text{C}\equiv\text{C}$  bond within the molecule. Attempts to isolate  $\text{Cp}^*_2\text{Sc-C}\equiv\text{C-H}$  give the second product in good yield. Presumably, concentration of the  $\text{Cp}^*_2\text{Sc-C}\equiv\text{C-H}$  solution accelerates the



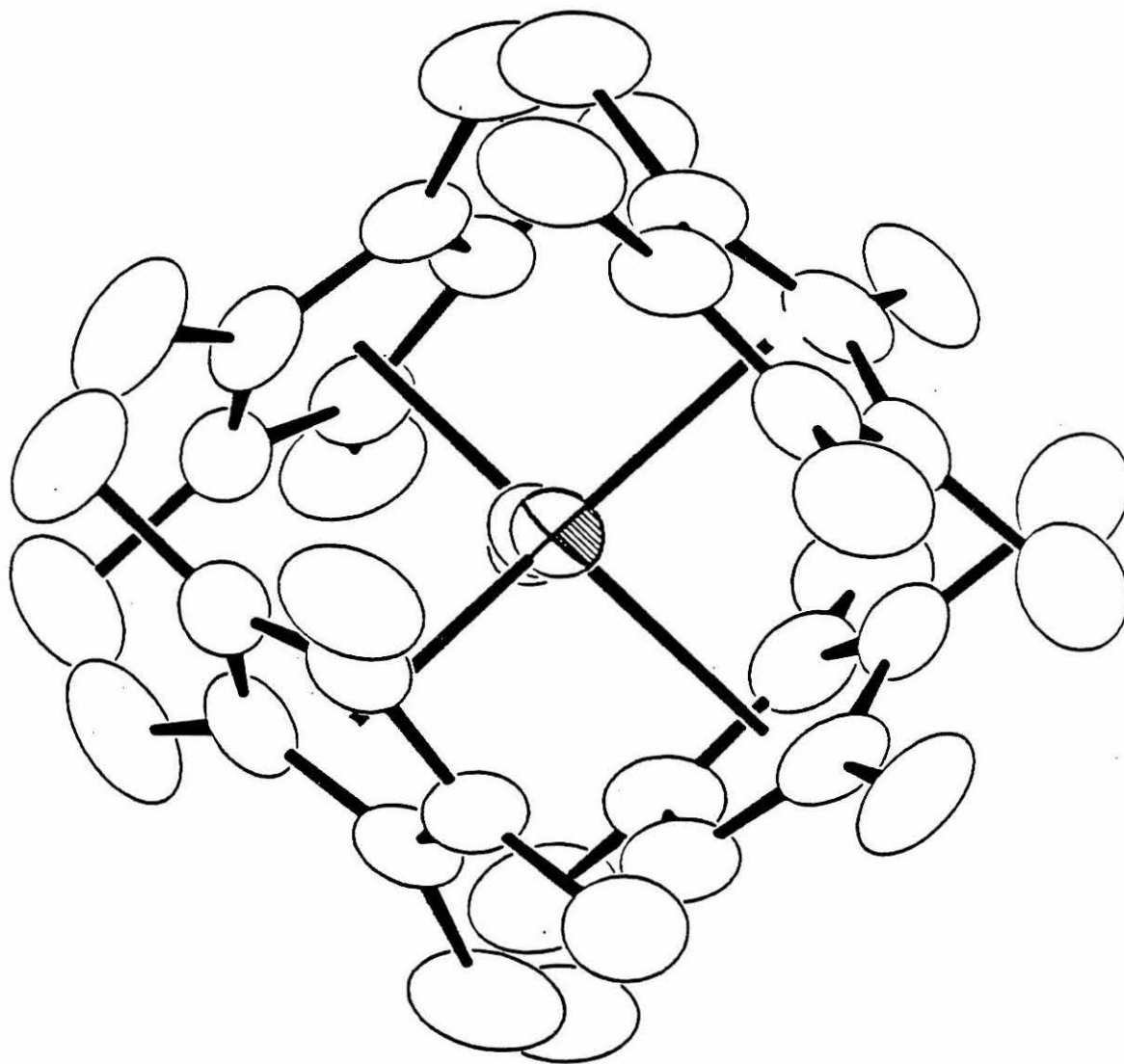
formation of the dimer by  $\sigma$ -bond metathesis of the terminal acetylide H and the  $\text{Sc-C}$  bond. A x-ray crystal structure determination of this molecule was carried out. An ORTEP drawing of the molecule is shown in Figure 1. The molecule crystallizes at a two-fold axis, which relates one  $\text{Cp}^*_2\text{Sc}$  unit and half of the bridging acetylene to the other half-molecule. Notable features are the  $\text{C}\equiv\text{C}$  bond and the staggered confirmation of



Figure 1. An ORTEP drawing of  $\text{Cp}^*_2\text{Sc-C}\equiv\text{C-ScCp}^*_2$ .



**Figure 2.** End view of the staggered  $[\text{Cp}^*_2\text{Sc}]$  units



**Table 2.** Selected Bond Distances and Angles for (Cp\*<sub>2</sub>ScC)<sub>2</sub>

	<u>Distance (Å)</u>		<u>Angle (°)</u>
Sc-Sc	5.600(2)	C1-C1-Sc	175.1(6)
Sc-C1	2.194(7)	CpR1-Sc-CpR2	143.1(1)
Sc-CpR1	2.171	CpR1-Sc-C1	108.7
Sc-CpR2	2.172	CpR2-Sc-C1	108.2
C1-C1	1.224(9)		

the Cp\*<sub>2</sub>Sc units (shown in Figure 2). The C≡C bond length is short, similar to that found in CaC<sub>2</sub> (1.195 Å)<sup>17</sup> and only slightly longer than that found in acetylene itself.<sup>18</sup> The dihedral angle between the two centroid-Sc-centroid planes of nearly 90° is to be expected, both to minimize steric interactions of the Cp\* rings and to maximize overlap with the C≡C p orbitals. The Sc-C-C angle is also close to the expected linear geometry. The M-C≡C-M structure is common among the alkali metals and the noble metals, where it generally results in extended polymeric bonding.<sup>19</sup> However, this structural unit has not previously been reported for early and middle transition metals.<sup>20</sup> There has been interest, however, in incorporating this unit into extended polymeric backbones of the type (M-C≡C-M-C≡C)<sub>n</sub>, where M = Ni, Pd, and Pt.<sup>21</sup> An x-ray crystal structure of [trans-(PMe<sub>3</sub>)<sub>2</sub>IPtC]<sub>2</sub> was recently published, which is the first simple μ<sup>2</sup>:η<sup>1</sup>,η<sup>1</sup> transition metal acetylide structurally characterized.<sup>22</sup> The only other crystallographically characterized M-C≡C-M complexes involve π bonding to the triple bond as well.<sup>23</sup> There are other structurally characterized MCCM units, however. For example, Wolczanski *et al.* have cleaved CO with (silox)<sub>3</sub>Ta (silox = t-Bu<sub>3</sub>SiO<sup>-</sup>) to give a compound formulated as (silox)<sub>3</sub>Ta=C=C-Ta(silox)<sub>3</sub>.<sup>24</sup> The C-C bond length of 1.32 Å supports this picture. (Though not structurally characterized, complexes with bonding believed to be M≡C-C≡M have also been synthesized.<sup>25</sup>) Spectroscopic and structural comparisons of the present work to other C≡C units are given in Table 3. The Sc-C

distance is 2.194 (7) Å, as compared to that found for  $\text{Cp}^*_2\text{Sc-CH}_3$  of 2.243(11)Å<sup>4</sup>. Rappe calculates the Sc-C bond length in  $\text{Cl}_2\text{Sc-CH}_3$  to be 2.17Å and in  $\text{Cl}_2\text{Sc-C}\equiv\text{C-H}$  to be 2.13Å; the same correction of 0.07Å added to his calculations give the experimentally determined numbers for the  $\text{Cp}^*_2\text{Sc}$  compounds.<sup>7</sup> Other features of the structure are similar to those found for other structurally characterized  $\text{Cp}^*_2\text{Sc}$  compounds.<sup>26</sup>

**Table 3.** Spectroscopic and Structural Data on the  $\text{C}\equiv\text{C}$  Unit

	<u><math>\nu(\text{C}\equiv\text{C})</math></u> <sup>1</sup>	<u><math>\delta\text{C}_{\text{acet}}</math></u>	<u><math>d(\text{C}\equiv\text{C})</math></u>	<u>Ref.</u>
$\text{C}_2\text{H}_2$	1947	71.6	1.21	18
$(\text{LiC})_2$	1885	75.0	-	27
$(\text{Cp}^*_2\text{ScC})_2$	1899	179.4	1.224(9)	this wk
$[\text{t}-(\text{PMe}_3)_2\text{IPtC}]_2$	2022	101.9 <sup>2</sup>	1.179(48)	24
$[(\text{Ph}_3\text{P})\text{AuC}]_2$	2040	-	-	28
$\text{t-Pt}(\text{PMe}_2\text{Ph})_2[\text{C}_2\text{W}_2(\text{OBu}^t)_5]_2$ <sup>3</sup>	-	233.9	1.33	25a
$\text{Ru}_4(\text{C}_2)(\text{PPh}_2)(\text{CO})_{12}$ <sup>4</sup>	-	-	1.28	25b

<sup>1</sup> $\nu(\text{C}\equiv\text{C})$  measured using Raman spectroscopy.

<sup>2</sup> $\delta\text{C}_{\text{acet}}$  is for  $[\text{t}-(\text{PMe}_3)_2\text{ClPdC}]_2$ ; <sup>13</sup>C NMR data was not reported for  $[\text{t}-(\text{PMe}_3)_2\text{IPtC}]_2$ .

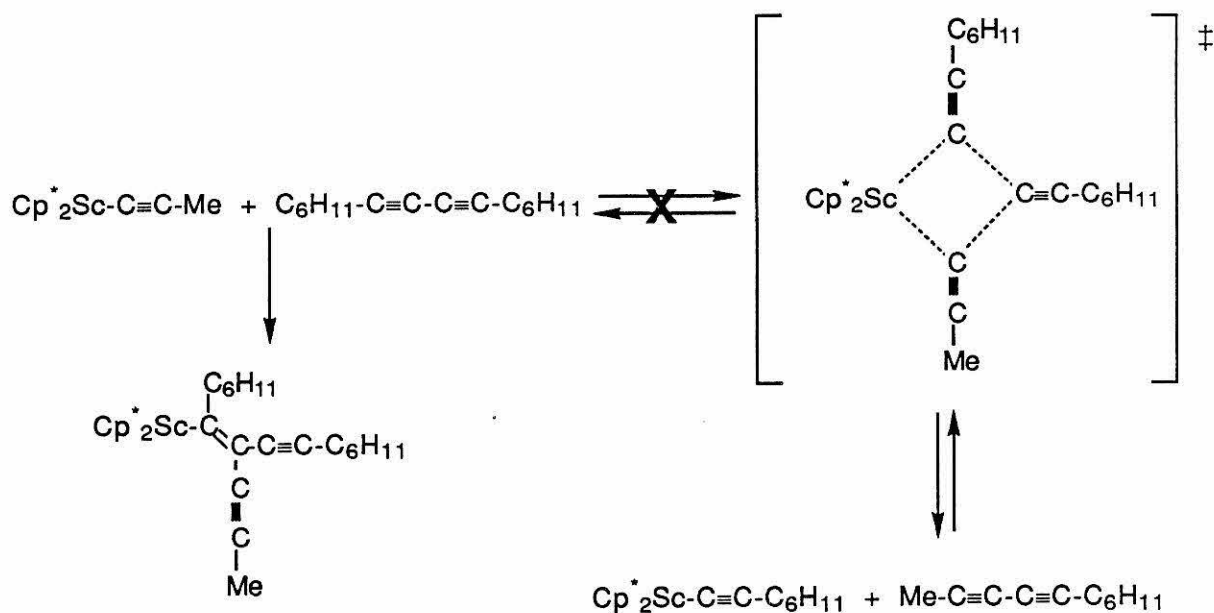
<sup>3</sup>Acetylide is  $\sigma$ -bonded to Pt and one W and  $\pi$ -bonded to one W.

<sup>4</sup>Acetylide is  $\sigma$ -bonded to 2 Ru and  $\pi$ -bonded to 2 Ru.

In view of the dimer's strong Sc-C bonds and its crowded coordination sphere, it is not surprising that its reactivity is somewhat limited. Unlike most other  $\text{Cp}^*_2\text{Sc}$  compounds, it is stable to chlorinated solvents, decomposing slowly at elevated temperatures. There is no apparent reaction with  $\text{H}_2$ , though a degenerate  $\sigma$ -bond metathesis reaction could occur. The dimer does react with excess ethylene at 80°C to give polyethylene; however, the  $\text{Cp}^*$  signal of the starting material remains unchanged.

Reaction with excess acetylene occurs to give  $\text{Cp}^*_2\text{Sc-C}\equiv\text{C-H}$ , which then can react with itself to generate the dimer. (Excess acetylene is polymerized.)

Given the current understanding of  $\sigma$ -bond metathesis, a possibility for C-C bond activation in this system seemed to lie with maximizing the s character of the C-C bonds to be broken and formed in the transition state. Presumably, the transition state consisting of sp carbons in all positions would be the most favorable for C-C  $\sigma$ -bond



**Scheme 3**

metathesis. We thus chose to examine the reaction of  $\text{Cp}^*_2\text{Sc-C}\equiv\text{C-Me}$  with  $\text{C}_6\text{H}_{11}\text{C}\equiv\text{C-C}\equiv\text{CC}_6\text{H}_{11}$ . The product of this reaction was most conclusively characterized by hydrolysis to give the free organic fragment which had a distinctive olefinic hydrogen with a  $^1\text{H}$  NMR  $\delta$  of 6.30. This observation indicates that insertion has occurred rather than C-C  $\sigma$ -bond metathesis.

## CONCLUSIONS

$\text{Cp}^*_2\text{ScR}$  compounds are capable of polymerizing acetylene; however,  $\sigma$ -bond metathesis is competitive with insertion under most conditions, leading to oligomers rather than polymers. The final organometallic product of this reaction,  $\text{Cp}^*_2\text{Sc-C}\equiv\text{C-ScCp}^*_2$ , is the first structurally characterized early transition metal bridging acetylide unit. Attempts to extend the observed chemistry of this system to activate C-C bonds were unsuccessful.

## EXPERIMENTAL

### General Considerations.

All manipulations were performed using glovebox and high vacuum line techniques.<sup>29</sup> Solvents were distilled from an appropriate drying agent under N<sub>2</sub> and stored over sodium/benzophenone or titanocene.<sup>30</sup> Acetylene (Matheson), which is normally stabilized with acetone and/or phosphine, was purified by passing through a trap filled with glass wool cooled to -78°C. **Caution: Acetylene can spontaneously explode at pressures greater than 2 atmospheres.**<sup>31</sup> <sup>13</sup>C<sub>2</sub>H<sub>2</sub> (90%, Stohler-Kor) was used to synthesize samples for <sup>13</sup>C NMR, and was used as received. 2-butyne (Aldrich) was freeze-pump-thawed before use. Diphenyldiacetylene (Farrachan) and dicyclohexyldiacetylene (Professor George Zweifel, UC Davis) were used as received. Cp<sup>\*</sup><sub>2</sub>ScCl<sub>2</sub>, Cp<sup>\*</sup><sub>2</sub>ScMe<sub>2</sub>, Cp<sup>\*</sup><sub>2</sub>Sc-C≡C-Me<sub>2</sub>, Cp<sup>\*</sup><sub>2</sub>ScCMe=CMe<sub>2</sub>, Cp<sup>\*</sup><sub>2</sub>ScC<sub>6</sub>H<sub>5</sub><sub>2</sub>, and Cp<sup>\*</sup><sub>2</sub>ScNMe<sub>2</sub><sup>32</sup>, were prepared by previously published routes. Elemental analyses and mass spectrometric measurements were provided by the Caltech microanalytical service. If not otherwise specified, reactivity studies were carried out by mixing the appropriate reagents in NMR tubes and monitoring the progress of the reaction by <sup>1</sup>H NMR. For example, a typical experiment involved dissolving 20 mg of Cp<sup>\*</sup><sub>2</sub>Sc-C≡C-Me in 0.5 ml C<sub>6</sub>D<sub>6</sub>, condensing Me-C≡C-Me (33.5 ml x 32 torr) into the NMR tube, and sealing the tube at -196°C.

NMR spectra were recorded on Varian EM-390 (<sup>1</sup>H, 90 MHz), JEOL FX-90Q (<sup>1</sup>H, 89.56 MHz), and Jeol GX400Q (<sup>1</sup>H, 400 MHz; <sup>13</sup>C, 100.38 MHz). IR spectra were measured in C<sub>6</sub>D<sub>6</sub> solution or as a Nujol mull and were recorded on a Perkin-Elmer 1600 Series FT-IR. The Raman spectrum was measured on a solid sample in a glass capillary using 488 nm laser excitation and 1 scan.

Table 4.  $^1\text{H}$  and  $^{13}\text{C}$  NMR Data<sup>a,b</sup>

<u>Compound</u>	<u>Assignment</u>	<u>Shift (ppm)</u>
$\text{Cp}^*_2\text{Sc-C}\equiv\text{C-H}^{\text{c,d}}$	$[(\text{CH}_3)_5\text{C}_5]$	1.93 s
	$-\text{C}\equiv\text{C}-\underline{\text{H}}$	2.87 dd ( $J_{\text{CH}}=215$ Hz, $^2J_{\text{CH}}=32$ Hz)
	$[(\underline{\text{C}}\text{H}_3)_5\text{C}_5]$	12.4
	$[(\text{CH}_3)_5\underline{\text{C}}_5]$	121.2
	$\text{Sc-C}\equiv\underline{\text{C}}-\text{H}$	99.0 ( $J_{\text{CC}}=87$ Hz)
$\text{Cp}^*_2\text{Sc-C}\equiv\text{C-ScCp}^*_2^{\text{c}}$	$[(\text{CH}_3)_5\text{C}_5]$	2.05 s
	$[(\underline{\text{C}}\text{H}_3)_5\text{C}_5]$	12.6
	$[(\text{CH}_3)_5\underline{\text{C}}_5]$	120.7
	$\text{Sc}-\underline{\text{C}}\equiv\underline{\text{C}}-\text{Sc}$	179.4

<sup>a</sup> Unless otherwise specified, spectra were obtained in benzene- $\text{d}_6$  at ambient temperature, 90 MHz. s = singlet, d = doublet. <sup>b</sup> Chemical shifts are referenced to internal  $\text{Si}(\text{CH}_3)_4$  or to solvent signals and indirectly referenced to  $\text{Si}(\text{CH}_3)_4$ . <sup>c</sup>  $^{13}\text{C}$  spectrum measured at 100.38 MHz. <sup>d</sup> Compound was not isolated.

$\text{Cp}^*_2\text{Sc-C}\equiv\text{C-H}$  could not be isolated, but was prepared in *situ* by condensing 34.3 torr x 33.5 ml of  $\text{C}_2\text{H}_2$  (0.06 mmol) into a  $\text{C}_6\text{D}_6$  solution of 20 mgs of  $\text{Cp}^*_2\text{ScMe}$  (0.06 mmol) in a sealable NMR tube. IR (soln, NaCl cell): 3265(m), 2907(s), 2861(s), 2267(m), 1928(w), 1489(w), 1436(m), 1380(m), 1025(m).

$\text{Cp}^*_2\text{Sc-C}\equiv\text{C-ScCp}^*_2$  was prepared by placing 420 mg (1.3 mmol) of  $\text{Cp}^*_2\text{ScMe}$  in a flask on a swivel frit assembly in the glove box. 30 ml of petroleum ether were vacuum transferred onto the solid on the vacuum line. 292 torr x 42.2 ml (0.65 mmol) of acetylene were admitted to the stirring solution at  $-78^\circ\text{C}$ , and allowed to stir for 40 minutes. The solution was then filtered at  $-78^\circ\text{C}$ . Yield: 312 mg (71%) of off-white powder. Analysis: calculated, C 77.03, H, 9.24; observed, C, 76.51, H, 9.08.

IR:(Nujol): 2716(w), 1460(s), 1379(s), 1165(w), 1064(w), 1025(m).

**Gas Evolution Measurement of  $\text{Cp}^*_2\text{ScCH}_3 + \text{C}_2\text{H}_2$**  84 mg (0.25 mmol) of  $\text{Cp}^*_2\text{ScCH}_3$  were dissolved in 10 ml of toluene. 319 torr x 42.2 ml (0.71mmol) of



acetylene was admitted to the stirring solution at  $-78^{\circ}\text{C}$  and allowed to warm to room temperature. The solution was then cooled to  $-78^{\circ}\text{C}$ , and gases were collected, through two  $-196^{\circ}\text{C}$  U-tubes, in a Toepler pump. 356 torr were collected in a volume of 12.77 ml, which corresponds to 0.95 equivalents of  $\text{gas/Cp}^*\text{ScCH}_3$ . The gas was identified as  $\text{CH}_4$  by mass spectrometry.

### **X-Ray Crystal Structure Determination of $\text{Cp}^*\text{Sc-C}\equiv\text{C-ScCp}^*\text{2} \cdot 1/2$**

**$\text{C}_7\text{H}_8$**  A long prism was cleaved with a razor blade in an argon atmosphere and a fragment was placed in a glass capillary. The crystal was centered on the diffractometer and preliminary cell dimensions plus an orientation matrix were calculated from the setting angles of 25 reflections. Two octants of data were collected and final cell dimensions were obtained from the setting angles of 24 reflections with  $25^{\circ} < \theta < 38^{\circ}$ . The data were corrected for a slight decay (2.2%) and Lorentz and polarization factors plus a Wilson scale factor were applied. The Laue group and the systematic absences in the diffractometer data were only consistent with the non-centrosymmetric space group  $\text{P4}_2\text{1c}$ . The scandium atom was located from a Patterson map and the remaining atoms of the molecule found with subsequent structure factor-Fourier cycles. Full matrix least squares converged with an R-index of 15%; the difference map contained many peaks, but none greater than  $|0.75| \text{e}\text{\AA}^{-3}$ . A region of positive density centered at  $1/2, 1/2, 0$  (a 4 point) was interpreted as a disordered toluene molecule<sup>33</sup>; because the atoms of toluene all have z coordinates nearly equal to 0, the disorder is effectively four-fold. An idealized toluene was fitted to the map (C-C ring, 1.38Å; C-CH<sub>3</sub>, 1.56Å) with isotropic thermal parameters, B, of  $10\text{\AA}^2$  assigned; the toluene parameters were not refined, but were readjusted once toward the end of the refinement. Hydrogen atoms were introduced on the  $\text{Cp}^*$  methyl groups at idealized positions based on difference maps calculated in the planes where they were expected; they were assigned isotropic thermal parameters of 20% greater than the isotropic thermal parameter of their carbon atom. These hydrogen atoms were also adjusted once toward the end of the refinement. Refinement of

the rest of the scandium dimer concluded smoothly, with the final R index for reflections with  $F_o^2 > 3\sigma(F_o^2)$  being 0.047. The labeling scheme is given in Figure 3, crystal data are given in Table 5, final parameters in Table 6, assigned parameters in Table 7,  $U_{ij}$ s in Table 8, and complete distances and angles in Table 9.

Calculations were done with programs of the CRYM Crystallographic Computing System and ORTEP. Scattering factors and corrections for anomalous scattering were taken from a standard reference.<sup>34</sup>  $R = \Sigma|F_o - |F_c|| / \Sigma F_o$ , for only  $F_o^2 > 0$ , and goodness of fit =  $[\Sigma w(F_o^2 - F_c^2)^2 / (n - p)]^{1/2}$  where n is the number of data and p the number of parameters refined. The function minimized in least squares was  $\Sigma w(F_o^2 - F_c^2)^2$ , where  $w = 1/\sigma^2(F_o^2)$ . Variances of the individual reflections were assigned based on counting statistics plus an additional term,  $0.0014|I|^2$ . Variances of the merged reflections were determined by standard propagation of error plus another additional term,  $0.0014<I>^2$ . The secondary extinction factor<sup>35</sup> refined to  $0.08(6) \times 10^{-6}$ .

**Figure 3.** Labeling Scheme for  $\text{Cp}^*_2\text{Sc-C}\equiv\text{C-ScCp}^*_2$

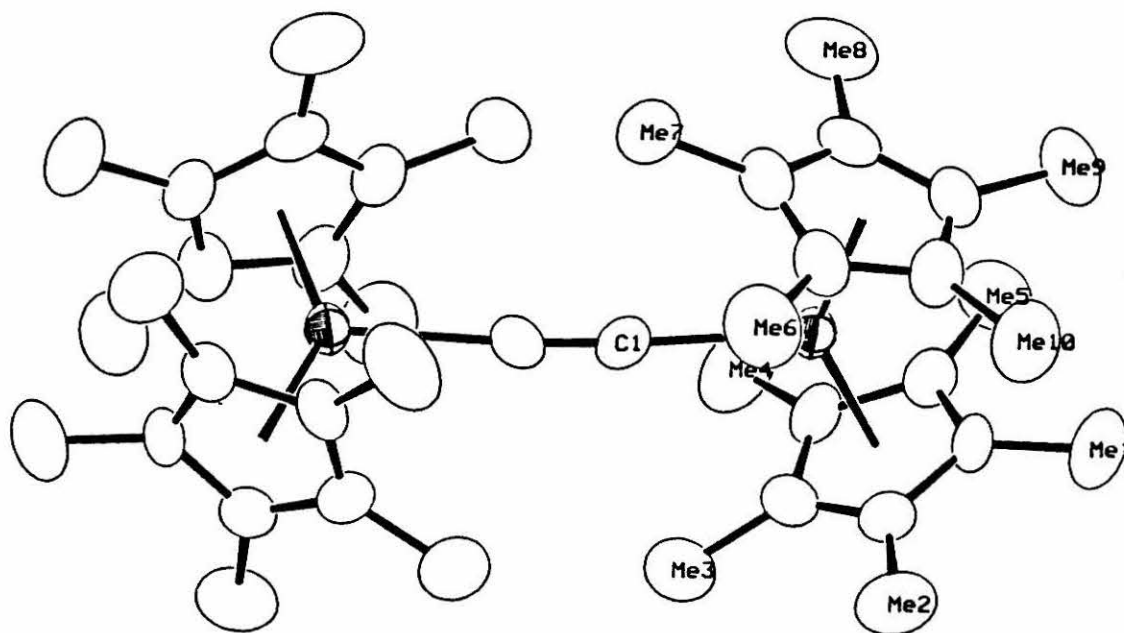


**Table 5.** Crystal and Intensity Collection Data

<b>Formula:</b>	<b>Formula Weight: 700.93</b>
<b>Crystal Color: pale yellow</b>	<b>Habit: prismatic</b>
<b><math>a = 15.057(3) \text{ \AA}</math></b>	
<b><math>c = 18.617(6) \text{ \AA}</math></b>	
<b><math>v = 4220.7(18) \text{ \AA}^3</math></b>	<b><math>z = 4</math></b>
<b><math>\lambda = 0.71073 \text{ \AA}</math></b>	<b>T: 22</b>
<b>Graphite monochromator</b>	
<b>Space group: P4<sub>2</sub>,c</b>	<b>Absences: <math>h00, h = 2n + 1; hhl, l = 2n + 1</math></b>
<b>Crystal Size: .22 x .35 x .48mm</b>	<b><math>\mu = 3.56 \text{ cm}^{-1}</math> (<math>\mu_{\text{rmax}} = 0.11</math>)</b>
<b>CAD-4 Diffractometer</b>	<b><math>\omega</math> scan</b>
<b><math>2\theta</math> range: <math>2^\circ - 40^\circ</math></b>	<b>Octants collected: <math>h, k, \pm l</math></b>
<b>Number reflections measured: 5284</b>	
<b>Number of independent reflections: 1460</b>	
<hr/>	
<b>Number with <math>F_o^2 &gt; 0</math>: 1327</b>	
<b>Number with <math>F_o^2 &gt; 3\sigma(F_o^2)</math>: 894</b>	
<b>Goodness of fit for merging data: 0.967</b>	
<b>Final R-index: 0.0835</b>	
<b>Final goodness of fit: 1.71</b>	

Table 6. Final Atom Coordinates and  $U_{ij}$ s ( $\times 10^4$ )

Atom	$x$	$y$	$z$	$U_{eq}$
Sc	3220(.8)	537(.9)	1529(.8)	370(4)
C1	4616(4)	133(5)	1451(4)	439(21)
Cp1	1852(5)	275(5)	815(4)	409(24)
Cp2	2552(6)	346(6)	326(4)	444(24)
Cp3	3110(5)	-393(6)	427(4)	486(26)
Cp4	2767(5)	-887(5)	997(4)	436(25)
Cp5	1976(5)	-483(5)	1240(4)	437(24)
Me1	1018(5)	840(5)	785(4)	721(29)
Me2	2682(6)	1053(6)	-240(4)	837(32)
Me3	3899(5)	-667(6)	-31(4)	808(28)
Me4	3135(6)	-1757(5)	1285(5)	855(32)
Me5	1350(5)	-864(5)	1787(4)	714(27)
Cp6	3602(6)	2026(5)	1985(5)	502(29)
Cp7	3873(6)	1434(6)	2535(5)	490(26)
Cp8	3095(7)	1027(5)	2785(4)	484(24)
Cp9	2357(6)	1404(6)	2428(5)	500(26)
Cp10	2675(6)	2006(5)	1927(5)	521(29)
Me6	4237(5)	2603(5)	1563(6)	817(28)
Me7	4792(5)	1328(5)	2836(4)	679(27)
Me8	3049(6)	356(6)	3392(5)	889(29)
Me9	1391(5)	1264(6)	2637(4)	720(30)
Me10	2143(5)	2653(5)	1489(5)	794(28)

$$^a U_{eq} = \frac{1}{3} \sum_i \sum_j [U_{ij}(a_i^* a_j^*)(\bar{a}_i \cdot \bar{a}_j)]$$

Table 7. Assigned Atom Coordinates and Bs

Atom	<i>x</i>	<i>y</i>	<i>z</i>	<i>B</i>
C2	4608	4880	31	10.0
C3	5418	4475	95	10.0
C4	6170	5000	104	10.0
C5	6125	5920	48	10.0
C6	5290	6301	-17	10.0
C7	4530	5780	-25	10.0
C8	3741	4310	21	10.0
H 1A	645	717	1197	6.2
H 1B	689	699	360	6.2
H 1C	1171	1450	785	6.2
H 2A	2127	1166	-473	7.9
H 2B	3090	819	-600	7.9
H 2C	2916	1564	-35	7.9
H 3A	4394	-687	213	8.2
H 3B	3925	-221	-431	8.2
H 3C	3733	-1218	-267	8.2
H 4A	3748	-1640	1417	7.8
H 4B	3130	-2170	900	7.8
H 4C	2812	-1945	1675	7.8
H 5A	1679	-1274	2076	6.8
H 5B	898	-1185	1531	6.8
H 5C	1110	-409	2058	6.8
H6AA	4030	3209	1551	7.6
H6AB	4334	2395	1095	7.6
H6AC	4816	2619	1813	7.6
H6BA	4381	3136	1849	7.6
H6BB	4003	2787	1122	7.6
H6BC	4796	2299	1488	7.6
H 7A	4911	1799	3172	6.5
H 7B	5225	1344	2464	6.5
H 7C	4835	772	3087	6.5
H 8A	3638	189	3545	7.4
H 8B	2756	-184	3227	7.4
H 8C	2730	579	3793	7.4
H9AA	1348	693	2904	6.4
H9AB	1006	1253	2256	6.4
H9AC	1219	1716	2985	6.4
H9BA	1382	1136	3168	6.4
H9BB	1146	756	2413	6.4
H9BC	1046	1769	2564	6.4
H10A	1531	2502	1542	7.4
H10B	2330	2641	1021	7.4
H10C	2236	3233	1703	7.4
H10D	1830	3031	1834	7.4
H10E	1734	2344	1213	7.4
H10F	2533	3001	1219	7.4

Table 8. Gaussian Amplitudes ( $\times 10^4$ )

Atom	$U_{11}$	$U_{22}$	$U_{33}$	$U_{12}$	$U_{13}$	$U_{23}$
Sc	284(9)	410(10)	415(8)	28(8)	-25(10)	-26(10)
C1	395(53)	489(47)	434(49)	-26(47)	-97(43)	-28(48)
Cp1	222(46)	471(60)	534(56)	6(48)	-72(52)	-90(47)
Cp2	416(57)	519(67)	397(53)	-64(57)	-44(49)	-15(50)
Cp3	358(57)	686(71)	413(51)	-138(63)	3(51)	-192(54)
Cp4	388(58)	338(55)	581(59)	37(44)	-160(51)	-96(49)
Cp5	388(59)	377(54)	545(58)	-40(51)	-51(47)	32(50)
Me1	433(54)	711(70)	1018(72)	12(54)	-250(58)	-179(59)
Me2	927(81)	968(85)	615(63)	-14(62)	8(60)	355(65)
Me3	657(60)	1152(82)	616(58)	-14(70)	-60(54)	-414(63)
Me4	869(68)	510(57)	1187(97)	11(57)	-375(67)	-64(63)
Me5	673(60)	706(67)	763(68)	-201(53)	102(53)	-40(53)
Cp6	449(64)	361(63)	695(71)	10(51)	79(55)	-63(54)
Cp7	361(58)	512(61)	596(63)	-70(53)	22(56)	-234(53)
Cp8	581(65)	481(53)	391(55)	25(58)	98(60)	-174(46)
Cp9	377(61)	553(64)	570(62)	26(53)	47(56)	-180(53)
Cp10	478(68)	358(61)	727(68)	107(52)	-41(58)	-12(52)
Me6	711(64)	634(59)	1107(77)	-248(54)	98(72)	2(74)
Me7	590(67)	802(70)	645(57)	50(52)	-182(52)	-364(55)
Me8	1154(78)	913(73)	601(55)	-107(67)	149(76)	-189(67)
Me9	472(62)	740(71)	949(73)	-11(52)	165(57)	-164(63)
Me10	759(65)	545(57)	1078(74)	147(50)	-129(71)	-128(68)

The form of the displacement factor is:

$$\exp -2\pi^2(U_{11}h^2a^{*2} + U_{22}k^2b^{*2} + U_{33}l^2c^{*2} + 2U_{12}hka^*b^* + 2U_{13}hla^*c^* + 2U_{23}klb^*c^*)$$

Table 9. Bond Lengths and Angles

Distance(Å)			Distance(Å)		
Sc	-C1	2.194(7)	Me6	-H6AA	0.964(9)
Sc	-Cp1	2.483(8)	Me6	-H6AB	0.937(9)
Sc	-Cp2	2.472(8)	Me6	-H6AC	0.989(9)
Sc	-Cp3	2.490(8)	Me6	-H6BA	0.987(9)
Sc	-Cp4	2.457(8)	Me6	-H6BB	0.936(9)
Sc	-Cp5	2.480(8)	Me6	-H6BC	0.968(9)
Sc	-Cp6	2.465(9)	Me7	-H 7A	0.963(8)
Sc	-Cp7	2.510(9)	Me7	-H 7B	0.951(8)
Sc	-Cp8	2.458(8)	Me7	-H 7C	0.961(8)
Sc	-Cp9	2.488(9)	Me8	-H 8A	0.964(9)
Sc	-Cp10	2.473(8)	Me8	-H 8B	0.975(9)
C1	-C1	1.224(9)	Me8	-H 8C	0.950(9)
Cp1	-Cp2	1.396(11)	Me9	-H9AA	0.995(8)
Cp1	-Cp5	1.401(11)	Me9	-H9AB	0.916(8)
Cp1	-Me1	1.518(11)	Me9	-H9AC	0.974(8)
Cp2	-Cp3	1.407(11)	Me9	-H9BA	1.007(8)
Cp2	-Me2	1.510(12)	Me9	-H9BB	0.946(8)
Cp3	-Cp4	1.396(11)	Me9	-H9BC	0.932(8)
Cp3	-Me3	1.520(12)	Me10	-H10A	0.954(8)
Cp4	-Cp5	1.411(11)	Me10	-H10B	0.916(8)
Cp4	-Me4	1.521(11)	Me10	-H10C	0.970(8)
Cp5	-Me5	1.502(11)	Me10	-H10D	0.979(8)
Me1	-H 1A	0.968(8)	Me10	-H10E	0.928(8)
Me1	-H 1B	0.957(8)	Me10	-H10F	0.933(8)
Me1	-H 1C	0.947(8)	C2	-C3	1.369(0)
Me2	-H 2A	0.956(9)	C2	-C7	1.364(0)
Me2	-H 2B	0.974(9)	C2	-C8	1.563(0)
Me2	-H 2C	0.928(9)	C3	-C4	1.381(0)
Me3	-H 3A	0.874(8)	C4	-C5	1.391(0)
Me3	-H 3B	1.004(8)	C5	-C6	1.387(0)
Me3	-H 3C	0.971(8)	C6	-C7	1.387(0)
Me4	-H 4A	0.971(8)			
Me4	-H 4B	0.949(8)			
Me4	-H 4C	0.919(8)			
Me5	-H 5A	0.957(8)			
Me5	-H 5B	0.961(8)			
Me5	-H 5C	0.925(8)			
Cp6	-Cp7	1.418(12)			
Cp6	-Cp10	1.401(12)			
Cp6	-Me6	1.512(12)			
Cp7	-Cp8	1.402(12)			
Cp7	-Me7	1.501(12)			
Cp8	-Cp9	1.415(12)			
Cp8	-Me8	1.517(12)			
Cp9	-Cp10	1.384(12)			
Cp9	-Me9	1.521(12)			
Cp10	-Me10	1.503(12)			



Table 9. Bond Lengths and Angles (cont.)

Angle(°)				Angle(°)			
C1	-C1	-Sc	175.1(6)	Me6	-Cp6	-Cp7	123.7(8)
Cp5	-Cp1	-Cp2	109.3(7)	Me6	-Cp6	-Cp10	127.1(8)
Me1	-Cp1	-Cp2	123.9(7)	Cp8	-Cp7	-Cp6	105.9(7)
Me1	-Cp1	-Cp5	125.9(7)	Me7	-Cp7	-Cp6	127.0(8)
Cp3	-Cp2	-Cp1	107.6(7)	Me7	-Cp7	-Cp8	126.9(8)
Me2	-Cp2	-Cp1	127.4(7)	Cp9	-Cp8	-Cp7	108.9(7)
Me2	-Cp2	-Cp3	124.9(7)	Me8	-Cp8	-Cp7	125.2(8)
Cp4	-Cp3	-Cp2	107.6(7)	Me8	-Cp8	-Cp9	125.6(8)
Me3	-Cp3	-Cp2	127.4(7)	Cp10	-Cp9	-Cp8	107.9(8)
Me3	-Cp3	-Cp4	124.8(7)	Me9	-Cp9	-Cp8	125.1(8)
Cp5	-Cp4	-Cp3	109.1(7)	Me9	-Cp9	-Cp10	126.4(8)
Me4	-Cp4	-Cp3	126.3(7)	Cp9	-Cp10	-Cp6	107.9(7)
Me4	-Cp4	-Cp5	124.5(7)	Me10	-Cp10	-Cp6	123.9(7)
Cp4	-Cp5	-Cp1	106.4(7)	Me10	-Cp10	-Cp9	127.3(8)
Me5	-Cp5	-Cp1	127.7(7)	H6AA-Me6	-Cp6		110.6(8)
Me5	-Cp5	-Cp4	125.6(7)	H6AB-Me6	-Cp6		112.9(8)
H 1A-Me1	-Cp1		110.2(7)	H6AC-Me6	-Cp6		109.1(8)
H 1B-Me1	-Cp1		109.6(7)	H6BA-Me6	-Cp6		109.0(8)
H 1C-Me1	-Cp1		110.0(7)	H6BB-Me6	-Cp6		112.9(8)
H 1B-Me1	-H 1A		108.2(8)	H6BC-Me6	-Cp6		110.7(8)
H 1C-Me1	-H 1A		109.0(8)	H6AB-Me6	-H6AA		110.1(9)
H 1C-Me1	-H 1B		109.9(8)	H6AC-Me6	-H6AA		105.8(8)
H 2A-Me2	-Cp2		109.2(8)	H6AC-Me6	-H6AB		108.0(8)
H 2B-Me2	-Cp2		107.9(8)	H6BB-Me6	-H6BA		108.3(8)
H 2C-Me2	-Cp2		110.3(8)	H6BC-Me6	-H6BA		105.7(8)
H 2B-Me2	-H 2A		107.7(9)	H6BC-Me6	-H6BB		109.9(9)
H 2C-Me2	-H 2A		111.7(9)	H 7A-Me7	-Cp7		109.6(7)
H 2C-Me2	-H 2B		110.1(9)	H 7B-Me7	-Cp7		111.0(7)
H 3A-Me3	-Cp3		112.6(8)	H 7C-Me7	-Cp7		109.7(7)
H 3B-Me3	-Cp3		105.3(7)	H 7B-Me7	-H 7A		109.1(8)
H 3C-Me3	-Cp3		106.4(7)	H 7C-Me7	-H 7A		108.2(7)
H 3B-Me3	-H 3A		112.1(8)	H 7C-Me7	-H 7B		109.3(8)
H 3C-Me3	-H 3A		115.3(9)	H 8A-Me8	-Cp8		110.6(8)
H 3C-Me3	-H 3B		104.3(8)	H 8B-Me8	-Cp8		110.0(8)
H 4A-Me4	-Cp4		106.2(7)	H 8C-Me8	-Cp8		111.9(8)
H 4B-Me4	-Cp4		107.1(7)	H 8B-Me8	-H 8A		107.0(8)
H 4C-Me4	-Cp4		110.5(8)	H 8C-Me8	-H 8A		109.0(8)
H 4B-Me4	-H 4A		108.5(8)	H 8C-Me8	-H 8B		108.3(8)
H 4C-Me4	-H 4A		111.2(8)	H9AA-Me9	-Cp9		108.1(7)
H 4C-Me4	-H 4B		113.1(8)	H9AB-Me9	-Cp9		114.1(8)
H 5A-Me5	-Cp5		107.6(7)	H9AC-Me9	-Cp9		109.1(7)
H 5B-Me5	-Cp5		107.5(7)	H9BA-Me9	-Cp9		106.9(7)
H 5C-Me5	-Cp5		109.3(7)	H9BB-Me9	-Cp9		111.9(8)
H 5B-Me5	-H 5A		108.8(8)	H9BC-Me9	-Cp9		112.5(8)
H 5C-Me5	-H 5A		111.8(8)	H9AB-Me9	-H9AA		109.3(8)
H 5C-Me5	-H 5B		111.6(8)	H9AC-Me9	-H9AA		104.7(8)
Cp10-Cp6	-Cp7		109.2(8)	H9AC-Me9	-H9AB		111.1(8)

Table 9. Bond Lengths and Angles (cont.)

Angle(°)

H9BB-Me9 -H9BA	105.9(8)
H9BC-Me9 -H9BA	107.0(8)
H9BC-Me9 -H9BB	112.2(8)
H10A-Me10-Cp10	107.6(7)
H10B-Me10-Cp10	109.8(8)
H10C-Me10-Cp10	106.5(7)
H10D-Me10-Cp10	106.1(7)
H10E-Me10-Cp10	109.2(8)
H10F-Me10-Cp10	108.7(7)
H10B-Me10-H10A	113.0(8)
H10C-Me10-H10A	108.2(8)
H10C-Me10-H10B	111.4(8)
H10E-Me10-H10D	109.6(8)
H10F-Me10-H10D	109.3(8)
H10F-Me10-H10E	113.7(9)
C7 -C2 -C3	121.7(0)
C8 -C2 -C3	120.1(0)
C8 -C2 -C7	118.2(0)
C4 -C3 -C2	118.4(0)
C5 -C4 -C3	121.9(0)
C6 -C5 -C4	117.6(0)
C7 -C6 -C5	121.0(0)
C6 -C7 -C2	119.3(0)

## REFERENCES

1. Collman, J.P.; Hegedus, L.S.; Norton, J.R.; Finke, R.G. "Principles and Applications of Organometallic Chemistry", 2nd ed.; University Science Books: Mill Valley, California, 1987, p. 578.
2. Thompson, M.E.; Baxter, S.M.; Bulls, A.R.; Burger, B.J.; Nolan, M.C.; Santarsiero, B.D.; Schaefer, W.P. *J. Am. Chem. Soc.* **1987**, *109*, 203-219.
3. a.) Burger, B.J., Ph.D. Dissertation, California Institute of Technology, Pasadena, California, 1986. b.) Cotter, W.D.; Bercaw, J.E. unpublished results.
4. Ito, T.; Shirakawa, H.; Ikeda, S. *J. Polym. Sci., Polym. Chem. Ed.* **1974**, *12*, 11.
5. Chien, J.C.W. "Polyacetylene: Chemistry, Physics, and Material Science"; Academic Press: Orlando, Florida; 1984.
6. Clarke, T.C.; Yannoni, C.S.; Katz, T.J. *J. Am. Chem. Soc.* **1983**, *105*, 7787-7789.
7. Rappe, A.K., submitted for publication to *Organometallics*.
8. Silvestre, J.; Calhorda, M.J.; Hoffman, R.; Stoutland, P.O.; Bergman, R.G. *Organometallics* **1986**, *5*, 1841-1851.
9. Bulls, A.R.; Bercaw, J.E.; Manriquez, J.M.; Thompson, M.E. *Polyhedron*, **1988**, *7*, 1409-1428.
10. a.) Raman: Herzberg, G. "Infrared and Raman Spectra of Polyatomic Molecules"; D. Van Nostrand & Co.: New York, 1945; p. 288. b.)  $^{13}\text{C}$  NMR: Graham, D.M.; Holloway, C.E. *Can. J. Chem.*, **1963**, *41*, 2114-2118.
11. Davison, A.; Selegue, J.P. *J. Am. Chem. Soc.* **1978**, *100*, 7763-7765.
12. Tsutsui, M.; Ely, N.; Gebala, A. *Inorg. Chem.* **1975**, *14*, 78-81.

13. a.) IR data: Sonogashira, K.; Fujikura, Y.; Yatake, T.; Toyoshima, N.; Takahashi, S.; Hagihara, N. *J. Organomet. Chem.* **1978**, *145*, 101-108. b.)  $^{13}\text{C}$  data: Sebald, A.; Stader, C.; Wrackmeyer, B.; Bensch, W. *J. Organomet. Chem.* **1986**, *311*, 233-242.
14. a.) IR data for  $\text{Me}_3\text{SnC}\equiv\text{C-H}$ : Guillermin, G.; Lequan, M.; Simonnin, M.P. *Bull. Chim. Soc. Fr.* **1973**, 1649-1651. b.)  $^{13}\text{C}$  NMR data: Kamienska-Traler, K. *J. Organomet. Chem.* **1978**, *159*, 15-21.
15. Atwood, J.L.; Tsutsui, M.; Ely, N.; Gebala, A.E. *J. Coord. Chem.*, **1976**, *5*, 209-215.
16. Cardin, D.J.; Lappert, M.F.; Raston, C.L. "Chemistry of Organo-Zirconium and -Hafnium Compounds"; Ellis Horwood Limited: Chichester, U.K., 1986; p.185.
17. Greenwood, N.N.; Earnshaw, A. "Chemistry of the Elements"; Pergamon Press: Oxford, 1986; p. 320.
18. Morrison, R.T.; Boyd, R.N. "Organic Chemistry"; Allyn & Bacon: Boston, 1980; p. 250.
19. Green, M.L.H. "Organometallic Compounds: The Transition Elements", Vol. 2; Methven & Co.: London, 1968; p. 275.
20.  $(\text{Cp}_2\text{TiC}\equiv\text{CTiCp}_2)_n$  is reported by Wailes as the product of the reaction of dimagnesium bromide acetylene with  $\text{Cp}_2\text{TiCl}$  in Wailes, P.C.; Coutts, R.S.P.; Weigold, H. "Organometallic Chemistry of Titanium, Zirconium, and Hafnium"; Academic Press: London, 1974; p. 220. However, the reference given is to "unpublished work" and no characterization is mentioned.
21. Sonogashira, K.; Takahashi, S.; Hagihara, N. *Macromolecules* **1977**, *10*, 879-880.
22. Ogawa, H.; Onitsuka, K.; Joh, T.; Takahashi, S.; Yamamoto, Y.; Yamakazi, H. *Organometallics* **1988**, *7*, 2257-2260.

23. a.) Bruce, M.I.; Snow, M.R.; Tiekink, E.R.T.; Williams, M.L. *J. Chem. Soc., Chem. Commun.*, **1986**, 701-702. b.) Blau, R.J.; Chisholm, M.H.; Folting, K.; Wang, R.J. *J. Chem. Soc., Chem. Commun.*, **1985**, 1582-1584.
24. LaPointe, R.E.; Wolczanski, P.T.; Mitchell, J.F. *J. Am. Chem. Soc.* **1986**, *108*, 6382-6384.
25. Listemann, M.L.; Schrock, R.R. *Organometallics* **1985**, *4*, 74-83.
26. a.)  $\text{Cp}^*_2\text{ScCH}_3$ ,  $\text{Cp}^*_2\text{Sc}(\text{NC}_5\text{H}_5)$ : see reference 2. b.)  $\text{Cp}(\text{CO})\text{CoC}(\text{CH}_3)\text{OScCp}^*_2$ : St.Clair, M.A.; Santarsiero, B.D.; Bercaw, J.E. *Organometallics* **1989**, *8*, 17-22.. c.)  $\text{Cp}^*_2\text{Sc}(\text{O}_2\text{C})\text{p-C}_6\text{H}_4\text{CH}_3$ : *Acta Cryst., Sec. C*, accepted for publication.
27. Rauscher, G.; Clark, T.; Poppinger, D.; Schleyer, P.R. *Angew. Chem., Intl. Ed., Engl.* **1978**, *17*, 276-278.
28. Cross, R.J.; Davidson, M.F. *J. Chem. Soc., Dalton Trans.* **1986**, 411-414.
29. Burger, B.J.; Bercaw, J.E. in "New Developments in the Synthesis, Manipulation, and Characterization of Organometallic Compounds"; Wayda, A. and Darensbourg, M., eds.; ACS Symposium Series, **1987**, *357*, 79-98.
30. Marvich, R.H.; Brintzinger, H.H. *J. Am. Chem. Soc.* **1971**, *93*, 2046-2048.
31. See Chien's book (reference 5) for more details of acetylene purification.
32. Bercaw, J.E.; Davies, D.L.; Wolczanski, P.T. *Organometallics* **1986**, *5*, 443-450.
33.  $^1\text{H}$  NMR of the remaining crystals confirmed the presence of a toluene of crystallization.
34. "International Tables for X-ray Crystallography"; Kynoch Press: Birmingham, 1974; Vol. IV, pp. 71, 149.
35. Larson, E.C. *Acta Cryst.* **1967**, *23*, 664, eqn. 3.

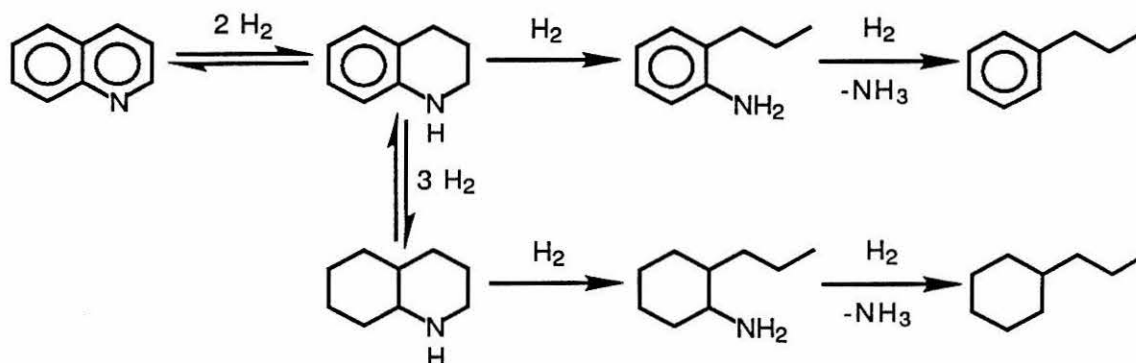
## Chapter 4

### Synthesis and Reactivity of $\text{Cp}^*_2\text{Ta}(\eta^2\text{-H}_2\text{C=NR})\text{H}$ and $\text{Cp}^*_2\text{Ta}(=\text{X})\text{H}$

## INTRODUCTION

Aside from interest in the late 1970s that was focused on "syn-gas" chemistry, the main thrust in organometallic research in the past decade has been in the area of C-H bond activation.<sup>1</sup> Recently, however, there has been considerable interest in organometallic reactions involving heteroatom (O, S, N, P) bonds to transition metals.<sup>2</sup> Much of this work involves attempts to model industrially important processes such as oxidation, hydrodenitrogenation (HDN), and hydrodesulfurization (HDS) and catalytic processes in metalloenzymes such as cytochrome P-450 and nitrogenase. In both the industrial and biological cases, reactive sites are often ill-defined and reaction conditions make detailed study of the processes involved quite difficult. Despite the experimental problems involved in directly probing these reactions, interest in them remains high due to the economic importance of the industrial processes and the ubiquity of the bioinorganic examples. Thus, in order to gain insight into these important types of reactions, it has been necessary to synthesize simpler homogeneous systems that are more amenable to study, but still perform the chemistry of interest.

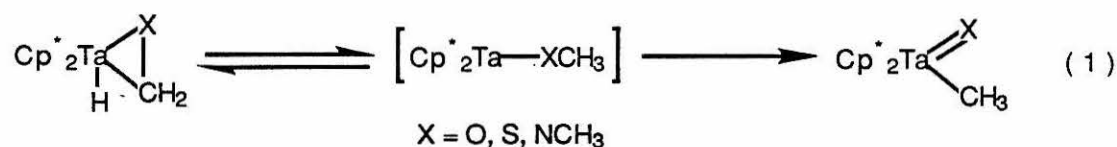
The HDN process is of particular interest to the petrochemical industry, as it removes nitrogen as  $\text{NH}_3$  from crude oil, coal, oil shale, and tar sands in the process of converting these materials to fuels or feed stocks.<sup>3</sup> Complete removal of nitrogen is critical, as it may act as a poison in catalytic processes later in the refining sequence.



Scheme 1.

Cobalt-molybdenum oxide or nickel oxide-molybdenum oxide heterogeneous catalysts are generally used. Studies of the heterogeneous system under working conditions have led to the proposed reaction sequence shown in Scheme 1, with C-N bond cleavage believed to be the rate determining step.<sup>4</sup>

Earlier work in these labs has shown the permethyltantallocene system to be a potentially interesting model for steps in the HDN process.<sup>5</sup> A number of synthetic routes are available to synthesize the  $\eta^2$   $H_2C=X$  species shown below in (1). These species, with heat, cleanly rearrange with cleavage of the C-X bond to give the



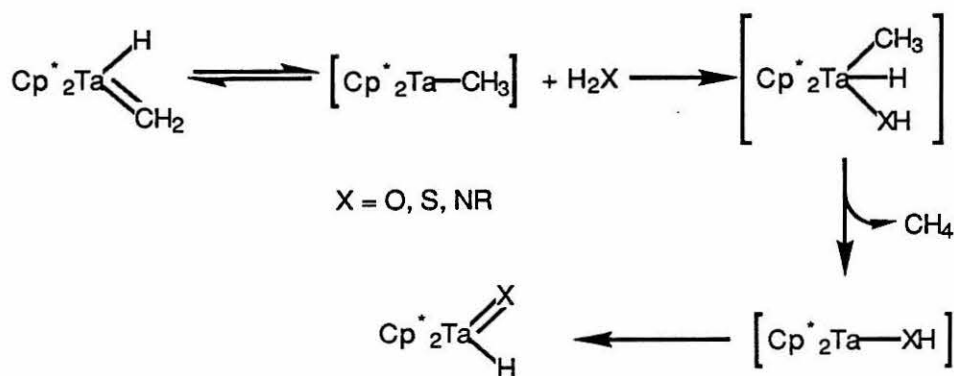
corresponding  $M=X(R)$  species. Similar chemistry has been observed in the thermal decomposition of pentakis(diethylamido)tantalum. Fractional distillation of this compound at temperatures greater than 100°C yields two products:  $(\eta^2\text{-CH}_3\text{CH}_2\text{N=CHCH}_3)\text{Ta}(\text{N}(\text{CH}_2\text{CH}_3)_2)_3$  and the imido  $(\text{CH}_3\text{CH}_2\text{N=})\text{Ta}(\text{N}(\text{CH}_2\text{CH}_3)_2)_3$ .<sup>6</sup> The observation of this type of reaction in the  $\text{Cp}^*_2\text{Ta}$  system suggested that these could serve as model compounds to investigate the mechanistic details of the C-N bond cleavage step. Thus, we decided to attempt to synthesize substituted aryl  $\eta^2$  imine complexes with which we could probe the electronics of this key reaction.

The permethyltantallocene system also offers the opportunity to explore the chemistry of the  $M=X$  unit, where  $X = \text{O, S, and NR}$ . Interest in organometallic oxo chemistry has been quite high in recent years, with the goal of using these species as controllable oxidizing agents<sup>7</sup>, as models for important processes such as alcohol oxidation<sup>8</sup> and, yet more challenging, alkane oxidation<sup>9</sup>. Significant work has also taken place in synthesizing metal oxo models of metalloenzymes such as cytochrome P-450.<sup>10</sup>



Research on metal sulfido species also has a significant bioinorganic component. For example, there has been a substantial amount of work aimed at modeling the reactivity and spectroscopic properties of xanthine oxidase, which is believed to have a  $\text{MoS}_4^{2-}$  in its active site.<sup>11</sup> Organometallic sulfido studies have largely focused on HDS model systems.<sup>12</sup> The study of  $\text{M}=\text{NR}$  has traditionally involved investigation of the role of that functional group in the reduction of dinitrogen; of particular interest in that regard are species such as  $\text{M}=\text{N}-\text{N}=\text{M}$ , which, upon hydrolysis, liberate hydrazine.<sup>13</sup> In recent years there has been significant work aimed at modeling the possible role of surface imido species in the ammoxidation process by which propylene is converted to acrylonitrile.<sup>14</sup>

Earlier work in these labs resulted in the synthesis of the first cis oxo-hydride compound,  $\text{Cp}^*_2\text{Ta}(=\text{O})\text{H}$ , by addition of water to  $\text{Cp}^*_2\text{Ta}(=\text{CH}_2)\text{H}$ , with concomitant loss of methane.<sup>5a</sup> Similarly, the sulfido-hydride  $\text{Cp}^*_2\text{Ta}(=\text{S})\text{H}$ , and numerous imido-hydrides  $\text{Cp}^*_2\text{Ta}(=\text{NR})\text{H}$ <sup>5b</sup> may be synthesized by the addition of  $\text{H}_2\text{X}$  ( $\text{X} = \text{S}, \text{NR}$ ) to

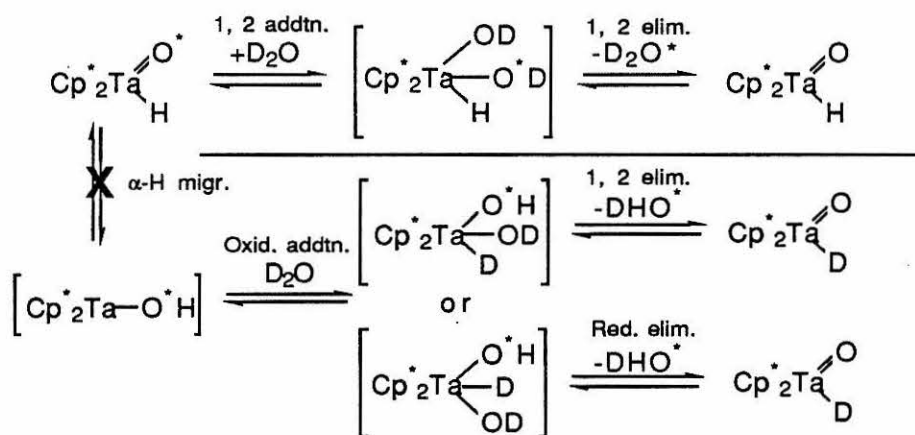


Scheme 2.

$\text{Cp}^*_2\text{Ta}(=\text{CH}_2)\text{H}$ . Alternative routes to some of these compounds have also been developed. And, as illustrated in equation (1), oxo, imido, and sulfido alkyl compounds

are accessible as well. With synthetic routes to these compounds available, we began to explore the reactivity of these compounds.

An intriguing observation by Dr. Ged Parkin first provided an example of what now appears to be one of the dominant modes of reactivity for these compounds. He noted that when  $\text{Cp}^*_2\text{Ta}(=\text{}^{18}\text{O})\text{H}$  is reacted with  $\text{D}_2\text{O}$ , there is facile exchange of  $^{18}\text{O}$ , but no incorporation of D into the organometallic product<sup>15</sup>. As shown in Scheme 3, this observation precludes reaction through an unsaturated 16 electron intermediate as seen for the reactions of water with  $\text{Cp}^*_2\text{Ta}(=\text{CH}_2)\text{H}$ . Instead, it indicates that the reactions



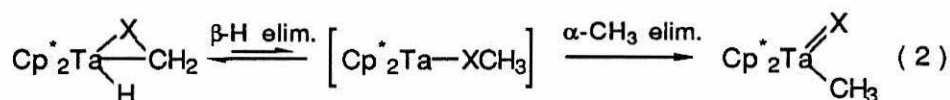
**Scheme 3.**

proceed through a net 1,2 addition/elimination pathway. It is this reaction pathway and its applications on which the second half of this chapter will focus.

## RESULTS AND DISCUSSION

### Synthesis of $\eta^2$ imine complexes

As mentioned earlier,  $(\text{CH}_3)_2\text{NH}$  reacts cleanly with  $\text{Cp}^*_2\text{Ta}(=\text{CH}_2)\text{H}$  to give (via  $\text{Cp}^*_2\text{Ta}-\text{N}(\text{CH}_3)_2$ )  $\text{Cp}^*_2\text{Ta}(\eta^2\text{-H}_2\text{C}=\text{NCH}_3)\text{H}$  and  $\text{CH}_4$ . Thermolysis of this complex results in formation of  $\text{Cp}^*_2\text{Ta}(=\text{NCH}_3)\text{CH}_3$ . It is useful to compare the properties of this system to those of the analogous  $\eta^2$  formaldehyde and thioaldehyde compounds that also have been synthesized with the permethyltantalocene system.<sup>5</sup>

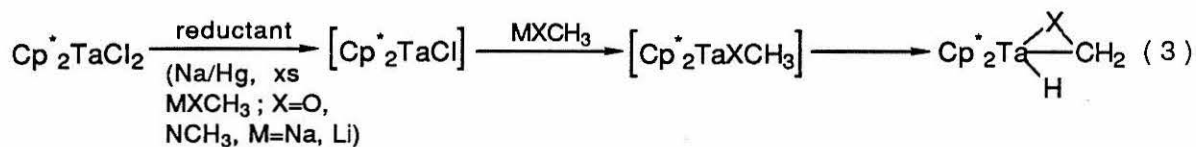


Measurements of magnetization transfer between  $\text{Cp}^*_2\text{Ta}(\text{H}_2\text{C}=\text{X})\text{H}$  and  $\text{Cp}^*_2\text{Ta}(\text{H}_2\text{C}=\text{X})\text{H}$  yield a barrier for  $\beta$ -H migratory insertion. When  $\text{X} = \text{NCH}_3$ , no magnetization transfer is observed up to  $100^\circ\text{C}$ , which indicates a lower limit for  $\Delta G^\ddagger$  of 22 kcal/mol. For comparison, when  $\text{X} = \text{S}$ ,  $\Delta G^\ddagger = 21.3(2)$  kcal/mol, and when  $\text{X} = \text{O}$ ,  $\Delta G^\ddagger = 19(1)$  kcal/mol. Similarly, the  $\Delta G^\ddagger$  for converting  $\text{Cp}^*_2\text{Ta}(\eta^2\text{-CH}_2\text{X})\text{H}$  to  $\text{Cp}^*_2\text{Ta}(=\text{X})\text{CH}_3$  is also highest for  $\text{X} = \text{NCH}_3$  ( $\Delta G^\ddagger = 35.4(1)$  kcal/mol at  $144^\circ\text{C}$ ;  $\text{X} = \text{O}$ ,  $\Delta G^\ddagger = 34.9(2)$  kcal/mol at  $140^\circ\text{C}$ ;  $\text{X} = \text{S}$ ,  $\Delta G^\ddagger = 31.8(1)$  kcal/mol at  $100^\circ\text{C}$ ).<sup>5b</sup> Indeed, while the intermediate  $[\text{Cp}^*_2\text{Ta}-\text{XCH}_3]$  can be trapped by  $\text{CO}$  or  $\text{CNCH}_3$  when  $\text{X} = \text{O}$  or  $\text{S}$ <sup>16</sup>, no trapping is observed when  $\text{X} = \text{NCH}_3$  up to  $140^\circ\text{C}$ .

Our attempts to synthesize aryl analogues of the  $\eta^2 \text{H}_2\text{C}=\text{NCH}_3$  species began with the reaction of  $\text{HN}(\text{CH}_3)(\text{C}_6\text{H}_5)$  with  $\text{Cp}^*_2\text{Ta}(=\text{CH}_2)\text{H}$ . Unfortunately, even with the amine in large excess, prolonged heating gave only "tuck-in" products. Similar behavior was observed with piperidine. Reactions of  $\text{Cp}^*_2\text{Ta}(\text{CH}_2)\text{H}$  with alcohols other than  $\text{CH}_3\text{OH}$  have also been unsuccessful.<sup>16</sup> However,  $\text{HN}(\text{CH}_3)(\text{CH}_2\text{C}_6\text{H}_5)$  does react with  $\text{Cp}^*_2\text{Ta}(=\text{CH}_2)\text{H}$  at  $130^\circ\text{C}$  over a period of days to give, among other products,  $\text{Cp}^*_2\text{Ta}(\eta^2\text{-CH}_2=\text{NCH}_2\text{C}_6\text{H}_5)\text{H}$ . As the N-H bond strengths of amines decrease in the

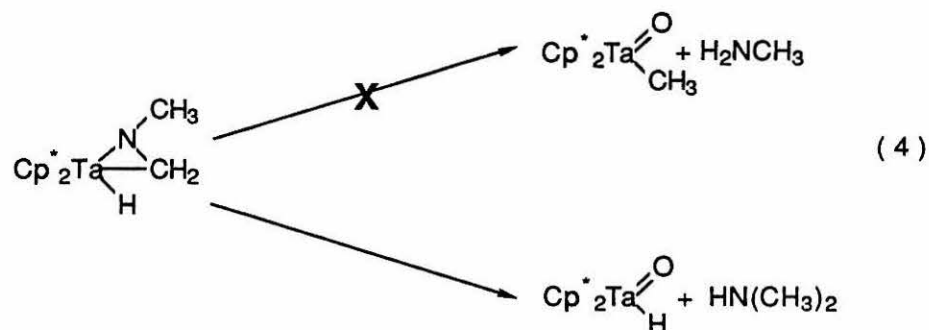
order  $\text{H-NH}_2 > \text{H-N(CH}_3)_2 > \text{H-N(C}_6\text{H}_5)(\text{CH}_3)$ <sup>17</sup>, it appears that perhaps steric factors prevent the formation of the intermediate aryl-alkyl amido complex. In contrast to the methyl-phenyl amine, the benzyl-methyl analogue could place the phenyl ring outside the sterically congested wedge. The 16 e<sup>-</sup> amido intermediate may adopt a configuration similar to that found in  $\text{Cp}^*_2\text{Hf(H)(NHCH}_3)$ , in which the amido group adopts the sterically less favored configuration in order to maximize overlap of the N lone pair with an empty metal orbital.<sup>18</sup>

An alternative route into this type of complex is shown in equation 3. Though direct mechanistic evidence is not yet available, reduction of  $\text{Cp}^*_2\text{TaCl}_2$  to  $\text{Cp}^*_2\text{TaCl}$  with subsequent metathesis to the 16 electron intermediate is a logical pathway to the



observed products. These reduction reactions are extremely condition-dependent. For example, while reduction of  $\text{Cp}^*_2\text{TaCl}_2$  in toluene with  $\text{LiN(CH}_3)_2$  is the preferred synthesis of  $\text{Cp}^*_2\text{Ta}(\eta^2\text{-H}_2\text{C=NCH}_3)\text{H}$ , the same reaction carried out in THF yields a ring cyclometalated complex. Reactions of excess  $\text{LiN(C}_6\text{H}_5)(\text{CH}_3)$  with  $\text{Cp}^*_2\text{TaCl}_2$  in THF, diethyl ether, dioxane, and toluene all led to the cyclometalated product. In the presence of stoichiometric amounts of  $\text{LiN(C}_6\text{H}_5)(\text{CH}_3)$  or  $\text{HN(C}_6\text{H}_5)(\text{CH}_3)$  and excess Na/Hg, the product obtained was the same as that observed from the reaction of  $\text{Cp}^*_2\text{TaCl}_2$  with Na/Hg alone. A weaker reducing agent, Mg, in THF, gave no reaction. Once again, similar results have been observed for reactions of alkoxides (other than methoxide) with  $\text{Cp}^*_2\text{TaCl}_2$ .

While attempts to synthesize the aryl analogue were unsuccessful, the reactivity of  $\text{Cp}^*_2\text{Ta}(\eta^2\text{-H}_2\text{C=NCH}_3)\text{H}$  did prove to be of some interest. Two pathways for the



reaction of water with  $\text{Cp}^*_2\text{Ta}(\eta^2\text{-H}_2\text{C}=\text{NCH}_3)\text{H}$  can be envisaged. Initial protonation of the N could induce cleavage of the C-N bond and migration of the H to the  $\text{CH}_2$ , giving a  $\text{Cp}^*_2\text{Ta}(\text{OH})(\text{NH}(\text{CH}_3))(\text{CH}_3)$  intermediate. This intermediate could then 1,2 eliminate to give the oxo-methyl species. Alternatively, 1,2 addition to the Ta-N bond would give a  $\text{Cp}^*_2\text{Ta}(\text{OH})(\text{CH}_2\text{NH}(\text{CH}_3))(\text{H})$  species, which could then 1,2 eliminate to give  $\text{Cp}^*_2\text{Ta}(=\text{O})\text{H}$ . The same end products could also be obtained by oxidative addition of water to a 16 electron amido intermediate. As shown in equation (5), the oxo-hydride is the only organometallic species observed. And, when  $\text{D}_2\text{O}$  is used, the hydride signal of  $\text{Cp}^*_2\text{Ta}(=\text{O})\text{H}$  is still clearly observable in the  $^1\text{H}$  NMR, while the integrated intensity of the  $\text{HN}(\text{CH}_3)_2$  peak is decreased by  $\sim 1/6$ . This is consistent with the 1,2 addition/elimination mechanism. The formaldehyde-hydride complex,  $\text{Cp}^*_2\text{Ta}(\eta^2\text{-H}_2\text{C}=\text{O})\text{H}$ , also reacts with water, presumably in the same manner, to give  $\text{Cp}^*_2\text{Ta}(=\text{O})\text{H}$ .

Spectroscopic observations in a related system also support the 1,2 addition/elimination mechanism. Reaction of  $\text{Cp}^*_2\text{Ta}(\eta^2\text{-H}_2\text{CNCH}_3)\text{H}$  with  $\text{H}_2\text{S}$  eventually yields  $\text{Cp}^*_2\text{Ta}(=\text{S})\text{H}$  as expected. However, an intermediate species is observed, which increases with depletion of  $\text{Cp}^*_2\text{Ta}(\eta^2\text{-H}_2\text{CNCH}_3)\text{H}$ , and decreases with the production of  $\text{Cp}^*_2\text{Ta}(=\text{S})\text{H}$ . The chemical shifts and intensities observed in the  $^1\text{H}$

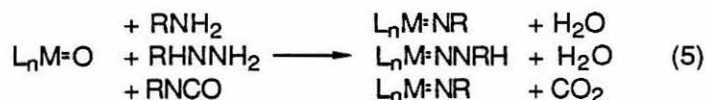
NMR are appropriate for a species such as  $\text{Cp}^*_2\text{Ta}(\text{SH})(\text{CH}_2\text{NH}(\text{CH}_3))(\text{H})$ , analogous to the proposed intermediate in the  $\text{H}_2\text{O}$  reaction.<sup>19</sup>

### Reactions of $\text{Ta}=\text{X}$ species

As mentioned earlier, observations by Parkin of the 1,2 addition/elimination pathway for the reaction of  $\text{Cp}^*_2\text{Ta}(=\text{O}^*)\text{H}$  with  $\text{D}_2\text{O}$  sparked interest as to the generality of this mechanism in this system. Similar results were noted for the reaction of  $\text{H}_2\text{O}$  and  $\text{D}_2\text{O}$  with  $\text{Cp}^*_2\text{Ta}(=\text{NC}_6\text{H}_5)\text{H}$ . Thus, a systematic investigation of the reactivity of the compounds  $\text{Cp}^*_2\text{Ta}(=\text{X})\text{Y}$  ( $\text{X} = \text{O}, \text{S}, \text{NR}$ ;  $\text{Y} = \text{H}, \text{CH}_3$ ) with  $\text{H}_2\text{Z}$  ( $\text{Z} = \text{O}, \text{S}, \text{NR}, \text{PR}$ ) was undertaken. In addition, attempts were made to synthesize the  $\text{X} = \text{PR}$  analogue of the imido species.

Reactions of  $\text{Ta}=\text{O}$  As demonstrated earlier,  $\text{Cp}^*_2\text{Ta}(=\text{O})\text{D}$  reacts with  $\text{H}_2\text{O}^*$  with exchange of labeled O for unlabeled O. In a similar fashion,  $\text{Cp}^*_2\text{Ta}(=\text{O})\text{H}$  reacts with  $\text{H}_2\text{S}$  at room temperature to give  $\text{Cp}^*_2\text{Ta}(=\text{S})\text{H}$ . Interestingly, reaction of the isoelectronic  $\text{Cp}_2\text{Mo}=\text{O}$  with  $\text{H}_2\text{S}$  leads to  $\text{Cp}_2\text{Mo}(\text{SH})_2$ .<sup>20</sup> There is considerable precedent for the reaction of  $\text{H}_2\text{S}$  with  $\text{M}=\text{O}$  to give  $\text{M}=\text{S}$  species in bioinorganic chemistry. In particular, this reaction has been used to convert oxo-molybdenum species into sulfido compounds as models for xanthine oxidases and dehydrogenases.<sup>21</sup>

Similarly, several reagents have been reported to convert metal oxos into metal imido species, as shown in equation 5.<sup>22</sup> However, neither  $\text{NH}_3$ ,  $(\text{C}_6\text{H}_5)\text{HNNH}_2$ ,



nor  $\text{C}_6\text{H}_5\text{NCO}$  reacts with  $\text{Cp}^*_2\text{Ta}(=\text{O})\text{H}$  to yield an imido complex. As  $\text{Re}=\text{O}$  bonds are known to react with aniline to give phenyl imido complexes,<sup>23</sup> it would be of considerable interest to investigate the reaction of  $\text{Cp}^*_2\text{W}=\text{O}$  with amines.  $\text{C}_6\text{H}_5\text{PH}_2$

also shows no reactivity toward  $\text{Cp}^*_2\text{Ta(=O)H}$ . No net reaction is seen with  $\text{Cp}^*_2\text{Ta(=O)(CH}_3\text{)}$  and  $\text{H}_2\text{O}$ ; however, the definitive labelling study was not attempted.

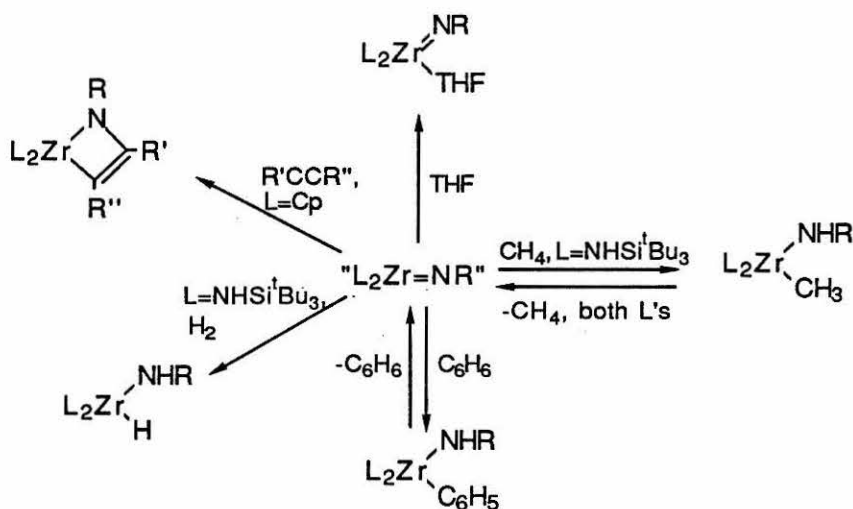
Reactions of Ta=S  $\text{Cp}^*_2\text{Ta(=S)H}$  reacts with water to give  $\text{Cp}^*_2\text{Ta(=O)H}$ , thus illustrating the facile reversibility of this reaction in the permethyltantalocene system. Heating this reaction mixture to  $50^\circ\text{C}$  yields an as yet unidentified product. While an unidentified  $\text{Cp}^*$  peak is observed to form (in  $<10\%$  yield) and then disappear during an  $^1\text{H}$  NMR experiment, no net transformation is observed upon reacting a 20-fold excess of  $\text{NH}_3$  with  $\text{Cp}^*_2\text{Ta(=S)H}$ .  $\text{Cp}^*_2\text{Ta(=S)H}$  has been found to be unreactive with  $\text{H}_2$  up to  $200^\circ\text{C}$ ; however,  $\text{Cp}^*_2\text{Ta(=S)CH}_3$  reacts with  $\text{H}_2$  at  $200^\circ\text{C}$  to give  $\text{CH}_4$  and  $\text{Cp}^*_2\text{Ta(=S)H}$ .<sup>24</sup> The forcing conditions involved and the reactivity of the Ta-CH<sub>3</sub> unit seem to indicate a mechanism other than 1,2 addition/elimination, which would be degenerate. One possibility could be initial 1,2 addition of  $\text{H}_2$  to the Ta=S bond to give  $\text{Cp}^*_2\text{Ta(SH)(H)(CH}_3\text{)}$  (possibly in equilibrium with  $\text{Cp}^*_2\text{Ta(=S)H}$ ), followed by reductive elimination of methane (which may require the high temperature).

Reactions of Ta=N-R More interesting reactivity was observed for  $\text{Cp}^*_2\text{Ta(=NR)H}$  ( $\text{R} = \text{H, CH}_3, \text{C}_6\text{H}_5$ ). Earlier work had shown that the N-phenyl imido reacted with water to give  $\text{Cp}^*_2\text{Ta(=O)H}$ , and with  $\text{D}_2\text{O}$  to give the same product. No exchange was observed by  $^{15}\text{N}$  NMR between excess  $\text{H}_2^{15}\text{NC}_6\text{H}_5$  and  $\text{Cp}^*_2\text{Ta(=NC}_6\text{H}_5\text{)H}$ . However, when  $\text{Cp}^*_2\text{Ta(=NH)H}$  was treated with  $^{15}\text{NH}_3$ , exchange did occur, as evidenced by a 60 Hz  $J_{\text{NH}}$ .  $\text{Cp}^*_2\text{Ta(=NC}_6\text{H}_5\text{)H}$  also reacts with  $\text{H}_2\text{S}$  to give  $\text{Cp}^*_2\text{Ta(=S)H}$ . A reaction does take place between  $\text{Cp}^*_2\text{Ta(=NH)H}$  and  $(\text{C}_6\text{H}_5)_2\text{PH}_2$ ; the product, though, is not believed to be a terminal phosphinidene. (See discussion of attempted syntheses of Ta=PR species below.)

While  $\text{Cl}_3(\text{THF})_2\text{Ta(NR)}$  has been found to be an effective imido transfer agent, reacting with organic carbonyls to yield the imine and (presumably) the metal oxo,<sup>25</sup>  $\text{Cp}^*_2\text{Ta(=NC}_6\text{H}_5\text{)H}$  does not react with acetone even with prolonged heating.  $\text{Cp}^*_2\text{Ta(=NC}_6\text{H}_5\text{)H}$  is also resistant to reduction by  $\text{LiAlH}_4$ , exchange with  $\text{NH}_3$  or

$\text{H}_2\text{NCH}_3$ , or alkylation by  $\text{CH}_3\text{I}$  or  $(\text{CH}_3)_3\text{SiCl}$  (though treatment with  $(\text{CH}_3)_3\text{O}^+\text{BF}_4^-$  results in decomposition).

Recent reports from the Bergman<sup>26</sup> and Wolczanski<sup>27</sup> groups have indicated that the Zr imidos are surprisingly reactive toward C-H bond activation, including  $\text{CH}_4$ . Some of this work is summarized in Scheme 4. Similarly, in the  $\text{Cp}^*_2\text{W}=\text{O}$  case recently examined by Parkin in these labs,  $\text{H}_2$  and  $\text{H-Si}(\text{CH}_3)_3$  can be added across the  $\text{W}=\text{O}$  bond (under forcing conditions) to give hydroxo- or siloxo-hydrides. We decided to examine the reactivity of  $\text{Cp}^*_2\text{Ta}(=\text{NH})\text{H}$  toward some of these types of substrates.

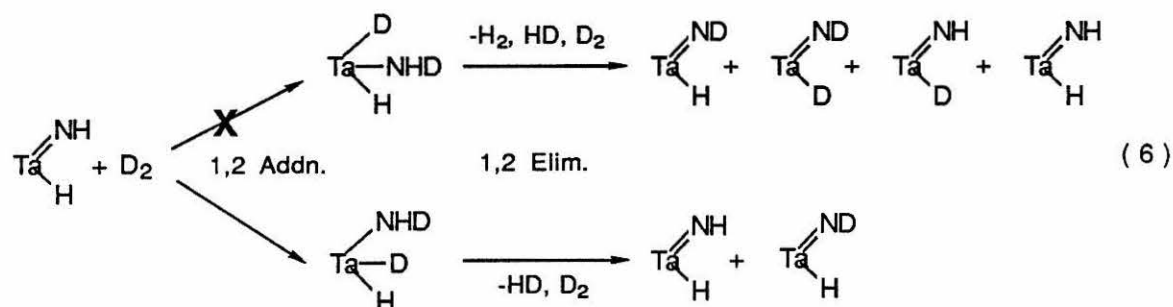


**Scheme 4.** (L = Cp and  $\text{NH}(\text{Si}^t\text{Bu}_3)$  unless otherwise specified)

This compound provides an ideal probe for these reactions, as the N-H provides an indicator of reaction with deuterated substrates that would be undetectable with the  $\text{Ta}=\text{O}$  or  $\text{Ta}=\text{S}$  (and likely the  $\text{Ta}=\text{NC}_6\text{H}_5$ ) analogues. While prolonged heating in  $\text{C}_6\text{D}_6$  does not result in H/D exchange, heating of  $\text{Cp}^*_2\text{Ta}(=\text{NH})\text{H}$  under 4 atmospheres of  $\text{D}_2$  does result in a decrease of intensity, and eventual near-disappearance, of the N-H signal in the  $^1\text{H}$  NMR. No decrease is observed in the Ta-H signal. While confirmation by  $^2\text{H}$  NMR would be advisable, this experiment suggests a non-symmetrical intermediate amido



species, which in turn implies initial attack by D<sub>2</sub> from the center rather than from the side.



Attempted Synthesis of Ta=PR Considerable effort has been expended in recent years in the "quest" for terminal phosphinidene compounds.<sup>28</sup> Indeed, it was only in 1987 that Lappert isolated and characterized the first of this class of compounds.<sup>29</sup> As a number of possible synthetic routes to Cp<sup>\*</sup><sub>2</sub>Ta(=PR)H are available, we decided to (briefly) join the quest. Reaction of C<sub>6</sub>H<sub>5</sub>PH<sub>2</sub> with Cp<sup>\*</sup><sub>2</sub>Ta(=CH<sub>2</sub>)H and with Cp<sup>\*</sup>(η<sup>5</sup>, η<sup>1</sup>(CH<sub>3</sub>)<sub>4</sub>C<sub>5</sub>(CH<sub>2</sub>))TaH<sub>2</sub> yielded only the phosphido compounds Cp<sup>\*</sup><sub>2</sub>TaH(PHC<sub>6</sub>H<sub>5</sub>)CH<sub>3</sub> and Cp<sup>\*</sup><sub>2</sub>TaH(PHC<sub>6</sub>H<sub>5</sub>)H, similar to the earlier reported Cp<sup>\*</sup><sub>2</sub>TaH(PH<sub>2</sub>)H<sup>5b</sup>. The reduction of Cp<sup>\*</sup><sub>2</sub>TaCl<sub>2</sub> with excess LiP(C<sub>6</sub>H<sub>5</sub>)H gave a mixture of products. Attempts to generate the phosphinidene complex via a 1,2 addition pathway were also unsuccessful. No reaction is observed when Cp<sup>\*</sup><sub>2</sub>Ta(=O)H or Cp<sup>\*</sup><sub>2</sub>Ta(=S)H is treated with H<sub>2</sub>P(C<sub>6</sub>H<sub>5</sub>). However, when Cp<sup>\*</sup><sub>2</sub>Ta(=NH)H is treated with H<sub>2</sub>P(C<sub>6</sub>H<sub>5</sub>) and heated to 80°C for a week, a new Cp<sup>\*</sup> signal is observed in the <sup>1</sup>H NMR. While the reaction is not clean (and not always reproducible), it appears that the Cp<sup>\*</sup> signal has the same chemical shift as the phosphido complexes synthesized by other routes.<sup>30</sup> This indicates that while 1,2 addition may have taken place to give an amido-phosphido complex, 1,2 elimination to the phosphinidene does not occur.

In a somewhat similar case, Schrock reports formation of imido-alkylidene compounds via intramolecular transfer of a proton from an amide group to an alkylidyne. When the corresponding phosphido-alkylidyne compound is synthesized, phosphinidene formation is not observed. An x-ray crystal structure determination of the phosphido compound reveals that, while the proton is oriented properly for transfer to the alkylidyne, the length of the W-P bond apparently puts the proton out of reach.<sup>31</sup> In our case it seems possible that while formation of the phosphido complexes is relatively facile, further reaction to give the phosphinidene is precluded by the distance involved in transferring a proton from the P to the Ta.

Equilibrium Studies The existence of the 1,2 addition/elimination reaction pathway in this system indicates a possibility of measuring equilibrium constants, and thus establishing relative bond strengths for these M=X functionalities. This would be of particular interest as there have been very few determinations of bond strengths for metal-heteroatom double bonds.<sup>2</sup> This method of establishing relative bond strengths has proven very useful in organometallic systems. In recent years, equilibrium studies have established relative Sc-C<sup>32</sup>, Ru-X<sup>33</sup>, Pd-X<sup>32</sup>, Ir-X<sup>34</sup> and Re-X<sup>35</sup> bond strengths.

Unfortunately, the only system for which we could obtain an equilibrium constant was the reaction of Cp<sup>\*</sup><sub>2</sub>Ta(=S)H with H<sub>2</sub>O. In dioxane, K<sub>eq</sub> was measured to be 1.1 x 10<sup>-3</sup>. The reaction was quite slow, taking over a week to reach equilibrium at room temperature. Heating the reaction mixture led to as yet unidentified products. As the first and second bond dissociation energies of H<sub>2</sub>O and H<sub>2</sub>S are known<sup>36</sup>, the relative bond strengths of Ta=O and Ta=S can be calculated (neglecting differences in solvation energies of H<sub>2</sub>O and H<sub>2</sub>S). As shown below, ΔG<sub>eq</sub>, when subtracted from the BDEs of H<sub>2</sub>O and H<sub>2</sub>S, yields a bond strength for Ta=O which is about 41 kcal greater than the Ta=S bond strength.

As mentioned above, equilibria were not observed in the other systems we investigated. However, we can place lower limits on the ΔBDE. These data, along with

the Ta=O/Ta=S data, are summarized below. The final differences in bond strengths for the M=X species are calculated by adding the difference in the sum of the total (first and second) BDEs of the two H<sub>2</sub>X species involved and then adding that to the experimentally determined  $\Delta G_{\text{eq}}$ .

	$\text{Ta} \begin{array}{c} \text{S} \\ \diagup \\ \text{H} \end{array} + \text{H}_2\text{O} \rightleftharpoons \text{Ta} \begin{array}{c} \text{O} \\ \diagup \\ \text{H} \end{array} + \text{H}_2\text{S} \quad K = 1.05 \times 10^{-3}$		
			$\Delta G_{\text{eq}} = +4.1 \text{ kcal/mol (dioxane)}$
$\Sigma 1^{\text{st}}$ and $2^{\text{nd}}$ BDE	- 221	- 176	$\implies \Delta \text{BDE}_{\text{H}_2\text{X}} = 45 \text{ kcal/mol}$
	Ta=O BDE greater than Ta=S BDE by 40.9 kcal/mol		

---

	$\text{Ta} \begin{array}{c} \text{NPh} \\ \diagup \\ \text{H} \end{array} + \text{H}_2\text{O} \rightleftharpoons \text{Ta} \begin{array}{c} \text{O} \\ \diagup \\ \text{H} \end{array} + \text{H}_2\text{NPh} \quad K > 2.6$		
			$\Delta G_{\text{eq}} < -0.6 \text{ kcal/mol (THF)}$
$\Sigma 1^{\text{st}}$ and $2^{\text{nd}}$ BDE	- 221	- 150 (est.)	$\implies \Delta \text{BDE}_{\text{H}_2\text{X}} = 71 \text{ kcal/mol}$
	Ta=O BDE greater than Ta=NPh BDE by >71.6 kcal/mol		

---

	$\text{Ta} \begin{array}{c} \text{NPh} \\ \diagup \\ \text{H} \end{array} + \text{H}_2\text{S} \rightleftharpoons \text{Ta} \begin{array}{c} \text{S} \\ \diagup \\ \text{H} \end{array} + \text{H}_2\text{NPh} \quad K > 8.0$		
			$\Delta G_{\text{eq}} < -1.2 \text{ kcal/mol (C}_6\text{D}_6\text{)}$
$\Sigma 1^{\text{st}}$ and $2^{\text{nd}}$ BDE	- 176	- 150 (est.)	$\implies \Delta \text{BDE}_{\text{H}_2\text{X}} = 26 \text{ kcal/mol}$
	Ta=S BDE greater than Ta=NPh BDE by >27.2 kcal/mol		

## CONCLUSIONS

The synthetic routes available for  $\text{Cp}^*_2\text{Ta}(\eta^2\text{-H}_2\text{C=NCH}_3)\text{H}$  were not found to be general for the synthesis of  $\text{Cp}^*_2\text{Ta}(\eta^2\text{-H}_2\text{C=NC}_6\text{H}_4\text{X})\text{H}$ , and thus we were unable to probe the electronics of the C-N bond breaking step. However, the reactivity of the parent N-methyl compound proved to be of some interest, as it reacts with  $\text{H}_2\text{O}$  and  $\text{H}_2\text{S}$  to form, respectively,  $\text{Cp}^*_2\text{Ta(=O)H}$  and  $\text{Cp}^*_2\text{Ta(=S)H}$ .

The reactivity of these doubly bonded  $\text{M=O}$  species was also investigated.  $\text{Cp}^*_2\text{Ta(=NH)H}$  reacts with  $\text{D}_2$  to give  $\text{Cp}^*_2\text{Ta(=ND)H}$ , implying a non-symmetrical amido-dihydride intermediate. Though not well characterized,  $\text{Cp}^*_2\text{Ta(=NH)H}$  appears to react with  $\text{H}_2\text{P(C}_6\text{H}_5)_3$  to give a phosphido complex, which does not 1,2 eliminate to give the phosphinidene. Other attempts to synthesize the  $\text{Ta=PR}$  unit were also unsuccessful.  $\text{Cp}^*_2\text{Ta(=S)H}$  reacts with  $\text{H}_2\text{O}$  to give an equilibrium mixture with  $\text{Cp}^*_2\text{Ta(=O)H}$  and  $\text{H}_2\text{S}$ . From the equilibrium constant and the known first and second BDEs of  $\text{H}_2\text{O}$  and  $\text{H}_2\text{S}$ , the  $\text{Ta=O}$  bond was found to be approximately 41 kcal stronger than the  $\text{Ta=S}$  bond. Though equilibria were not observed for the reactions of  $\text{Cp}^*_2\text{Ta(NC}_6\text{H}_5)\text{H}$  with  $\text{H}_2\text{O}$  and  $\text{H}_2\text{S}$ , lower limits for the difference in  $\text{Ta=NC}_6\text{H}_5$  and  $\text{Ta=O}$  (>71.6 kcal) and  $\text{Ta=NC}_6\text{H}_5$  and  $\text{Ta=S}$  (>27.2 kcal) could also be obtained.

## EXPERIMENTAL

### General Considerations.

All manipulations were performed using glovebox and high vacuum line techniques.<sup>37</sup> Solvents were distilled from an appropriate drying agent under N<sub>2</sub> and stored over sodium/benzophenone or titanocene.<sup>38</sup> H<sub>2</sub>O was deionized and degassed before use. NH<sub>3</sub>, H<sub>2</sub>S, HN(CH<sub>3</sub>)<sub>2</sub> (all Matheson), and <sup>15</sup>NH<sub>3</sub> (Stohler-Kor) were freeze-pump-thawed before use. (**Caution:** H<sub>2</sub>S is extremely toxic.) H<sub>2</sub>N(C<sub>6</sub>H<sub>5</sub>), HN(CH<sub>3</sub>)(C<sub>6</sub>H<sub>5</sub>), and acetone (all Aldrich) were dried over 4Å molecular sieves. LiP(C<sub>6</sub>H<sub>5</sub>)H was prepared by metalation of H<sub>2</sub>P(C<sub>6</sub>H<sub>5</sub>) with n-BuLi in toluene, filtered, and used as a solution. H<sub>2</sub>P(C<sub>6</sub>H<sub>5</sub>), LiAlH<sub>4</sub>, CH<sub>3</sub>I, (CH<sub>3</sub>)<sub>3</sub>SiCl, and (CH<sub>3</sub>)<sub>3</sub>OBf<sub>4</sub> (all Aldrich) and H<sub>2</sub><sup>15</sup>N(C<sub>6</sub>H<sub>5</sub>) (Stohler-Kor) were used as received. Cp\*<sub>2</sub>TaCl<sub>2</sub><sup>39</sup>, Cp\*<sub>2</sub>Ta(=CH<sub>2</sub>)H<sup>5a</sup>, Cp\*<sub>2</sub>Ta(=O)H<sup>5a</sup>, Cp\*<sub>2</sub>Ta(=N(C<sub>6</sub>H<sub>5</sub>))H<sup>5b</sup>, Cp\*<sub>2</sub>Ta(=NH)H<sup>5b</sup>, Cp\*<sub>2</sub>Ta(η<sup>2</sup>-H<sub>2</sub>C=NCH<sub>3</sub>)H<sup>5b</sup>, Cp\*<sub>2</sub>Ta(=O)CH<sub>3</sub><sup>5b</sup>, Cp\*<sub>2</sub>Ta(=NCH<sub>3</sub>)CH<sub>3</sub><sup>5b</sup>, and Cp\*<sub>2</sub>Ta(=S)H<sup>40</sup>, were prepared as described in other works.<sup>41</sup> Elemental analyses and mass spectrometric measurements were provided by the Caltech microanalytical service.

NMR spectra were recorded on Varian EM-390 (<sup>1</sup>H, 90 MHz), JEOL FX-90Q (<sup>15</sup>N, 9.03 MHz), and Jeol GX400Q (<sup>1</sup>H, 400 MHz).

**Reactivity Studies** Typically, studies were carried out by mixing the appropriate reagents in an NMR tube and monitoring the progress of the reaction by NMR. For example, 0.020 g of Cp\*<sub>2</sub>Ta(=O)H (4.58 × 10<sup>-5</sup> moles) was dissolved in 0.5 ml of C<sub>6</sub>D<sub>6</sub> in a sealable NMR tube and attached to a calibrated gas volume. The tube and gas volume were evacuated on the vacuum line, and 33.5 ml × 260 torr of NH<sub>3</sub> (46 × 10<sup>-5</sup> moles) was condensed into the tube at -196°C. The tube was then sealed, and the reaction was monitored by <sup>1</sup>H NMR.

**Equilibrium Studies** In general, the equilibrium studies were carried out as follows: A sealable NMR tube was loaded with the Cp\*<sub>2</sub>Ta(=X)H compound to be studied.

The tube was evacuated on the vacuum line, and an appropriate solvent vacuum transferred in. If  $\text{H}_2\text{S}$  or  $\text{NH}_3$  were to be added, it was done with a calibrated gas bulb;  $\text{H}_2\text{O}$ ,  $(\text{C}_6\text{H}_5)\text{NH}_2$ , and  $(\text{C}_6\text{H}_5)\text{PH}_2$  were added via syringe against an Ar flush. The tube was then cooled to  $-196^\circ\text{C}$ , evacuated, and sealed. The reactions were monitored by  $^1\text{H}$  NMR.

Equilibrium constants were calculated from ratios of reactants and products observed in the  $^1\text{H}$  NMR spectra. In all cases, the non-organometallic product of the reaction was not quantifiable in the spectrum and thus one  $\text{H}_2\text{X}$  was assumed as product per  $\text{Cp}^*_2\text{Ta}(=\text{Y})\text{H}$  product. First and second X-H BDEs have been measured experimentally for  $\text{H}_2\text{O}$  and  $\text{H}_2\text{S}$ ; only the first N-H BDE is known for  $\text{H}_2\text{N}(\text{C}_6\text{H}_5)$ . An estimate of the second BDE was obtained simply by subtracting 10 kcal from the first BDE, as this is approximately the difference between the first and second BDEs in  $\text{H}_2\text{O}$  and  $\text{H}_2\text{S}$ . Differences in solvation energy between reactants and products were assumed to be negligible.

## REFERENCES

1. a.) Parshall, G.W. *Chemtech* **1984**, 628-638. b.) Crabtree, R.H. *Chem. Rev.* **1985**, *85*, 245-269. c.) Rothwell, I.P. *Polyhedron* **1985**, *4*, 177-200.
2. Mayer, J.M.; Nugent, W. "Metal-Ligand Multiple Bonds"; Wiley-Interscience: New York, 1988.
- 3 See, for example, Laine, R.M. *J. Mol. Catal.* **1983**, *21*, 119-132.
4. Satterfield, C.N.; Gultekin, S. *Ind. Eng. Chem. Proc. Des. Dev.* **1981**, *20*, 62.
5. a.) van Asselt, A.; Burger, B.J.; Gibson, V.C.; Bercaw, J.E. *J. Am. Chem. Soc.* **1986**, *108*, 5347-5349. b.) Parkin, G.; Bunel, E.; Burger, B.J.; Trimmer, M.S.; van Asselt, A.; Bercaw, J.E. *J. Mol. Catal.* **1987**, *41*, 21-39.
6. Takahashi, Y.; Onoyama, N.; Ishikawa, Y.; Motojima, S.; Sugiyama, K. *Chem. Let.*, **1978**, 525-528.
7. Sharpless, K.B. *Chemistry in Britain* **1986**, *22*, 38-44.
8. Day, V.W.; Klemperer, W.G.; Schwartz, C.; Wang, R.-C. in "Surface Organometallic Chemistry: Molecular Approaches to Surface Catalysis", Jean-Marie Basset, *et al.*, eds.; Kluwer Academic Publishers: Boston, 1988; 173-186.
9. Labinger, J.A. *Catal. Lett.* **1988**, *1*, 371-376.
10. Dawson, J.H.; Elbe, K.S. *Adv. Inorg. Bioinorg. Mech.* **1986**, *4*, 1-64.
11. Hille, R.; Massey, V. In "Molybdenum Enzymes", Spiro, T., ed.; Wiley-Interscience: New York, 1985; 443-518 .
12. Angelici, R.J. *Acc. Chem. Res.* **1988**, *21*, 387-394 and references therein.
13. Rocklage, S.M.; Schrock, R.R. *J. Am. Chem. Soc.* **1982**, *104*, 3077-3081.
14. Chan, D.M.T.; Fultz, W.C.; Nugent, W.A.; Roe, D.C.; Tulip, T.H. *J. Am. Chem. Soc.* **1985**, *107*, 251-253.

15. Parkin, G.; Bercaw, J.E. *Polyhedron* **1988**, *7*, 2053-2082
16. Burger, B.J., Ph.D. dissertation, California Institute of Technology, Pasadena, California, 1987. Interestingly, reactions with thiols seem to be more general (Nelson, J.; Bercaw, J.E. unpublished observations).
17. Lowry, T.H.; Richardson, K.S. "Mechanism and Theory in Organic Chemistry", 2nd ed.; Harper and Row: New York, 1981.
18. Hillhouse, G.L.; Bulls, A.R.; Santarsiero, B.D.; Bercaw, J.E. *Organometallics*, **1988**, *7*, 1309-1312.
19. Peaks at 2.20 ( $\text{NCH}_3$ ) and 1.02 ( $\text{TaCH}_2\text{N}$ ) are observed with proper integration ratios relative to the new  $\text{Cp}^*$  signal. However, a peak at 1.54 with an intensity of  $\sim 5$  protons is also observed to grow in and decrease concomitantly with these signals. Its identity is unknown.
20. Green, M.L.H.; Lynch, A.H.; Swanwick, M.G. *J. Chem. Soc., Dalton Trans.* **1972**, 1445-1447.
21. Garner, C.D.; Bristow, S. In "Molybdenum Enzymes", Spiro, T., ed.; Wiley-Interscience: New York, 1985; p 385.
22. Nugent, W.A.; Haymore, B.L. *Coord. Chem. Rev.*, **1980**, *31*, 123-175.
23. Clark, G.R.; Nielson, A.J.; Rickard, C.E.F. *Polyhedron*, **1988**, *7*, 117-128.
24. Nelson, J.; Bercaw, J.E. unpublished results.
25. Rocklage, S.M.; Schrock, R.R. *J. Am. Chem. Soc.* **1982**, *104*, 3077-3081.
26.  $\text{L} = \text{Cp}$ ; Walsh, P.J.; Hollander, F.J.; Bergman, R.G. *J. Am. Chem. Soc.* **1988**, *110*, 8729-8731.
27.  $\text{L} = \text{NHSi}^t\text{Bu}_3$ ; Cummins, C.C.; Baxter, S.M.; Wolczanski, P.T. *J. Am. Chem. Soc.*, **1988**, *110*, 8731-8733.
28. Cowley, A.H.; Barron, A.R. *Acc. Chem. Res.* **1988**, *21*, 81-87.



29. Hitchcock, P.B.; Lappert, M.F.; Leung, W.-P. *J. Chem. Soc., Chem. Commun.* **1987**, 1282.
30.  $^1\text{H}$  NMR data:  $\text{Cp}^*_2\text{Ta}(\text{H})(\text{CH}_3)(\text{PH}(\text{C}_6\text{H}_5))$ :  $\text{Cp}^*$ , 1.85(s);  $\text{C}_6\text{H}_5$ , 7.77-8.08(m, br).  $\text{Cp}^*_2\text{Ta}(\text{H})_2(\text{PH}(\text{C}_6\text{H}_5))$ :  $\text{CH}_3$ , 0.14(s);  $\text{Cp}^*$ , 1.87(s); Ta-H, 5.22(t,  $^2J_{\text{PH}}=4.5$  Hz);  $\text{C}_6\text{H}_5$ , 7.73-7.98(m, br).  $\text{Cp}^*_2\text{Ta}(\text{H})(\text{NH}_2)(\text{PH}(\text{C}_6\text{H}_5))$ :  $\text{Cp}^*$ , 1.84(s);  $\text{C}_6\text{H}_5$ , 7.77-8.08(m, br). All chemical shifts are in parts per million from TMS, and were recorded in  $\text{C}_6\text{D}_6$  on a Varian EM-390.
31. Rocklage, S.M.; Schrock, R.R.; Churchill, M.R.; Wasserman, H.J. *Organometallics*, **1982**, *1*, 1332-1338.
32. Bulls, A.R.; Bercaw, J.E.; Manriquez, J.M.; Thompson, M.E. *Polyhedron*, **1988**, *7*, 1409-1428.
33. Bryndza, H.E.; Fong, L.K.; Paciello, R.A.; Tam, W.; Bercaw, J.E. *J. Am. Chem. Soc.* **1987**, *109*, 1444-1456.
34. Buchanan, J.M.; Stryker, J.M.; Bergman, R.G. *J. Am. Chem. Soc.* **1986**, *108*, 1537-1550.
35. Erikson, T.K.G.; Bryan, J.C.; Mayer, J.M. *Organometallics*, **1988**, *7*, 1930-1938.
36. a.)  $\text{H}_2\text{O}$ : Kerr, J.A. *Chem. Rev.* **1966**, *66*, 465-500. b.)  $\text{H}_2\text{S}$ : Benson, S.W. *Chem. Rev.* **1978**, *78*, 23-35.
37. Burger, B.J.; Bercaw, J.E. in "New Developments in the Synthesis, Manipulation, and Characterization of Organometallic Compounds"; Wayda, A. and Darensbourg, M., eds.; ACS Symposium Series, **1987**, *357*, 79-98.
38. Marvich, R.H.; Brintzinger, H.H. *J. Am. Chem. Soc.* **1971**, *93*, 2046-2048.
39. Gibson, V.C.; Bercaw, J.E.; Bruton, W.J.; Sanner, R.D. *Organometallics* **1986**, *5*, 976-979.
40. Parkin, G.; Bercaw, J.E. unpublished results.

- 41. Complete synthetic procedures and characterizations for these compounds will be included in manuscripts in preparation by G. Parkin and J.E. Bercaw.